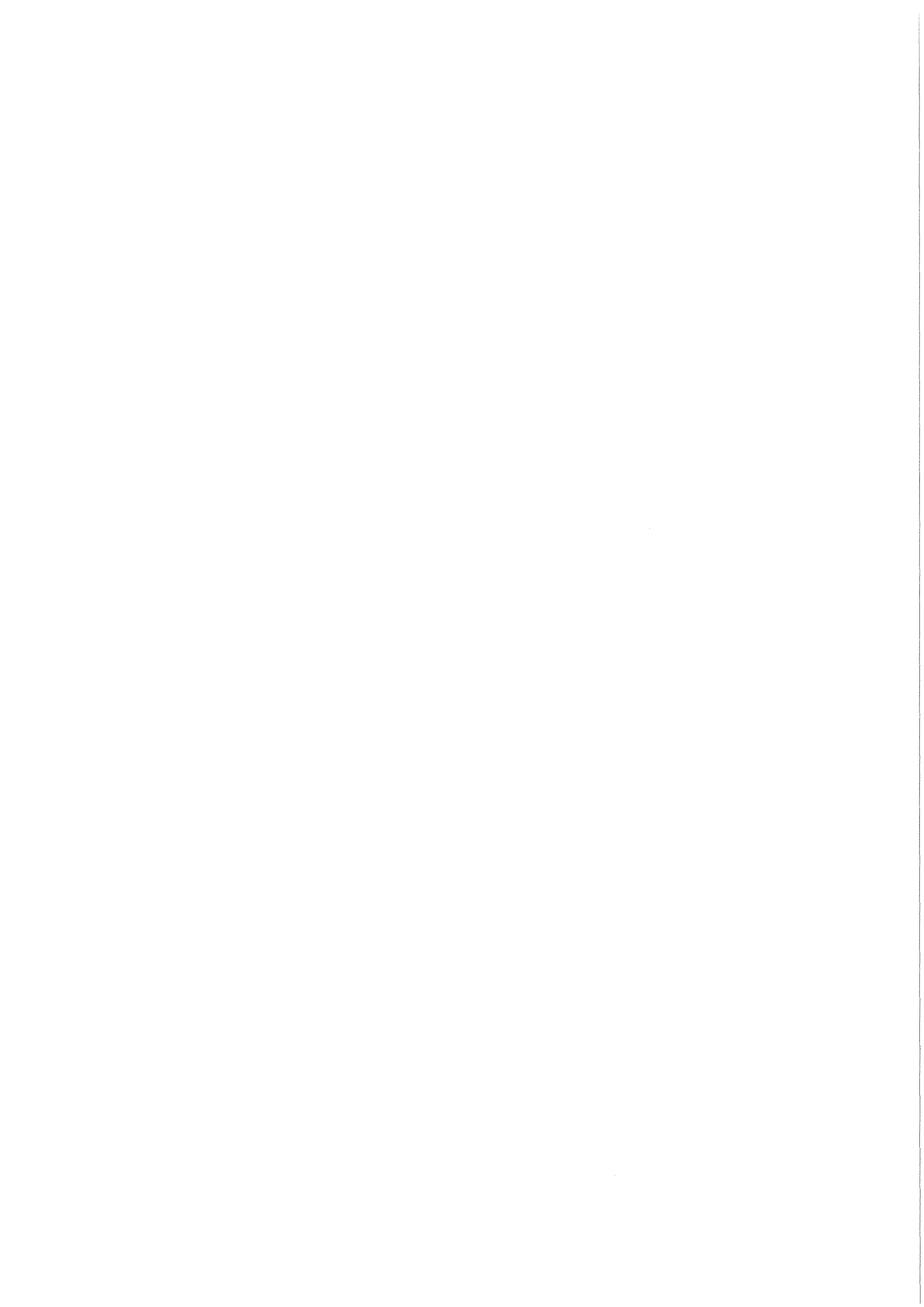


KfK 3719
März 1984

**Über die wissenschaftliche Arbeit
von
Leonardo Caldarola**

Kernforschungszentrum Karlsruhe



KERNFORSCHUNGSZENTRUM KARLSRUHE
Institut für Reaktorentwicklung

KfK 3719

Über die wissenschaftliche Arbeit
von
Leonardo Caldarola

Kernforschungszentrum Karlsruhe GmbH, Karlsruhe

Als Manuskript vervielfältigt
Für diesen Bericht behalten wir uns alle Rechte vor

Kernforschungszentrum Karlsruhe GmbH
ISSN 0303-4003

Leonardo Caldarola

geb. 22. Oktober 1933

gest. 27. März 1983

D. Smidt

Wir trauern um unseren lieben Freund und Kollegen Leonardo Caldarola. Unser tiefes Mitgefühl gilt seiner Gattin und seinen beiden Kindern. Mit großer Betroffenheit haben wir alle die Nachricht von seinem so plötzlichen Tode aufgenommen. Wir können es nicht fassen, daß dieser brillante, lebenswerte und humorvolle Mann uns nicht mehr begegnen wird, uns nicht mehr in seinem lebhaften Stil seine originellen Gedanken vortragen wird und uns nicht mehr durch die Erzählung einer der vielen Geschichten aus dem Schatz seiner Erlebnisse erheitern wird.

Der Tod, gegen den wir Menschen machtlos sind, hat einer glänzenden und international anerkannten wissenschaftlichen Laufbahn ein allzu frühes Ende gesetzt. Die, die ihm am nächsten standen und die er nun zurückläßt, können Trost nur in ihrem Glauben finden. Aber wir wissen, daß er nicht umsonst gelebt hat. Seine Kinder werden seinen Namen weitertragen, und seine wissenschaftlichen Leistungen werden sein Gedenken bei Menschen buchstäblich in der ganzen Welt lebendig halten.

Unsere freundschaftliche Erinnerung aber wird ihn weiter sehen als einen Mann voller wahrhaft schöpferischer Gedanken, einen unermüdeten Arbeiter, dabei mit wachem Sinn für die vielfältige Komik im menschlichen Leben. So, als im wahrsten Sinne des Wortes "liebenswert", werden wir an ihn denken.

M. Dalle Donne

Caro Leonardo, caro Cavaliere,

io, noi, non ti vogliamo ricordare com'eri gli ultimi giorni: stanco, ammalato, con gli occhi pieni di paura. Ti vogliamo ricordare come eri ai tempi dell' Agip, o ai tempi dell' Inghilterra: pronto allo scherzo o alla discussione interminabile di politica o di fisica.

Di quando passeggiavi avanti indietro, vestito di nero, nei corridori di Durley Hall, di quando andavi in Cornovaglia con gli amici scozzesi, o di quella volta dell' urlo del giaguaro. O di quando si cantava insieme: "Mamma son tanto felice" nella camera attigua a quella di Häfele. O di quando, dopo un anno appena qui a Karlsruhe, presentasti, unico straniero, una relazione allo Status Bericht del Reattore Veloce. O di quando ti apprestavi a tornare in Italia, convinto di dare un contributo al risolle-
vamento dell' energia nucleare italiana.

Se, adesso, tu mi vedi, Leonardo, se mi senti, mi capisci al volo. Per gli altri, per quelli che non ti conoscono così bene, come ti conoscevo io, posso dire che eri un uomo buono, generoso, a volte ingenuo; serio, pessimista, poco facile alle confidenze; prudente, tranquillo, generalmente controllato; profondamente intelligente, con una capacità straordinaria, sbalorditiva, di concentrarsi su un soggetto, di sviscerarlo nei suoi minimi particolari. Un Italiano del Sud: con i difetti e i pregi, soprattutto i pregi, dell' Italiano del Sud: per te la tua famiglia, tuo padre, tua madre, tuo fratello, tua sorella, tua moglie e i tuoi figli, soprattutto i figli, e il tuo lavoro scientifico erano tutto. E in questo avevi ragione, perchè sono queste due cose, i figli e il tuo lavoro scientifico, che ti permettono di vivere ancora un po', oltre la morte.

Ciao Leonardo.

Die Zeit von 1960 bis 1975

Leonardo Caldarola im Institut für Angewandte Reaktorphysik (IAR)
des Kernforschungszentrums Karlsruhe

Wolf Häfele

1960 war der Beginn des Projektes Schneller Brüter im Kernforschungszentrum Karlsruhe. Bald kam es zu der Assoziation mit Euratom, ein Schritt, der für das Projekt von wesentlicher Bedeutung war. Im Vollzug dieser Assoziation kam Leonardo Caldarola als italienischer Wissenschaftler, der Euratom-Bediensteter war, in das damals gerade neu gegründete Institut für Angewandte Reaktorphysik (IAR). Dieses Institut war sehr stark auf das Projekt Schneller Brüter ausgerichtet; die Personalunion Projektleiter Schneller Brüter - Institutsleiter legte das nahe.

Im Institut für Angewandte Reaktorphysik verfolgte Leonardo Caldarola im Laufe der Zeit drei große Problemkreise, die alle für das Projekt Schneller Brüter von erheblicher Bedeutung waren. Bei allen drei Problemkreisen machte Leonardo Caldarola von seiner großen theoretischen Begabung Gebrauch, die in höchst seltener Art und Weise Mathematik und Ingenieurkunst miteinander vereinte.

Der erste Problemkreis betraf die wissenschaftliche Nutzung des SEFOR-Reaktors. Dieses deutsch-amerikanische Reaktorexperiment in Arkansas, USA, diente der Messung des Dopplerkoeffizienten unter weitgehend echten Bedingungen des Betriebes eines Leistungsreaktors. Insbesondere waren auch Oszillatorexperimente vorgesehen, die zunächst in gewohnter Weise vorsahen, eine Reaktivitätsoszillation zustande kommen zu lassen, um aus den so hervorgerufenen Leistungsschwankungen die Größe und Dynamik des wirksamen Leistungskoeffizienten herzuleiten. Natürlich sind immer mehrere Koeffizienten im Spiel, der Dopplerkoeffizient ist keineswegs der einzige. Hier brachte nun Leonardo Caldarola den Gedanken ein,

die Leistungsschwankungen durch eine zweite Oszillation, nämlich die des Kühlmittelstroms, zu kompensieren. Es liegt in der Natur der Sache, daß durch ein solches Balanced Oscillator Experiment deutlich mehr Informationen gewonnen werden können als bei einem einfachen Oszillatorexperiment, insbesondere konnte der Dopplerkoeffizient besser von den übrigen Koeffizienten getrennt werden. Leonardo Caldarola hat aber nicht nur die Theorie dieses Balanced Oscillator-Experimentes entworfen, sondern auch die dazugehörigen Apparaturen technisch entwickelt und das Experiment dann schließlich mit großem Erfolg durchgeführt.

Anfang der siebziger Jahre griff Leonardo Caldarola ein anderes großes Arbeitsgebiet auf, das für das Projekt Schneller Brüter wohl von noch größerer Bedeutung war: Die auf das seit längerer Zeit bekannte Phänomen der Dampfexplosion zurückgehende Brennstoff-Natrium-Wechselwirkung. Heute überblicken wir deutlicher, wie sehr sich das Genehmigungsverfahren für kommerzielle und prototypische Kernkraftwerke Anfang der siebziger Jahre verschärfte. Insbesondere galt das auch für den SNR 300, den deutschen MWel Prototyp eines Schnellen Brütters. In solchem Zusammenhang war deutlich geworden, daß die Dynamik des sogenannten Bethe-Tait-Störfalles eingeht. Es war entscheidend, zu verstehen, ob der Wärmeübergang aus Brennstoffpartikeln an das Natrium instantan oder, wegen der Bildung eines Dampffilmes, verzögert vonstatten gehen würde. Wieder zeigte Leonardo Caldarola eine ungeheure analytische Kraft beim Angehen dieser Fragestellung. Insbesondere kamen seine Resultate so rechtzeitig, daß insoweit das Genehmigungsverfahren wie vorgesehen ablaufen konnte. In den siebziger Jahren weitete sich diese Fragestellung noch aus, und es kam an mehreren Stellen der Welt auch zu gezielten Experimenten. In diesem weltweiten Dialog um die Natrium-Dampfexplosion hat Leonardo Caldarola eine wesentliche Rolle gespielt.

In den späten sechziger Jahren kam aber noch eine andere Entwicklung in Gang, die Leonardo Caldarola während seiner Zeit am Institut für Angewandte Reaktorphysik aufgriff: Die Fehlerbaumanalyse. Als solche war sie schon während der frühen sechziger Jahre im Bereich der Raumfahrt und Elektronik entwickelt worden. Es schien aber zunächst überhaupt nicht klar zu sein, ob diese Art von Analyse auf das Gebiet der Reaktortechnik übertragbar sein würde, wo gerade nicht viele gleichartige oder sehr ähnliche Komponenten ein System ausmachen. Erneut bedurfte es großer analytischer Kraft, hier erste Schritte zu tun, und erneut profi-

tierte Leonardo Caldarola von seiner glücklichen Begabung, Mathematik und Ingenieurkunst auf ungewöhnliche Weise zu verbinden. Dieses Arbeitsgebiet lag in der Luft, auch an anderen Stellen wurde intensiv daran gearbeitet. Für Leonardo Caldarola wurde das Gebiet der Fehlerbaumanalyse zu seinem Hauptarbeitsgebiet, das er in den siebziger Jahren - dann freilich im Institut für Reaktorentwicklung des Kernforschungszentrums Karlsruhe - mit großem Erfolg bearbeitete.



Die Zeit von 1975 bis 1983

Leonardo Caldarola im Institut für Reaktorentwicklung des Kernforschungszentrums Karlsruhe

Dieter Smidt

Nachdem Professor Dr. Häfele, der Leiter des Instituts für Angewandte Reaktorphysik und Systemanalyse des Kernforschungszentrums Karlsruhe, neue Aufgaben übernommen hatte, entschied sich Leonardo Caldarola für den Übertritt in das Institut für Reaktorentwicklung des Kernforschungszentrums Karlsruhe, das sich vorwiegend mit Problemen der Reaktorsicherheit beschäftigt. Er brachte seine beiden Arbeitsgebiete Zuverlässigkeitsanalyse und Erforschung der Grundlagen der Dampfexplosion mit.

Für die weitere Erforschung der Phänomene der Dampfexplosion mußten zunächst die experimentellen Kenntnisse erweitert werden. Durch mehrere von ihm betreute Doktorarbeiten nahm Caldarola diese Aufgabe systematisch in Angriff. Aus den bereits vor Caldarolas Eintritt in das Institut dort durchgeführten Experimenten, bei denen die Reaktion zwischen Wasser und geschmolzenem Kupfer mit einer handelsüblichen Hochgeschwindigkeitskamera (5000 Bilder/sec) aufgenommen wurde, hatten trotz vieler interessanter Einsichten gezeigt, daß der eigentliche Explosionsvorgang so schnell vor sich geht, daß er mit dem zur Verfügung stehenden zeitlichen Auflösungsvermögen nicht erfaßt werden konnte. Eine kurz vor seinem Tode fertig gewordene Dissertation von M. Ando führte hier erheblich weiter. Erstmals war es gelungen, durch Aufnahmegeschwindigkeiten von 100000 Bildern/sec den Explosionsvorgang in Einzelaufnahmen aufzulösen und die dabei ablaufenden Vorgänge genauer zu betrachten. Die Beobachtungen geben starke Hinweise dafür, daß es sich in der Tat, wie Caldarola schon früher vermutet hatte, um die Ausbildung hydrodynamischer Instabilitäten beim Zusammenbruch des Dampfes handelte. Erste Nachrechnungen zeigten, daß diese Vermutung größenordnungsmäßige Übereinstimmung mit

den beobachteten Phänomenen gab. Bereits im Dezember 1977 erstellte Caldarola zusammen mit S. J. Board einen umfassenden Bericht /49/, der zum damaligen Zeitpunkt der beste Bericht über den state of the art der Dampfexplosion darstellte. Obwohl die Bedeutung der Dampfexplosion aus übergeordneten Erwägungen nicht mehr den gleichen großen Stellenwert für die Reaktorsicherheit hat wie dies vor etwa 5 bis 10 Jahren der Fall war, war es doch wichtig, auf die lange Zeit unverstandener Phänomene ein neues Licht zu werfen. Dies ist Caldarola zu einem großen Teil möglich gewesen.

Die Auswertung großer und komplexer Fehlerbäume kann nur durch Rechenprogramme erfolgen. Während hierfür weitgehend Monte-Carlo-Techniken eingesetzt wurden, entschied sich Caldarola für eine analytische Behandlung der dem Fehlerbaum entsprechenden Booleschen Ausdrücke. Es zeigte sich bald, daß mit dieser Methode nicht nur wesentlich kürzere Rechenzeiten erzielt werden, sondern daß bei sehr großen Fehlerbäumen alle anderen Methoden schließlich versagen.

In den meisten Fehlerbaumuntersuchungen, wie sie z. B. auch noch in der Rasmussen-Studie zugrunde liegen, geht man davon aus, daß die betrachteten Systemkomponenten nur zwei Zustände haben können: intakt bzw. ausgefallen. Dadurch wird die Behandlung komplexerer Teilsysteme außerordentlich schwierig und aufwendig. Eine wesentliche Leistung Caldarolas ist die Entwicklung von Verfahren für die Behandlung von Komponenten mit mehreren Zuständen durch Einführung einer Booleschen Algebra mit beschränkten Variablen. Mit einer ausführlichen Arbeit hierüber habilitierte er sich am 16. Januar 1980. Seine Rechenverfahren sind international in hohem Maße anerkannt worden. Als Beispiel sei eine Untersuchung der Firma Control Data erwähnt, die für ihre Benutzer-Software das auf der Welt verfügbare leistungsfähigste System auswählte und dabei sich für die Programme von Caldarola entschied.

In zunehmendem Maße wurde neben der theoretischen Vervollkommnung der Hilfsmittel die praktische Anwendung erweitert. Als wichtigster Beitrag auf diesem Gebiet ist die Untersuchung des Schnellabschaltsystems des SNR und des Superphénix zu nennen, die in Zusammenarbeit mit der Firma Siemens durchgeführt wurde, die beide Systeme entwickelt und baut.

Der Wert, den man seiner hohen Sachkenntnis auf seinen Arbeitsgebieten beimaß, zeigte sich auch in seiner Berufung in zahlreiche deutsche und internationale Sachverständigenausschüsse:

- Ad hoc-Gruppe Zuverlässigkeit und Risiko des BMFT
- Reliability experts working group des IRC Ispra im Rahmen von EURATOM
- OECD/NEA-CSNI-Specialists' Group on Vapour Explosions and Fuel Coolant Interaction
- Group of Experts on fuel-coolant-interaction des IRC Ispra im Rahmen von EURATOM

Außerdem nahm Caldarola als "principal scientific officer" der Europäischen Gemeinschaft Einfluß auf die Begutachtung von Arbeitsprogrammen des Europäischen Forschungszentrums in Ispra.

Neben seinen wissenschaftlichen Arbeiten ist auch sein Erfolg und sein Engagement als wissenschaftlicher Lehrer hervorzuheben. Sein außerordentlich lebendiger Vortragsstil bleibt sowohl für die Hörer seiner Vorträge als auch für seine Studenten unvergeßlich.

Der Tod dieses Mannes, der mit seiner hohen wissenschaftlichen Begabung, seinem Ideenreichtum und seinem unermüdlichen Arbeitseinsatz wichtige Beiträge auf seinen Fachgebieten geleistet hat, wird von seinen Kollegen in aller Welt als ein schmerzlicher Verlust empfunden.



Der folgende Artikel

L. Caldarola

The Balanced Oscillator Experiment

aus

NUKLEONIK, Bd. 7 (1965) S. 120-127

wurde mit freundlicher Genehmigung des
Springer-Verlags, der das Copyright an
dieser Arbeit besitzt, nachgedruckt



Sciences, Washington. — [6] PRESTWOOD, R.J., and B.P. BAYHURST: Phys. Rev. **121**, 1438 (1961). — [7] JERONIMO, J.M.F., G.S. MANT, J. OLKOWSKY, A. SADEGHI, and C.F. WILLIAMSON: Nuclear Phys. **47**, 157 (1963). — [8] PRUD'HOMME, J.T., I.L. MORGAN, J.H. MCCRARY, J.B. ASHE, and O.M. HUDSON jr.: Texas Nuclear Corporation, Report AFSWC-TR-60-30 (1960). — [9] BORMANN, M., S. CIERJACKS, E. FRETWURST, K.-J. GIESECKE, H. NEUERT u. H.

POLLEHN: Z. Physik **174**, 1 (1963). — [10] RAYBURN, L.A.: Phys. Rev. **130**, 731 (1963). — [11] GABBARD, F.: Private Mitteilung.

Anschrift: A. PAULSEN und H. LISKIEN
EURATOM
Zentralbüro für Kernmessungen
Geel/Belgien

The Balanced Oscillator Experiment*

Von L. CALDAROLA **

(Institut für Angewandte Reaktorphysik Kernforschungszentrum Karlsruhe)

With 12 figures in the text

(Received November 3, 1964)

Abstract. The "Balanced Oscillator Experiment" is a new type of oscillator experiment to measure transfer functions of nuclear fast reactors.

The technique consists in injecting in a reactor at the same time sinusoidal signals of reactivity and coolant flow of the same frequency and related each other in such a way that the coolant temperatures remain constant.

In addition to the Doppler reactivity coefficient, this new method allows to measure the fuel thermal conductivity and the heat transfer coefficient between fuel and coolant.

Numerical examples are included with reference to the Southwest Experimental Fast Oxide Reactor (Sefor). (Bibl. 3.)

1. Introduction

The "Balanced Oscillator Experiment" consists in injecting in a fast reactor at the same time sinusoidal signals of reactivity and coolant flow of the same frequency and related each other in such a way that the coolant temperatures remain constant.

frequency in such a way that the outlet coolant temperature, Θ_{out} , remains constant. That is:

$$\Delta\Theta_{out} = 0. \tag{3}$$

The outlet coolant temperature is measured by a thermocouple (Fig. 2). $\Delta\mu_m/\Delta k_m$ and " α " are obviously function of " ω ".

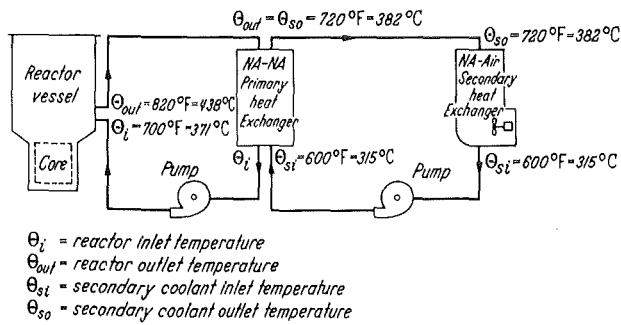


Fig. 1. Schematic reactor flow diagram (Sefor)

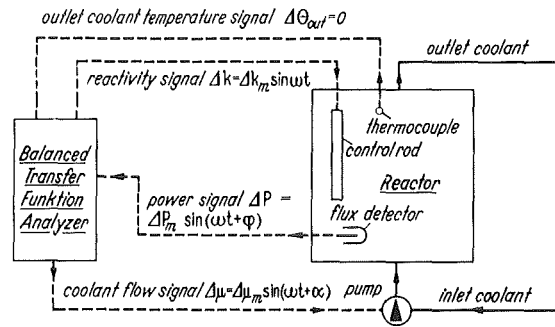


Fig. 2. Balanced oscillator experiment — Schematic Diagram of the signals

During the experiment the inlet coolant temperature must be kept constant by other means which are discussed later in para 6.

In this way the Doppler effect is the only reactivity temperature effect which is present during the experiment.

Fig. 1 shows the schematic reactor flow diagram.

Fig. 2 shows a schematic diagram of all the signals. The input signals to reactor are:

(i) reactivity signal $\Delta k = \Delta k_m \sin \omega t$, (1)

(ii) coolant flow signal $\Delta \mu = \Delta \mu_m \sin(\omega t + \alpha)$. (2)

The amplitude ratio, $\Delta\mu_m/\Delta k_m$, and the phase shift " α " of the two input signals must be chosen at any

The power signal ΔP is measured by means of a flux detector (Fig. 2). The "Balanced Transfer Function Analyser" (Fig. 2) allows us to evaluate the two transfer functions

$$\frac{\Delta\mu^*(j\omega)/\mu_0}{\Delta P^*(j\omega)/P_0} \tag{4}$$

and

$$\frac{\Delta P^*(j\omega)/P_0}{\Delta k^*(j\omega)/\beta} \tag{5}$$

where

- "*" indicates Laplace transform
- subscript "0" indicates steady state condition
- β = fraction of delayed neutrons.

2. Physical Fundamentals

In this paragraph we intend to find out which conditions should the amplitude ratio $\Delta\mu_m/\Delta k_m$ and the phase shift " α " satisfy in order to keep the coolant temperatures constant.

* This paper has been prepared within the framework of the association Euratom-Gesellschaft für Kernforschung mbH. in the field of fast breeder development.

** Euratom, Brussels, delegated to the Karlsruhe Fast Reactor Project Institut für Angewandte Reaktorphysik.

The reactor can be considered as divided in "n" cooling channels each including a fuel rod and its associated coolant. The heat balance equation of the coolant in an average channel is the following:

$$\frac{2\pi R h}{c} \frac{T_s - \Theta}{\mu/n} = \frac{\partial \Theta}{\partial z} + \frac{1}{v} \frac{\partial \Theta}{\partial t} \quad (1)$$

where

- h = heat transfer coeff. between fuel surface and coolant (including the cladding)
- R = radius of fuel rod
- c = specific heat capacity of the coolant
- T_s = fuel surface temperature
- Θ = coolant temperature
- z = axial coordinate
- v = coolant speed
- t = time
- n = number of cooling channels.

Eq. (1) can give $\partial \Theta / \partial t = 0$ only if:

$$\frac{T_s - \Theta}{\mu} = \frac{T_{s0} - \Theta_0}{\mu_0} = \text{function of "z" only} \quad (2)$$

where subscript "0" indicates initial steady state conditions. Taking into account (2), eq. (1) becomes:

$$\frac{2\pi R h}{c} \frac{T_{s0} - \Theta_0}{\mu_0/n} = \frac{\partial \Theta}{\partial z} + \frac{1}{v} \frac{\partial \Theta}{\partial t} \quad (3)$$

If we introduce the change of coolant temperature, $\Delta \Theta$

$$\Delta \Theta = \Theta - \Theta_0 \quad (4)$$

eq. (3) becomes:

$$\frac{2\pi R h}{c} \frac{T_{s0} - \Theta_0}{\mu_0/n} = \frac{d\Theta_0}{dz} + \frac{\partial \Delta \Theta}{\partial z} + \frac{1}{v} \frac{\partial \Delta \Theta}{\partial t} \quad (5)$$

It is:

$$\frac{2\pi R h}{c} \frac{T_{s0} - \Theta_0}{\mu_0/n} = \frac{d\Theta_0}{dz} \quad (6)$$

Eq. (5) becomes therefore:

$$\frac{\partial \Delta \Theta}{\partial z} + \frac{1}{v} \frac{\partial \Delta \Theta}{\partial t} = 0 \quad (7)$$

Eq. (7) associated to the boundary condition that the inlet coolant temperature, Θ_i , is constant ($\Delta \Theta_i = 0$), gives:

$$\Delta \Theta = 0 \quad (8)$$

We have therefore shown that condition (2) is necessary and sufficient in order to keep the coolant temperatures constant with time.

Taking into account (4) and (8), condition (2) may be written as follows:

$$\frac{\mu}{\mu_0} = \frac{T_s - \Theta}{T_{s0} - \Theta_0} = \frac{T_s - \Theta_0}{T_{s0} - \Theta_0} \quad (9)$$

Introducing

$$\Delta \mu = \mu - \mu_0 \quad (10)$$

and

$$\Delta T_s = T_s - T_{s0} \quad (11)$$

eq. (9) becomes:

$$\frac{\Delta \mu}{\mu_0} = \frac{\Delta T_s}{T_{s0} - \Theta_0} \quad (12)$$

The Laplace transform of eq. (12) is:

$$\frac{\Delta \mu^*}{\mu_0} = \frac{\Delta T_s^*}{T_{s0} - \Theta_0} \quad (13)$$

It is:

$$T_{s0} - \Theta_0 = \frac{R}{2h} \frac{P_0}{V_f} M(z) \quad (14)$$

where:

- P_0 = reactor power at steady state
- V_f = volume of fuel in reactor = $n\pi R^2 H$ (H being the height of the fuel rod)

$M(z)$ = normalized function expressing power distribution along the axis of a fuel rod

$$\left[\frac{1}{H} \int_0^H M(z) dz = 1 \right]$$

Since the coolant temperatures are constant, it is [according to Ref. 2, para 2, eq. (20)]:

$$\Delta T_s^* = \frac{R}{2h} \frac{1}{V_f} F_s(s \cdot t_r) M(z) \Delta P^*(s) \quad (15)$$

where

$\Delta P^*(s)$ = Laplace transform of the power change

and

$F_s(s \cdot t_r)$ = normalized transfer function between fuel surface temperature and power [$F_s(0) = 1$]

$$t_r = \text{radial time scale} = \frac{\rho_f c_f}{\lambda} R^2 = \text{fuel density} \times \text{fuel specific heat capacity} \times \text{fuel thermal conductivity} \times (\text{radius})^2$$

Putting (14) and (15) in (13), we have:

$$\frac{\Delta \mu^*}{\mu_0} = \frac{\Delta T_s^*}{T_{s0} - \Theta_0} = F_s(s \cdot t_r) \frac{\Delta P^*}{P_0} \quad (16)$$

which is independent on the axial coordinate "z".

In the time domain eq. (16) becomes:

$$\frac{\Delta \mu}{\mu_0} = \frac{\Delta T_s}{T_{s0} - \Theta_0} = \frac{1}{P_0} \int_0^t f_s(x) \Delta P(t-x) dx \quad (17)$$

where

$$f_s(t) = L^{-1} [F_s(s \cdot t_r)] \quad (18)$$

and L^{-1} indicates antitransformation.

The demonstration given in this paragraph starts from the assumption (2) where μ can be dependent on "z" which is physically impossible. At the end [eqs. (16) and (17)] we find out that μ is function only of the time.

In Appendix 1 a more refined demonstration is given: starting from condition (17) where μ is only a time dependent function, it is shown that the coolant temperatures remain constant.

Eq. (16) allows us to find which conditions should the amplitude ratio $\Delta \mu_m / \Delta k_m$ and the phase shift "α" satisfy, in order to keep the coolant temperatures constant.

It is:

$$D(j\omega) = \frac{\Delta P^*(j\omega)/P_0}{\Delta k^*(j\omega)/\beta} = \text{reactor power transfer function.} \quad (19)$$

Taking into account (16) and (19) we have:

$$\frac{\Delta \mu^*(j\omega)}{\Delta k^*(j\omega)} = \frac{\Delta \mu^*(j\omega)}{\Delta P^*(j\omega)} \cdot \frac{\Delta P^*(j\omega)}{\Delta k^*(j\omega)} = \frac{\mu_0}{\beta} D(j\omega) F_s(j\omega t_r) \quad (20)$$

and therefore:

$$\frac{\Delta\mu_m}{\Delta k_m} = \frac{\mu_0}{\beta} |D(j\omega)| \cdot |F_s(j\omega t_r)| \quad (21)$$

$$\alpha = \varphi_D(j\omega) + \varphi_s(j\omega t_r). \quad (22)$$

φ_D and φ_s being the phases respectively of the functions $D(j\omega)$ and $F_s(j\omega t_r)$.

3. Results obtainable from the new oscillator experiment

We have already said in para 1 that the "Balanced Transfer Function Analyser" allows us to evaluate

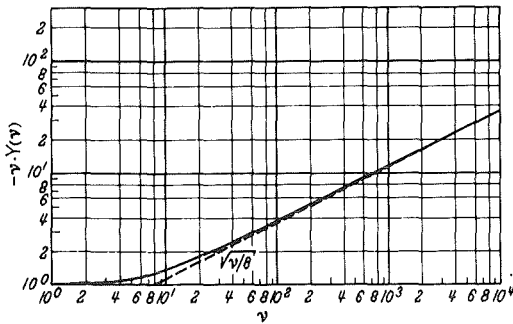


Fig. 3. Diagram of the function $-\nu Y(\nu)$

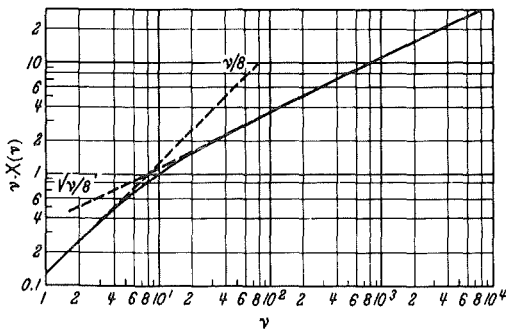


Fig. 4. Diagram of the function $\nu X(\nu)$

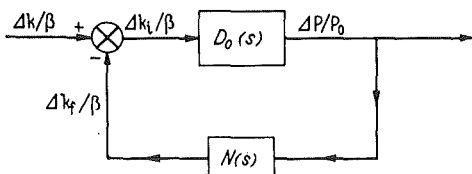


Fig. 5. Block diagram of reactor transfer functions

the two following transfer functions:

$$F_s(j\omega t_r) = \frac{\Delta\mu^*(j\omega)\mu_0}{\Delta P^*(j\omega)/P_0} \quad (1)$$

and

$$D(j\omega) = \frac{\Delta P^*(j\omega)/P_0}{\Delta k^*(j\omega)/\beta}. \quad (2)$$

As we have already shown in para 2 [eq. (16)], $F_s(j\omega t_r)$ is the transfer function between fuel surface temperature and power.

3.1. Determination of the parameters t_r and γ from the transfer function $F_s(j\omega t_r) = \frac{\Delta\mu^*(j\omega)\mu_0}{\Delta P^*(j\omega)/P_0}$

The author has found the following theoretical expression for $F_s(\sigma)$ with $\sigma = st_r$ (Ref. 2):

$$F_s(\sigma) = \frac{1/\sigma Z(\sigma)}{1 + \gamma/Z(\sigma)} \quad (3)$$

where

$$t_r = \text{radial time scale} = \frac{\rho_f c_f}{\lambda} R^2 = \frac{\text{fuel density} \times \text{fuel specific heat capacity}}{\text{fuel thermal conductivity}} \times (\text{radius})^2 \quad (4)$$

$$\gamma = \frac{\lambda}{2hR} = \frac{\text{fuel thermal conductivity}}{2 \times \text{heat transfer coefficient} \times \text{radius}} \quad (4')$$

$$Z(\sigma) = - \frac{J_0(\sqrt{\sigma})}{2\sqrt{\sigma} J_1(\sqrt{\sigma})} \quad (5)$$

J_0 and J_1 being Bessel functions of the first kind.

Putting $\sigma = j\nu = j\omega t_r$, we can write:

$$Z(j\nu) = X(\nu) + j Y(\nu). \quad (6)$$

With $X(\nu)$ and $Y(\nu)$ respectively real and imaginary part of $Z(j\nu)$. Introducing (6) in (3), we can write:

$$\frac{1}{F_s(j\nu)} = -\nu Y(\nu) + j[\nu X(\nu) + \gamma t_r \omega]. \quad (7)$$

$F_s(j\omega t_r)$ is also determined experimentally by means of eq. (1). Indicating with $M_s(\omega t_r)$ and $\varphi_s(\omega t_r)$ respectively modulus and phase of $F_s(j\omega t_r)$, we have:

$$\frac{1}{F_s(j\omega t_r)} = \frac{\cos \varphi_s}{M_s} - j \frac{\sin \varphi_s}{M_s}. \quad (8)$$

By comparing (7) with (8) we have:

$$\frac{\cos \varphi_s}{M_s} = -\nu Y(\nu) \quad (9)$$

and

$$-\frac{\sin \varphi_s}{M_s} = \nu X(\nu) + \gamma t_r \omega. \quad (10)$$

The functions $-\nu Y(\nu)$ and $\nu X(\nu)$ have been calculated and are given respectively in Figs. 2 and 4.

For a chosen value of ω we can evaluate $\cos \varphi_s/M_s$ experimentally. Using eq. (9), and Fig. 3 we get ν and, since $\nu = \omega t_r$, t_r is determined.

In eq. (10) the term $-\sin \varphi_s/M_s$ on the left side is evaluated experimentally for the chosen ω . $\nu X(\nu)$ is also known because ν is known, and we can therefore determine $\gamma \cdot t_r$.

The functions $-\nu Y(\nu)$ and $\nu X(\nu)$ have been programmed on the IBM 7070 computer, so that t_r and γ can be more precisely determined by means of numerical methods instead of using the graphs of Figs. 3 and 4. From t_r and γ , it is possible to evaluate the thermal conductivity, λ , and the heat transfer coefficient, h , if the density, ρ , the specific heat capacity, c , and radius, R , of the fuel rod have been previously determined.

3.2. Determination of the Doppler power coefficient and of the parameter $\sigma_1 t_r$ from the reactor transfer function,

$$D(j\omega) = \frac{\Delta P^*(j\omega)/P_0}{\Delta k^*(j\omega)/\beta}$$

Fig. 5 shows a schematic block diagram of the reactor transfer functions defined as:

$$D_0(s) = \frac{\Delta P^*(s)/P_0}{\Delta k^*(s)/\beta} = \text{zero power transfer function}, \quad (11)$$

$$N(s) = \frac{\Delta k_f^*(s)/\beta}{\Delta P^*(s)/P_0} = \text{feedback transfer function,} \quad (12)$$

$$D(s) = \frac{\Delta P^*(s)/P_0}{\Delta k^*(s)/\beta} = \frac{D_0(s)}{1 + D_0(s) \cdot N(s)} \quad (13)$$

= power transfer function

where:

$$\Delta k = \Delta k_i + \Delta k_j. \quad (14)$$

Since the coolant temperatures are constant, the reactivity feedback (Δk_j) will depend only on the fuel temperatures. It is:

$$\Delta k_j = \gamma_f \Delta T_{\text{eff}} \quad (15)$$

where:

γ_f = fuel temperature coefficient (mainly Doppler)
 T_{eff} = effective fuel temperature.

The effective fuel temperature is defined by:

$$\Delta T_{\text{eff}} = \frac{\int_{\text{all rods}} \Phi \Phi' \Delta T_{\text{av}} dV}{\int_{\text{all rods}} \Phi \Phi' dV}. \quad (16)$$

Φ and Φ' being respectively flux and adjoint flux, V volume and T_{av} the average temperature of a section of a fuel rod. Since the coolant temperatures are constant, ΔT_{av} will depend only on ΔP . It is [according to Ref. 2 para 2 eq. (22)]:

$$\Delta T_{\text{av}} = \frac{R}{2h} \left(1 + \frac{1}{8\gamma}\right) F_{\text{av}}(s \cdot t_r) \frac{M(z)}{V_f} \Delta P^*(s) \quad (17)$$

where:

$F_{\text{av}}(s \cdot t_r)$ = normalized transfer function between average fuel temperature and power [$F_{\text{av}}(0) = 1$].

Putting (16) and (17) in (15), and taking into account that $V_f = n\pi R^2 H$, we get:

$$\Delta k_j^* = G \cdot F_{\text{av}}(s \cdot t_r) \frac{1}{nH} \Delta P^*(s) \quad (18)$$

where:

$$G = \text{Doppler power coefficient} \quad (19)$$

$$= \gamma_f A_f \frac{1}{2\pi R h} \left(1 + \frac{1}{8\gamma}\right),$$

$$A_f = \frac{\int_{\text{all rods}} \Phi \Phi' M(z) dV}{\int_{\text{all rods}} \Phi \Phi' dV}. \quad (20)$$

Taking into account (18), eq. (12) becomes:

$$N(s) = \frac{P_0}{nH} \cdot \frac{1}{\beta} G \cdot F_{\text{av}}(s \cdot t_r). \quad (21)$$

The author has shown in Ref. 2 that the function $F_{\text{av}}(s \cdot t_r)$ with very good approximation is given by:

$$F_{\text{av}}(s \cdot t_r) \cong \frac{1}{1 + s t_r / \sigma_1}. \quad (22)$$

— σ_1 being the first root of the Bessel functions equation:

$$\frac{J_0(\sqrt{-\sigma})}{2\sqrt{-\sigma} J_1(\sqrt{-\sigma})} = \gamma. \quad (23)$$

Putting (22) in (21), we get:

$$N(s) \cong \frac{P_0}{nH} \frac{1}{\beta} G \frac{1}{1 + s t_r / \sigma_1}. \quad (24)$$

From eq. (13) we have

$$N(s) = \frac{1}{D(s)} - \frac{1}{D_0(s)}. \quad (25)$$

From (24) and (25) we obtain (putting $s = j\omega$):

$$\frac{P_0}{nH} \frac{G}{\beta} \frac{1}{1 + j\omega t_r / \sigma_1} = \frac{1}{D(j\omega)} - \frac{1}{D_0(j\omega)}. \quad (26)$$

If φ_D and φ_{D_0} are the phases respectively of $D(j\omega)$ and $D_0(j\omega)$, from (26) we have:

$$\frac{P_0}{nH} \frac{G}{\beta} = \frac{1}{|D| \cos \varphi_D} \times \left. \begin{aligned} &1 + \left| \frac{D}{D_0} \right|^2 - 2 \left| \frac{D}{D_0} \right| \cos(\varphi_D - \varphi_{D_0}) \\ &\times \frac{1}{1 - \left| \frac{D}{D_0} \right| \frac{\cos \varphi_{D_0}}{\cos \varphi_D}} \end{aligned} \right\} \quad (27)$$

and

$$\frac{\sigma_1}{t_r} = \omega \operatorname{ctg} \varphi_D \cdot \frac{1 - \left| \frac{D}{D_0} \right| \frac{\cos \varphi_{D_0}}{\cos \varphi_D}}{1 - \left| \frac{D}{D_0} \right| \frac{\sin \varphi_{D_0}}{\sin \varphi_D}}. \quad (28)$$

It is:

$$\lim_{\omega \rightarrow 0} \left| \frac{D}{D_0} \right| = 0, \quad (29)$$

$$\lim_{\omega \rightarrow 0} \cos \varphi_{D_0} = 0, \quad (30)$$

$$\lim_{\omega \rightarrow 0} \cos \varphi_D = 1. \quad (31)$$

Taking into account (29); (30) and (31), eq. (27) becomes:

$$\lim_{\omega \rightarrow 0} \frac{1}{|D|} = \frac{P_0}{nH} \frac{G}{\beta}. \quad (32)$$

For ω very small (in Sefor smaller than $3 \cdot 10^{-3} \text{ sec}^{-1}$), the power transfer function $D(j\omega)$ tends to the asymptotic value $nH\beta/P_0G$. Since P_0/nH and β are known, eq. (32) allows to determine the Doppler power coefficient G . We can conclude that G can be determined by measuring the transfer function $D(j\omega)$ only.

Eq. (28) allows to determine the parameter, σ_1/t_r . From the point of view of the accuracy, it is convenient to carry out this evaluation when $\operatorname{ctg} \varphi_D \cong 1$ that is when $\omega \cong \sigma_1/t_r$.

The determination of σ_1/t_r implies in the most general cases the measurement of both the transfer functions $D(j\omega)$ and $D_0(j\omega)$. In some cases the conditions (29) and (30) are already satisfied in the frequency region under consideration and σ_1/t_r is than more simply given by

$$\frac{\sigma_1}{t_r} = \omega \operatorname{cotg} \varphi_D. \quad (33)$$

This happens when:

$$\frac{\sigma_1}{t_r} \ll \lambda_\infty \quad (34)$$

where

$$\lambda_\infty = \frac{1}{\sum_{i=1}^6 \frac{\beta_i}{\lambda_i}}, \quad (35)$$

β_i and λ_i being respectively fraction and decay constant associated to the "i" th group of delayed neutrons. The determination of σ_1/t_r can be used as a countercheck of the results obtained in para 3.1. Since t_r and γ have already been determined (para 3.1) and σ_1 is function of γ (Fig. 6), the ratio σ_1/t_r can be also theoretically calculated and compared with that obtained experimentally.

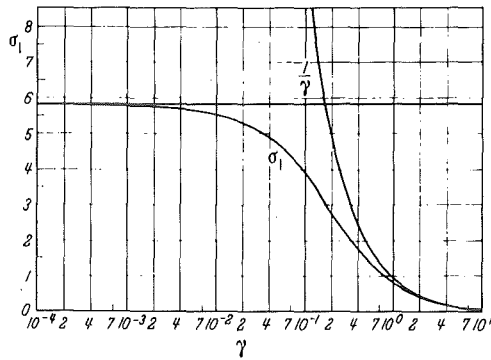


Fig. 6. First root $-\sigma_1$ of the equation $\frac{J_0(\nu-\sigma)}{2\nu-\sigma J_1(\nu-\sigma)} = \gamma$ as function of γ

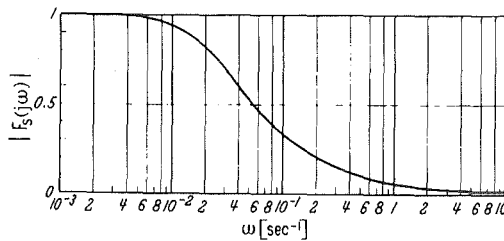


Fig. 7. Frequency response of the transfer function $F_s(j\omega)$ —Amplitude diagram (Sefor)

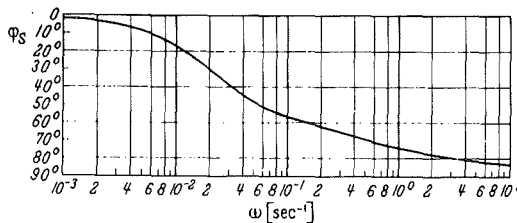


Fig. 8. Frequency response of the transfer function $F_s(j\omega)$ — Phase diagram (Sefor)

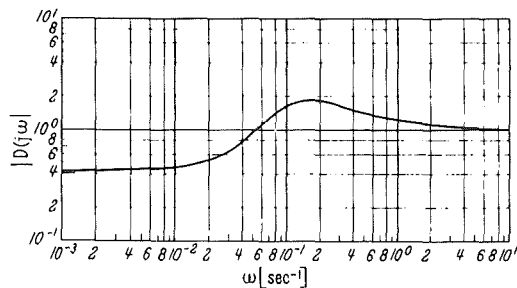


Fig. 9. Frequency response of the reactor power transfer function $D(j\omega)$ —Amplitude diagram (Sefor)

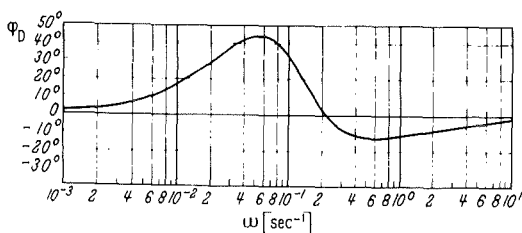


Fig. 10. Frequency response of the reactor power transfer function $D(j\omega)$ —Phase diagram (Sefor)

4. Numerical examples for Sefor reactor

Figs. 7 and 8 show respectively amplitude (M_s) and phase (φ_s) of the function $F_s(j\omega)$ as it is expected to be in Sefor.

Taking for example $\omega = 0.0625$ rad/sec, we have:

$$M_s = 0.4537 \quad \text{from Fig. 7,} \quad (1)$$

$$\varphi_s = -51.5^\circ \quad \text{from Fig. 8.} \quad (2)$$

From (1) and (2), we have:

$$\cos \varphi_s = \frac{0.6225}{0.4537} = 1.375 = -\nu Y(\nu), \quad (3)$$

$$-\sin \varphi_s = \frac{0.7826}{0.4537} = 1.73 = \nu X(\nu) + \gamma t_r \omega. \quad (4)$$

From Fig. 3, we see that:

$$-\nu Y(\nu) = 1.375 \quad \text{when } \nu = 10. \quad (5)$$

We can therefore determine t_r :

$$t_r = \frac{\nu}{\omega} = \frac{10}{0.0625} = 160 \text{ secs.} \quad (6)$$

From Fig. 4, when $\nu = 10$, we have

$$\nu X(\nu) \approx 1.03. \quad (7)$$

From eq. (4) we get:

$$\gamma t_r = \frac{1.73 - 1.03}{0.0625} = 11.2 \text{ secs} \quad (8)$$

and therefore we determine γ

$$\gamma = \frac{11.2}{160} = 0.07. \quad (9)$$

From Fig. 6 for $\gamma = 0.07$ we get:

$$\sigma_1 = 4.4068 \quad (10)$$

and

$$t_r = \frac{4.4068}{160} = 0.0276 \text{ rad/sec.} \quad (11)$$

Figs. 9 and 10 show respectively amplitude and phase of the power transfer function $D(j\omega)$ in the low frequency region as it is expected to be in the case of Sefor.

For $\omega < 3 \cdot 10^{-3} \text{ sec}^{-1}$, $|D(j\omega)|$ tends to the asymptotic value of $0.424 \text{ \$}^{-1}$. From eq. (28) of para 3.2 putting $\omega = 0$, we get

$$\frac{P_0}{nH} \beta = \frac{1}{0.424} = 2.36 \text{ \$}. \quad (12)$$

Since:

$$P_0 = 20 \text{ MW}, \quad (13)$$

$$nH = 500 \text{ m}, \quad (14)$$

$$\beta = 3.395 \cdot 10^{-3}. \quad (15)$$

G can be determined

$$G = \frac{2.36 \cdot 500 \cdot 3.395 \cdot 10^{-3}}{20} \approx 0.2 \text{ Ak} \cdot \text{m/MW}. \quad (16)$$

For $\omega = 0.029 \text{ sec}^{-1}$ (which is not too different from the theoretical value of σ_1/t_r , given by 11), we have:

$$|D_0| = 4.24 \quad \text{(from Fig. 11),} \quad (17)$$

$$|D| = 0.622 \quad \text{(from Fig. 9),} \quad (18)$$

$$\varphi_{D_0} = -55^\circ \quad \text{(from Fig. 12),} \quad (19)$$

$$\varphi_D = +36.8 \quad \text{(from Fig. 10).} \quad (20)$$

Using eq. (28) of para 3.2, we have:

$$\left. \begin{aligned} \frac{\sigma_1}{t_r} &= 0.029 \cdot 1.33 \left\{ \frac{1 - \frac{0.622}{4.24} \frac{0.82}{0.8}}{1 + \frac{0.622}{4.24} \frac{0.57}{0.598}} \right\} \\ &= 0.029 \cdot 1.33 \cdot 0.740 = 0.0286 \text{ (sec}^{-1}\text{)}. \end{aligned} \right\} \quad (21)$$

The value of σ_1/t_r calculated by (21) differs slightly from that given by (11) because the reactivity feedback transfer function is only approximately expressed by one pole [eqs. (22) and (24) of para 3.2].

5. Comparison with the traditional oscillator experiment

With the traditional oscillator experiment only the reactivity signal is introduced in the reactor. The advantages of the "balanced oscillator experiment" in comparison with the traditional one, are mainly the following:

(i) Since the coolant temperatures are constant, it is possible to separate the Doppler temperature effect on reactivity from the other temperature effects. It is a real clean oscillator experiment.

(ii) The normalized transfer function $F_s(j\omega t_r)$ between fuel surface temperature and power is determined by indirect measurements. The direct measurement of $F_s(j\omega t_r)$ would imply the measurement of the fuel surface temperature, which is technically difficult and inaccurate. The measurement of $F_s(j\omega t_r)$ allows to determine the parameters γ and t_r and therefore the fuel conductivity, λ , and the heat transfer coefficient, h , can be calculated.

(iii) The normalized transfer function $F_{av}(j\omega t_r)$ between average fuel temperature and power is determined and therefore the parameter σ_1/t_r can be calculated.

With the traditional type of oscillator experiment the transfer function $F_s(j\omega)$ cannot be determined and therefore γ and t_r cannot be evaluated.

In addition, since the coolant temperatures are not kept constant, the Doppler temperature effect on reactivity is not rigorously separated from the other temperature effects. The calculation of the Doppler power coefficient, G , and of the parameter, σ_1/t_r , from the power transfer function $D(j\omega)$ is therefore more complicated and it is dependent upon the knowledge of the other reactivity coefficients and their associated time constants.

6. Final Comments

The method of introducing in a system two or more sinusoidal signals related in such a way that a specific physical quantity easily measurable does not change, can be considered a very general method to measure transfer functions indirectly. This "balance technique" may have a wide application especially when it is difficult to carry out the direct measurement of a transfer function.

A simple and well known example of "balance technique" is the Wheatstone Bridge to measure electric impedences. In the Wheatstone Bridge the impedences are balanced in modulus and phase in such a way that no current passes through the diagonal. When this condition is fulfilled, the unknown

impedence can be determined by a simple relationship with the other three known impedences.

To end our comments about the application of the "balanced oscillator experiment" on Sefor, we must say that the coolant flow signal may cause a noticeable disturbance in the inlet coolant temperature, Θ_i , through the primary heat exchanger. Since Θ_i must be kept constant during the experiment, it is necessary to balance this effect. This may be obtained by introducing in the system a third signal $\Delta\xi = \Delta\xi_m \sin(\omega t + \delta)$ to the pump of the secondary coolant circuit (Fig. 1). $\Delta\xi_m$ and δ must of course be chosen in such a way that no change occurs in Θ_i .

A better solution could be obtained by putting a by-pass valve across the primary heat exchanger from

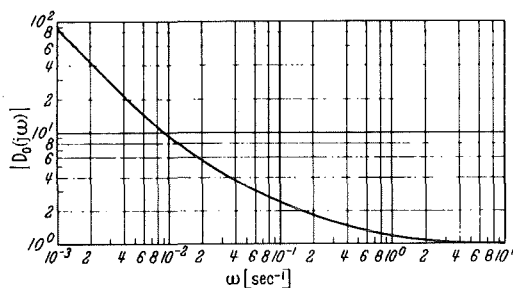


Fig. 11. Frequency response of the zero power transfer function $D_s(j\omega)$ - Amplitude diagram (Sefor)

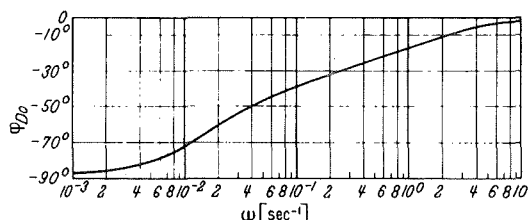


Fig. 12. Frequency response of the zero power transfer function $D_s(j\omega)$ - Phase diagram (Sefor)

the side of the primary coolant circuit (Fig. 1). This valve should of course be operated in such a way that Θ_i remains constant during the experiment.

In the analysis developed in this paper, the thermal capacity of the fuel cladding has been purposely neglected in order to show the essential parts of the new experiment. In the heat transfer coefficient "h" are included the heat transfer coefficients fuel to cladding, internal to external surface of the cladding and cladding to coolant. However, if the thermal capacity of the fuel cladding must be taken into account, the philosophy of the experiment is still valid, but the mathematical relationships will be slightly more complicated.

Appendix I

Demonstration that the coolant temperatures, Θ , remain constant during the experiment [$A\Theta(z; t) = 0$]

The heat balance equation of the coolant in a cooling channel is the following:

$$\frac{2\pi R h}{c} \frac{T_s - \Theta}{\mu/n} = \frac{\partial \Theta}{\partial z} + \frac{1}{v} \frac{\partial \Theta}{\partial t} \quad (1)$$

where:

- R = radius of fuel rod
- h = heat transfer coefficient between fuel and coolant (including the cladding)
- c = specific heat capacity of the coolant
- μ = coolant flow
- T_s = surface fuel temperature
- z = axial coordinate
- v = coolant speed
- t = time
- n = number of cooling channels.

We introduce:

$$T_s = T_{s0} + \Delta T_s, \quad (2)$$

$$\Theta = \Theta_0 + \Delta \Theta, \quad (3)$$

$$\mu = \mu_0 + \Delta \mu \quad (4)$$

where subscript "0" indicates initial steady state conditions and "Δ" variation from steady state condition.

The fuel surface temperature, T_s , may be expressed as function of the coolant temperature, Θ , and of the power, P [according to Ref. 2 para 2 eq. (20)]:

$$\left. \begin{aligned} \Delta T_s^*(s, t_r; z) = G_s(s, t_r) \Delta \Theta^*(s; z) + \\ + \frac{R}{2h} F_s(s, t_r) \frac{\Delta P^*(s)}{V_f} M(z) \end{aligned} \right\} \quad (5)$$

where:

- "*" indicates Laplace transform
- s = complex variable of Laplace transformation

V_f = volume of fuel in reactor = $n\pi R^2 H$ (H being the height of the fuel rod)

$M(z)$ = normalized function expressing power distribution along the axis of a fuel rod

$$\left[\frac{1}{H} \int_0^H M(z) dz = 1 \right]$$

$$\begin{aligned} t_r = \text{radial time scale} &= \frac{\rho_f c_f}{\lambda} R^2 = \\ &= \frac{\text{fuel density} \times \text{specific heat capacity}}{\text{fuel thermal conductivity}} \times \\ &\quad \times (\text{radius})^2 \end{aligned}$$

$G_s(s, t_r)$ = normalized transfer function given in Ref. 2 para 2 eq. (23) [$G_s(0) = 1$]

$F_s(s, t_r)$ = normalized transfer function given in Ref. 2 para 2 eq. (24) [$F_s(0) = 1$].

It is [Ref. 2 para 2 eq. (24)]:

$$G_s(s, t_r) = 1 - \gamma t_r s F_s(s, t_r) \quad (6)$$

where:

$$\gamma = \frac{\lambda}{2hR} = \frac{\text{fuel thermal conductivity}}{2 \times \text{heat transfer coefficient} \times \text{Radius}} \quad (7)$$

Eq. (5) becomes:

$$\left. \begin{aligned} \Delta T_s^*(s, t_r; z) = \Delta \Theta^*(s; z) [1 - \gamma t_r s F_s(s, t_r)] + \\ + \frac{R}{2h} F_s(s, t_r) \frac{M(z)}{V_f} \Delta P^*(s). \end{aligned} \right\} \quad (8)$$

Antitransforming to the time domain, (8) gives:

$$\left. \begin{aligned} \Delta T_s = \Delta \Theta - \gamma t_r \int_0^t \frac{df_s(x)}{dx} \Delta \Theta(z; t-x) dx + \\ + \frac{R \cdot M(z)}{2h V_f} \int_0^t f_s(x) \Delta P(t-x) dx \end{aligned} \right\} \quad (9)$$

where:

$$f_s(t) = L^{-1}[F_s(s, t_r)] \quad (10)$$

and L^{-1} indicates antitransformation.

We shall also remember that, at steady state conditions, it is:

$$\frac{2\pi R h (T_{s0} - \Theta_0)}{c \mu_0 / n} = \frac{\pi R^2 P_0}{c \mu_0 V_f / n} M(z) = \frac{d\Theta_0}{dz} \quad (11)$$

Taking into account (2); (3); (4) and (9), eq. (1) becomes:

$$\left. \begin{aligned} \pi R^2 \frac{P_0 M(z)}{c \mu_0 V_f / n} \left[1 + \frac{1}{P_0} \int_0^t f_s(x) \Delta P(t-x) dx \right. \\ \left. \frac{1 + \frac{\Delta \mu}{\mu_0}}{1 + \frac{\Delta \mu}{\mu_0}} \right] \\ = \frac{d\Theta_0}{dz} + \frac{\partial \Delta \Theta}{\partial z} + \frac{1}{v} \frac{\partial \Delta \Theta}{\partial t} + \\ + \frac{2\pi R h \gamma t_r}{c \mu / n} \int_0^t \frac{df_s(x)}{dx} \Delta \Theta(z; t-x) dx. \end{aligned} \right\} \quad (12)$$

We must demonstrate that the condition

$$\frac{\Delta \mu}{\mu_0} = \frac{1}{P_0} \int_0^t f_s(x) \Delta P(t-x) dx \quad (13)$$

is necessary and sufficient to give $\Delta \Theta(z; t) = 0$.

Eq. (13) is equal to condition (17) of para 2.

In the Laplace domain eq. (13) is equivalent to:

$$\frac{\Delta \mu^*(s)}{\mu_0} = F_s(s, t_r) \frac{\Delta P^*(s)}{P_0} \quad (14)$$

which is equal to condition (16) of para 2.

Condition (13) is necessary because eq. (12) can give $\Delta \Theta = 0$ only if (13) is satisfied.

Taking into account (11) and (13), eq. (12) becomes:

$$\left. \begin{aligned} \frac{\partial \Delta \Theta}{\partial z} + \frac{1}{v} \frac{\partial \Delta \Theta}{\partial t} + \\ + \frac{2\pi R h \gamma t_r}{c \mu / n} \int_0^t \frac{df_s(x)}{dx} \Delta \Theta(z; t-x) dx = 0 \end{aligned} \right\} \quad (15)$$

with the boundary condition

$$\Delta \Theta(0; t) = 0 \quad (16)$$

that is inlet coolant temperature constant.

The solution of (15) is of the type

$$\Delta \Theta = \Delta \Theta(0; t) + \sum_{m=1}^{m=\infty} \frac{1}{m!} \left(\frac{\partial^m \Delta \Theta}{\partial z^m} \right)_{z=0} \cdot z^m \quad (17)$$

where all the $(\partial^m \Delta \Theta / \partial z^m)_{z=0}$ are functions of the time.

If in (15) we put $z = 0$, we get:

$$\left(\frac{\partial \Delta \Theta}{\partial z} \right)_{z=0} = 0. \quad (18)$$

Differentiating (15) in respect to "z" and putting $z = 0$, we get [taking into account (18)]:

$$\left(\frac{\partial^2 \Delta \Theta}{\partial z^2} \right)_{z=0} = 0. \quad (19)$$

By successive differentiations we get for each "m"

$$\left(\frac{\partial^m \Delta \Theta}{\partial z^m} \right)_{z=0} = 0. \quad (20)$$

We can conclude that the solution of eq. (15) with the boundary condition (16) is:

$$\Delta\theta(z; t) = 0. \quad (21)$$

Acknowledgements

The author wishes to thank Prof. HÄFELE for the encouragement and for the useful discussions during the development of this work.

The author thanks also Miss FERRANTI who carried out the necessary calculations on the IBM 7070 computer.

References: [1] HÄFELE, W., K. OTT, L. CALDAROLA, SCHIKARSKI, COHEN, WOLFE, GREEBLER, and REYNOLDS: Static and Dynamic Measurements on the Doppler Effect in an Experimental Power Reactor. Geneva Conference 1964, A/CONF. 28/P/644. — [2] CALDAROLA, L., and SCHLECHTENDAHL: Reactor Temperature Transients with Spatial Variables — First Part: Radial Analysis. KFK 223, May 1964. — [3] COHEN, GREEBLER, HORST, and WOLFE: The Southwest Experimental Fast Oxide Reactor. GE-APED-4281 (June 1963).

Address: L. CALDAROLA
Institut für Angewandte Reaktorphysik
Kernforschungszentrum Karlsruhe
75 Karlsruhe

On Flux Depressions due to Absorber Rods

By **KARL-HEINZ MÜLLER**

Ispra (Italy)*

With 5 Figures in the Text

(Received November 10, 1964)

Summary. The rate of absorption of neutrons in probes, cooling pipes etc., is appreciably greater than in the surroundings. The resulting flux depressions are of great importance but difficult to estimate.

Using the diffusion treatment of neutron migration, an elementary theory is developed to describe the behaviour of the flux in simple arrangements of fuel elements and absorber imbedded in an infinite homogeneous medium. The investigation is divided into three sections:

1. Discrete fuel-rods combined with a single absorber-rod, all rods being assumed to be very slender and the neutrons to be monoenergetic.
2. Two and multigroup calculation for the same geometry.
3. Discrete absorber-rods.

Introduction

Flux measurements often involve the use of Indium probes or other activation detectors which disturb the flux distribution. The same effect is also produced by other heterogeneities, for example cooling-pipes, control rods etc. We consider two cases (Fig. 1) and refer to both, for simplicity, as an absorber.

In the interior and vicinity of the absorber the absorber the diffusion-approximation is not valid. Thus we surround this domain by a control surface Γ . The material of the whole space is assumed to have a constant cross-section Σ_0 and diffusion-coefficient D_0 , but inside Γ the cross-section and diffusion-coefficient have to be corrected by additive terms Σ_1 and D_1 respectively.

The corresponding additive absorption-rate is assumed to be caused by a sink-distribution localized inside Γ .

1. Source, absorber, monoenergetic neutrons

If Γ is a sphere or, in the two dimensional case, a circle, one can use, as a first approximation to a sink distribution, a point-sink at the center $r=r_1$. Its intensity is proportional to $\int_{\Gamma} \partial\Phi/\partial n \cdot ds$. For a one point-source of strength $2\pi S_0 D_0$ at $r=r_0$ and one absorber centered at $r=r_1$, the flux Φ can be described using the diffusion model, by the integrodifferential-equation:

$$\Delta\Phi - \kappa_0^2\Phi = \left. \begin{aligned} & \left(C \int_{\Gamma} \frac{\partial\Phi}{\partial n} ds \right) \times \\ & \times \delta(r-r_1) - 2\pi S_0 \delta(r-r_0), \end{aligned} \right\} \quad (1)$$

* CCR Euratom, TCR.

where C is a constant, denoting the blackness, and $\kappa_0^2 = \Sigma_0/D_0$. For reasons of clarity we confine our argument to the two-dimensional case. The extension to three dimensions will be obvious later.

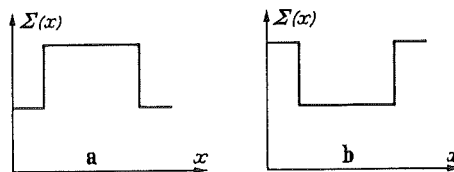


Fig. 1 a and b. Total cross section depending on x . Shape (a) is significant of an absorber and (b) of a duct

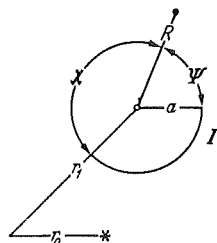


Fig. 2. Control surface Γ surrounds the absorbing domain

Thus, we shall base our argument on the two dimensional form of the above equation, i.e.

$$\left. \begin{aligned} \left(\frac{\partial^2}{\partial x^2} + \frac{\partial^2}{\partial y^2} - \kappa_0^2 \right) \Phi = & \left(C a \int_0^{2\pi} \frac{\partial\Phi}{\partial R} d\Psi \right) \times \\ & \times \delta(r-r_1) - 2\pi S_0 \delta(r-r_0). \end{aligned} \right\} \quad (2)$$

To solve this equation we use a Fourier-transformation:

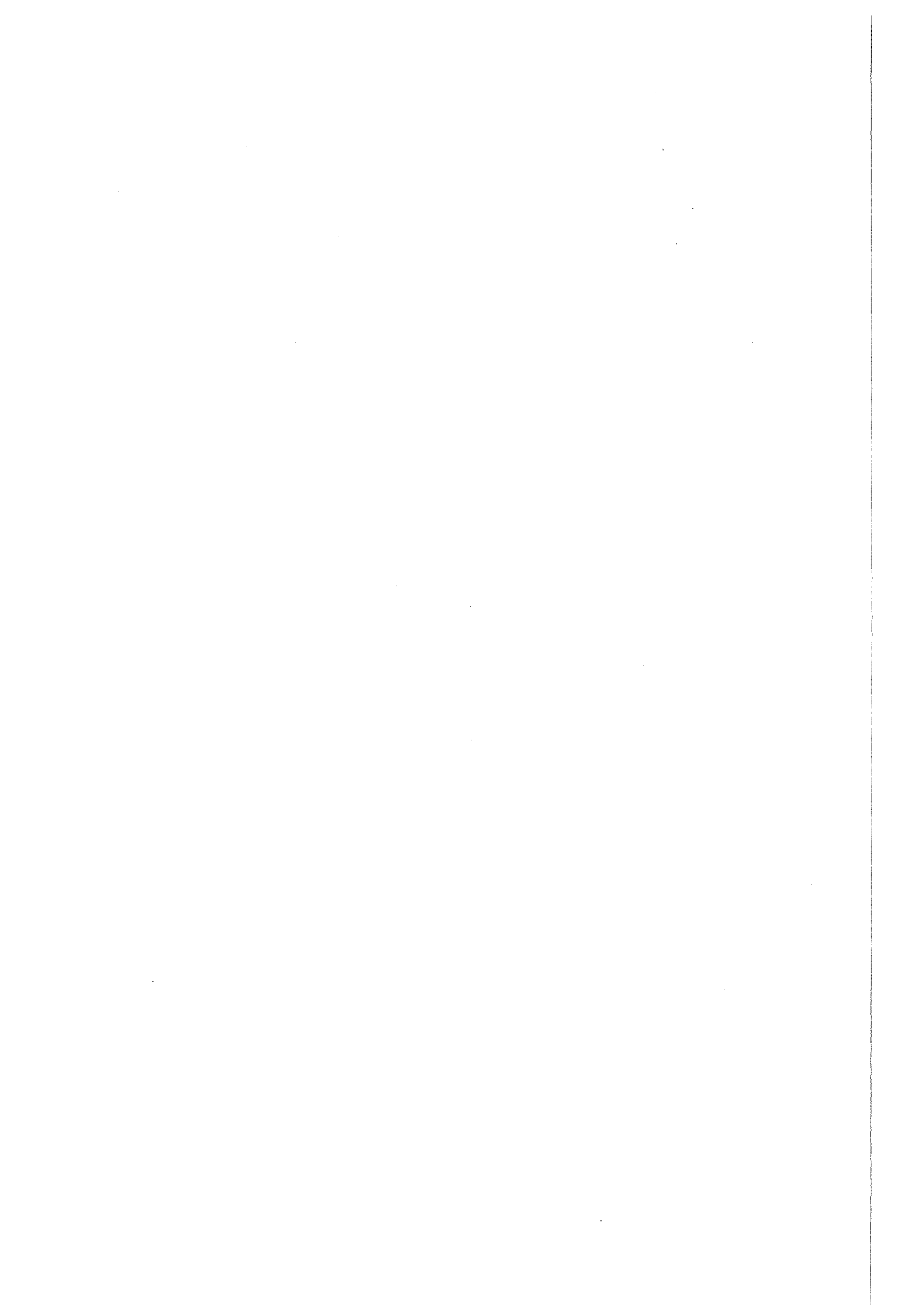
Der folgende Artikel

S.J. Board, L. Caldarola
Fuel Coolant Interaction in Fast Reactors

aus

Symposium on the Thermal and Hydraulic
Aspects of Nuclear Safety,
Vol. 2: Liquid Metal Fast Breeder Reactors,
(1977) pp 195-222

wurde mit freundlicher Genehmigung der
American Society of Mechanical Engineers (ASME)
nachgedruckt



Fuel Coolant Interaction in Fast Reactors

S. J. BOARD

C.E.G.B. Berkeley Nuclear Laboratories
Berkeley, Gloucestershire
Great Britain

and

L. CALDAROLA

Institut für Reaktorentwicklung
Gesellschaft für Kernforschung m.b.H.
Federal Republic of Germany

ABSTRACT

Fuel-coolant interactions are an important problem in fast reactor safety. After a brief historical review, the most significant experiments are described and their results discussed and compared. The experiments range from basic studies with nonreactor materials to in-pile fuel failure tests. In all those involving fast reactor materials, only low efficiency interactions have occurred, apart from the case of sodium injection into fuel.

The main theoretical models are critically reviewed in the light of the experimental evidence. It is now widely believed that there are three main stages in energetic FCIs,

- 1) An initial quiescent period in which the two fluids coarsely intermix (the interpenetration stage), which appears to require some kind of film boiling,
- 2) A small disturbance (trigger) which induces a local interaction,
- 3) A coherent propagation through the interacting masses.

Behind the propagating front, fuel fragmentation occurs, but it is not yet clear which of the three following mechanisms is dominant: pure hydrodynamic fragmentation, blanket collapse, or violent boiling.

It is not yet possible to define completely the conditions under which these stages can occur, and there is not yet enough evidence to be completely confident that this description applies to the injection experiments of sodium into UO_2 .

Some experiments which should be able to resolve the key remaining problems are identified.

INTRODUCTION

We begin by defining the term "Fuel Coolant Interaction" (FCI). Let us suppose that a cold liquid (coolant) comes in contact with molten material (fuel) whose temperature is

well above the boiling point of the coolant. For such a system an FCI is said to occur if heat is transferred from the fuel to the coolant on a time-scale much shorter than that of normal boiling processes, leading to a sudden rise in pressure.

If the time-scale for heat transfer between the two fluids is small compared with that for overall expansion of the fuel-coolant mixture, a significant fraction of the available thermal energy may be converted into mechanical work on the surroundings. In this case, we speak of an energetic FCI or vapor explosion.

Energetic FCIs have been observed in the metal industry [1]; [2], in the paper industry [3] in the liquid natural gas (LNG) industry [4] and in the nuclear industry in "ad hoc" water reactor experiments [5]. A summary of early work is given in [6]. The possibility that an FCI could occur in accident situations in a liquid metal cooled fast breeder reactor (LMFBR) was first examined by Hicks and Menzies [7], who showed that the potential mechanical work could place a significant load on the containment system. In the last decade, considerable scientific effort has been devoted to this topic, particularly to determining whether or not an energetic FCI can occur with fast reactor materials. Since in fast reactors the core is not in its most reactive configuration, low energy FCIs may be also of concern.

Experimental observations have shown that the way in which the molten fuel and the coolant are brought together (mode of contact) is important in that it affects the probability of occurrence of the FCI as well as the mechanical energy yield.

An important characteristic of FCIs is that if frozen fuel debris is recovered, it is observed to be finely fragmented (typically 100 μm radius). While it is possible that this may be merely a consequence of the explosion, it seems more likely that it may be a cause, since a large surface area is necessary for rapid heat transfer rates. We note, however, that fine fragmentation occurs in low efficiency FCIs, showing that it is not a sufficient condition for energetic events. The mechanisms of fragmentation and their relation to energy yield need to be understood.

BRIEF HISTORICAL REVIEW

The early experimental results [8] showed that the interactions for many materials were primarily physical (thermal) rather than chemical and identified conditions under which vapor explosions occurred.

Wright (1965) carried out a series of Al/water experiments in various modes of contact and showed that a necessary condition for production of significant pressures is that the fuel must be molten [9]. This allowed the fine scale intermixing which is necessary for very rapid heat transfer. It was initially assumed that the interaction involved two distinct processes: fuel fragmentation and heat transfer with pressure generation. Many fragmentation mechanisms were suggested, such as coolant entrapment [8] impact fragmentation [10] vapor bubble growth and collapse [11] and others. For UO_2/Na a commonly proposed mechanism was thermal stress fragmentation [12]. Many parametric models were developed in various countries [13], [14], [15], [74]: these models assumed that fragmentation and mixing takes place at a given rate and calculate the pressure transient.

In 1973, Fauske [24] suggested that spontaneous nucleation (SN) of the coolant might play an important role in large scale energetic FCIs. Both this and more recent models put forward by, e.g., Colgate [25], by Board et al., [26] and by Cho et al. [27] suggest that the fragmentation and pressure generation processes are coupled together, so that large scale explosions become self-propagating. While there are significant differences between the various coupled models, they all have as a common basis the concept that

energetic FCIs involve three main stages: first an initial (quiescent) period in which the two fields can come together and may coarsely intermixed; second a disturbance (trigger) which induces a local interaction; and third, a propagating process wherein the interaction spreads rapidly through the interacting masses. Since film boiling plays an important role in establishing the first stage (coarse mixing), a summary on this topic is given in Appendix 1.

The Nuclear Energy Agency of the Organization for Economic Co-operation and Development (OECD/NEA) has sponsored specialist international conferences in 1972 [16], 1973 [17] and 1976 [18]. Fast reactor conferences sponsored by the American Nuclear Society (ANS) in 1974 (Beverly Hill) and in 1976 (Chicago) have also given attention to this subject. Reviews have been carried out periodically by various authors: e.g. Witte et al. in 1970 [6], Teague in 1972 [19], Caldarola in 1974 [20], Fauske in 1975 [21], Buxton and Nelson in 1975 [22] and Benz, Frölich and Unger in 1976 [23], and Board and Hall [51] in 1976.

DESCRIPTION OF SOME BASIC EXPERIMENTS WHICH ARE SIGNIFICANT TO THE PHYSICAL UNDERSTANDING OF FCI PHENOMENA

Three basic modes of contact have been investigated: (1) dropping experiments (small scale and large scale), (2) shock tube experiments, and (3) injection experiments.

Small Scale Dropping Experiments (fuel dropped into coolant)

A large number of experiments have been performed with this mode of contact. Table 1 gives a summary, both for UO_2/Na and other materials.

1) All experiments show a delay time (dwell) between first contact and interaction. In experiments in which the dwell time was investigated, this increased systematically with both fuel temperature and coolant temperature. This, together with the visual evidence of vapor blankets, suggests that stable film boiling inhibits FCI until the fuel cools down to some threshold temperature at which the film becomes unstable and breaks down. This is confirmed by the CEGB experiments [39] in which the vapor blanket was collapsed by an external perturbation.

2) If the bulk of the fuel has solidified when the vapor blanket collapses, no interaction occurs. An important exception is the experiment with molten copper which may be understood in terms of an oxide layer destabilizing film boiling when the copper is still molten.

3) For experiments on tin, temperatures lower than the threshold value of 300°C yielded no fragmentation. This threshold is independent of the water temperature and above the melting point of tin (232°C). The calculated contact temperature is about 255°C and is lower than the homogeneous nucleation temperature of water (300°C). It is, however, not possible to determine that the contact temperature is higher than the spontaneous nucleation temperature because the latter is not well defined (it can in fact take any value between the saturation temperature and the homogeneous nucleation temperature depending upon the contact angle which cannot be known for these conditions). There is some evidence of a maximum interaction pressure at a temperature of 700°C [38].

4) By comparing the results of the UO_2/Na tests with those of the other materials, one might deduce that the conditions for stable film boiling may have been satisfied at least for a short time (30 to 200 msec) in the case of UO_2/Na systems for the particular set of conditions of these experiments.

Table 1
Small scale dropping and injection experiments

Laboratory and Reference	Mode of Contact	Fuel			Coolant			Results				Comments on Results
		Type	Mass (gr)	Temp. Range (°C)	Type	Mass (gr)	Temp. Range (°C)	Dwell Time (msecs.)	Peak Pressure (atm)	Energy (Joule)	Efficiency	
ANL(35)	Drop	UO ₂	25	2900	Na	300	200-600	30-300	45	8	0.1 %	Pressure rise time 30 to 600 μsecs. - 100 gr. of Na ejected by the interaction. Ejected UO ₂ fragments smooth and rounded - Fragments in tank angular.
ANL(35)	Drop	SS	30	1800-2300	Na	300	200-600	3-18	4	1		All SS fragments smooth and rounded. Pressure event before complete submergence.
Culham(36)	Drop	Sn	12	300-900	H ₂ O	3000	0-100	15-200	-	-	-	300 tests. Temperature interaction zone (TIZ) for spontaneous fragmentation limited by a fuel temp. threshold at 300°C and a cool. temp. threshold around 60°C which decreases with increasing fuel temp. Cyclic escalation.
ANL(37)	Drop	Sn	1	200-700	H ₂ O		4-70	-	-	-	-	Fragmentation increases with entrance velocity and decreases with increasing water temp. Fragmentation reaches a maximum at a tin temp. of 500°C. Similar results with bismuth, lead and silver chloride.
MIT(38)	Drop	Sn	1	300-1100	H ₂ O	10 ⁵	22	10-200	0.2	-	-	Results consistent with Culham - Pressure pulses low because of large tank - Single interaction
CEGB(39)	Fuel placed in crucible	Sn	60	600	H ₂ O	1000	40	triggered externally	4	10	0.3 %	Sudden increase in ambient pressure triggers interaction.
UCLA(41)	Drop	Sn	25	340-790	H ₂ O	6·10 ⁴	8-52	-	2	-	-	Multiple interactions - Results consistent with other laboratories - Fuel temp. threshold reduced by temp. stratification in water.
GfK(42)	Drop	Cu	0.5	1000-1800	H ₂ O	50	20	up to 700	20	-	-	Single interaction, only when copper heated in air. Temp. measurements in Cu show oxide layer causes film breakdown when Cu still molten.
Un. Stuttgart(43)	Drop	Pb	up to 100	350-650	H ₂ O		0-60	-	-	-	-	Fragmentation decreases with increasing water temperature and reaches a maximum with lead temp. of 500°C.
ANL(29)	Injection	UO ₂	100	2900	Na	5	400	10-400		40	7 %	Rapid vapour generation prior to explosion. Wide spread of results.
ANL(33)	Injection	NaCl	80	1100	H ₂ O	3	20	100-300		60	14	Vapour layer around water prior to explosion. Energy yields require rapid fragmentation
CEA(Correct!) (28)	Injection	UO ₂	4000	2900	Na	300	300-615		10 in cover gas			Work done in compressing the gas: 100 KJ in a time of about 30 msecs. Time scale too slow for an energetic FCI
Harwell(30,31)	Injection	Fe	54	1600	Na	2	200	50-60		0.1		
Harwell(32,104)	Injection	Sn	300	275-650	H ₂ O	1-2	20	70-150				Dwell time increases with fuel temperature.

5) The energy yields for all materials including UO_2 and Na in this configuration are similarly low.

6) For small masses (~ 1 gm) single interactions were observed, which lead to complete fragmentation. For larger masses (at least with tin), multiple interactions may occur. For UO_2/Na , single drops produced single interactions.

7) The observation that the UO_2 fragments ejected from the tank [35] were smooth and rounded suggests that at least part of the fragmentation took place with UO_2 still in the molten state. The angular and rough-surfaced UO_2 fragments which were found inside the tank indicate that some of the fragmentation took place after the UO_2 had frozen.

Large Scale Dropping Experiments (fuel dropped into coolant)

These experiments involve much larger volumes of materials than those used in the single drop experiments.

Material pairs which have been investigated include aluminum/water, Freon/oil, Freon/water, tin/water, LNG/water, copper/water, steel/water, and UO_2/Na . All the materials except UO_2/Na in this mode have been observed to explode coherently under some circumstances. Considerable progress towards understanding the mechanisms for coherent explosions has been made as a result of some of these studies.

Aluminum/Water

Long's early experiments [8] demonstrated violent explosions of a physical nature could occur between ~ 25 kg aluminum and cold water in a relatively small tank. Explosions occurred only for very specific conditions of drop height, water depth, and temperature, and could be inhibited by changing the properties of the base of the tank by painting. Similar experiments were carried out by Hess [49] who filmed the interaction through perspex windows and later by Briggs [50] with very much better instrumentation. Briggs films show aluminum entering the tank during a relatively long dwell time (~ 1 sec), spreading over the base, and filling the lower half of the tank with a coarse dispersion (~ 1 cm scale) of aluminum and water. The interaction starts usually at the base, and spreads rapidly through the coarse dispersion, the interaction front moving at a velocity ~ 200 m sec^{-1} . Behind the front the coarse dispersion is no longer visible, but it is not clear if this is because fragmentation has occurred, or merely that the aluminum/vapor/liquid interfaces are no longer clearly defined. Pressures up to 400 bars have been recorded in some events, but it is not yet established whether or not the pressure rise at the visible front is sharp, i.e., a shock front. Analysis suggests that the efficiency of the explosions is in the range $\sim 10\%$ of the thermodynamic maximum.

Tin/Water

Early experiments on propagation of explosions [40] used $\sim 1/2$ kg molten tin distributed along a narrow trough, initially in an open tank, and later in a narrow (quasi 2D) vessel. Coherent propagation was observed when the tin and water became intermixed due to a minor local interaction.

In experiments involving up to 2 kg of molten tin distributed along a 1 meter long water filled shock tube [51], the interaction took the form of a single shock wave (~ 50 bar with ~ 100 μs rise time and ~ 10 ms width) which travelled up the tube with a velocity of 100-200 m/sec. The magnitude and nature of the interaction was unaffected by

the use of a detonator instead of spontaneous triggering.

Larger amounts (20 kg) of molten tin have been poured into a water tank in the aluminum/water facility at Winfrith [52]. For tin at 500°C and cold water (when in small scale experiments the dwell times are short) the materials interacted continuously but incoherently. For tin at 800°C and water at 60°C, initial coarse mixing (as in the aluminum tests) was observed and a similar propagating interaction occurred.

Freon Experiments

Large scale pouring experiments using Freon 22 (boiling point -40°C) as the vaporizable coolant, and water or mineral oil as the fuel, were originated at ANL, and have proved particularly informative both in respect of the requirements for initial intermixing and mechanisms for propagation. The first ANL experiments [53] showed, by plotting peak pressure as a function of fuel temperature, that there was a relatively narrow range of fuel temperatures in which vigorous explosions occurred. The lowest limit (threshold) was identified as that which produced an instantaneous contact temperature equal to the homogeneous nucleation temperature of the Freon (54°C). Subsequent Freon/water experiments [54] suggested that the fuel threshold temperature was insensitive to Freon subcooling though Freon/mineral oil experiments [56] show the opposite. Films of the interactions [56] showed that the threshold was associated with a sudden increase in the intermixing (dwell) time. This has subsequently been quantified by Armstrong [55], who showed that the pressure increased linearly with dwell. The results also suggest that the peak pressure increases with increasing drop height (i.e., potential energy for mixing). Measurements of the dwell time as a function of the fuel temperature [51] show that it increases in a manner very similar to that for single drops of tin in water, suggesting that the mechanism for dwell and trigger in the two materials may be similar (i.e., spontaneous breakdown of film boiling), despite large differences in scale and geometry. More recent data [56] indicate that explosions are unaffected by large quantities of gas (20% void fraction) but can be completely inhibited by an increase of the ambient pressure to 2.2 bars absolute.

The propagation stage has been studied using a thin (2D) vessel [51], so that propagation is restricted to one plane. High speed cinephotography with simultaneous pressure measurement within the interaction zone shows that when the interaction occurs, a dark region spreads rapidly throughout the intermixed zone. The region has a well defined front which has been shown to be coincident with the sharp pressure front. The shock front moves at a velocity of ~ 100 m/sec. As in the case of the aluminum water experiments [50], the details of the processes behind the front are obscured.

Steel/Water

A series of experiments at Ispra [57], in which ~ 10 kg molten steel between 1500-1800°C was poured into a large water tank, produced no pressure pulses and no fine fragmentation. On the other hand, a single test with 5 kg steel in a smaller tank [58] produced a very violent interaction, confirming widespread foundry experience of the hazards of this combination. The above results together with difficulties which have been experienced in obtaining explosions with aluminum and water [50], illustrate that it is difficult to determine the true explosive potential of a material pair from experiments in which the initial mixing or triggering conditions are left to chance. Factors such as the shape and size of the vessel, pouring height and rate, and experiment scale can exert controlling influence on the mixing behavior and triggering probability.

UO₂/Na

Large scale experiments with UO₂/Na have been performed at Ispra [59] and Argonne [60]. Similar masses of UO₂ (a few kg) were used in each case. The Argonne experiments were with a pyrotechnic mixture, released into a 20 cm dia sodium pot, (Na to UO₂ volume ratio ~ 20), whereas the Ispra experiments dropped 4 kg UO₂ into a 0.28 m³ tank. Neither Laboratory obtained violent interactions in the range of conditions investigated, though the Argonne experiment showed evidence of incoherent interactions (pressure spikes up to 30 bar occurring 200-700 msec after entry of UO₂ into Na).

Other observations of significance were that in one test, molten UO₂ reached the base of the pot and spread out to the corners before solidifying, and that the vapor generation during UO₂ entry was an order of magnitude lower in a run with hot (600°C) sodium than when the sodium was cooler (300°C). The latter effect was attributed to partial vapor blanketing, or interference between adjacent bubbles in the boiling pool. The Ispra results also showed a number of minor pressure pulses, though of much lower amplitude (~ 1 bar).

While these tests show that coherent interactions did not occur in these conditions, caution is necessary since they did show that UO₂ can interpenetrate and mix with sub-cooled sodium while remaining molten.

Concluding Remarks on the Large Scale Dropping Experiments

The following conclusions can be drawn:

- 1) All experiments in which an energetic interaction occurred show a quiescent intermixing phase (coarse mixing) prior to the explosion. There is some evidence [55] that the pressure produced increases with the dwell time which may be related to the degree of intermixing.
- 2) In these experiments the quiescent intermixing phase was always associated with a vapor film separating the molten fuel from the liquid coolant.
- 3) It seems reasonable to suppose that, similarly to small scale dropping experiments, vapor blanket collapse (either spontaneous or induced) is important in triggering the interaction.
- 4) The Freon/water data show that interactions can occur at a contact temperature below the homogeneous nucleation temperature (54°C) but not necessarily below the spontaneous nucleation temperature, which is not well defined as already pointed out. Visual evidence [54] suggests that the threshold is associated with the onset of film boiling (see point 2 above), which could be due to spontaneous nucleation of the Freon.
- 5) Propagation velocities were of the order of 100 m/sec, which is lower than the speed of sound in the liquid (1000 m/sec), but probably (and in one case [51] certainly) higher than the speed of sound in the interaction region where vapor is present. For this reason the presence of vapor may be important in allowing supersonic propagation at relatively low velocities.
- 7) The experimental results give no definite information about the mechanism of fragmentation and energy transfer behind the propagating front.
- 8) In all UO₂/Na dropping tests no energetic FCI occurred, although there is evidence of incoherent interactions. However, it is not yet clear whether this was due to specific properties of the materials preventing propagation (such as contact temperature lower than spontaneous nucleation temperature) or because a suitable configuration for coherence was not obtained. The fuel to coolant volume ratio in these experiments was

1 : 20. In the Al/water experiments [50] this ratio has to be decreased from 1 : 30 to 1 : 5 before a coherent FCI could be obtained.

9) The observation that an increase to 2.2 bars in the ambient pressure inhibits explosions in Freon systems is not well understood.

Henry [56] suggests this is due to the fact that bubble growth is thermally limited early in life at elevated pressures, though the change in pressure is in fact rather small. The sensitivity of spontaneously triggered interactions to small changes in initial conditions has already been demonstrated (e.g., [50]). The results might simply be explained by the absence of a sufficiently energetic trigger in these particular experiments.

“Shock Tube” Experiments

Experimental Results

Another method of bringing two liquids into contact was developed by Wright [9] who used a strong vertical tube in which a water column was impacted onto molten aluminum. The simple ID geometry allows straightforward determination of the pressure within the interaction zone. Wright observed typical pressures ~ 200 bar lasting for ~ 1 ms. Similar experiments at Foulness [61] showed that the column may bounce several times, and that the maximum pressure often occurs on a bounce after the first. The measurement of pressures up to 600 bars confirmed that super-critical pressures can be produced in FCIs. Efficiencies, determined from the kinetic energy (KE) of the column after impact, were $\sim 10\%$ of the maximum thermodynamic. A transparent shock tube developed at Windscale [62] with molten salt and water showed that in a long series of bounces, each impact engulfed molten salt to a depth ~ 1 tube diameter. Further experiments without viewing facilities showed evidence of vigorous FCIs with molten tin/water for tin temperature $> 300^\circ\text{C}$ (with peak pressure of the order of 100 bars always on the first bounce) and also for molten Bi_2O_3 /water at 900°C (150 bars). The one Bi_2O_3 test with a lower temperature (500°C) apparently produced fragmentation but no pressure pulse.

At Ispra [63] a UO_2/Na shock tube has been developed: the high pressures characteristic of most other shock tube experiments are not apparently observed in this system.

Experiments in Grenoble in the apparatus Correct 2 differ from normal shock tube experiments in that the coolant enters the interaction chamber through a side arm over a period of 0.5 secs. The one published result [65] shows a pressure pulse of ~ 72 bars which the authors attribute to water hammer effect. The sodium is expelled at a velocity very similar to its initial (downward) velocity, and most of the thermal energy remains in the UO_2 .

Concluding Remarks on Shock Tube Experiments

Following conclusions can be drawn:

1) Results of Al/water and Tin/water experiments seem to be consistent with those of the large scale dropping experiments. However it is not understood why the largest interaction occurred at the second bounce in the Al/water case but at the first bounce in the Tin/water case.

2) Energetic FCIs were also obtained with Bi_2O_3 and water. This shows that energetic interactions with a fuel having a lower conductivity than that of the coolant are possible (see also injection experiments). In this experiment the interface temperature was higher than the homogeneous nucleation temperature of the coolant.

3) There is no evidence of violent interaction with Na/ UO_2 , though it appears that a true shock tube impact has not yet been obtained with these materials.

4) As a general comment, it must be said that despite the significant amount of quantitative data, no serious analysis has been carried out, and neither has there been a systematic study of the effects of the major variables.

Injection Experiments (coolant injected into fuel)

Experimental results are summarized in Table 1. The following observations can be made:

1) Energetic FCIs have resulted from the injection of small quantities of Na into UO_2 . Similar interactions have been obtained for water injected into molten salt.

2) A common feature of both these experiments is the existence of a dwell time which in the case of UO_2/Na systems may be as long as few hundred milli-seconds. During this dwell time violent boiling accompanied by the production of copious quantities of Na vapor was observed [29]. This, together with the visual analysis of the salt H_2O experiments [33], might suggest that even in the case of UO_2/Na , vapor generation inhibits the interaction initially, allowing the possibility of coarse intermixing during the dwell, thus setting up the conditions for a coherent vapor explosion. In fact, if it is assumed that the small Na droplets rapidly reach the saturation temperature, the occurrence of some kind of film boiling cannot be excluded.

3) Analysis of the water/salt experiments [33] suggests that the energy yield is greater than the thermal energy that could be conducted into the water during the dwell time. The author concludes that rapid fragmentation must have occurred in a timescale less than $70 \mu\text{secs}$. This interpretation is consistent with the interpretation of FCIs under other modes of contact. It seems plausible that the Na/ UO_2 results can be explained on the same basis. However, a special explanation for the Na/ UO_2 experiments, based on heating a drop to the S.N. temperature by conduction without fragmentation, has been put forward by Fauske [34] (see section on Superheated Drop Model). In support of this, data on Freon II globules in hot water [34] and pentane/silicone oil [78] has been quoted. However, these systems from the UO_2/Na system because, e.g., the UO_2 surface will solidify and crack, thus increasing the likelihood of nucleation with little superheat.

4) Injection of water into molten tin at Harwell (104) produced explosions over the temperature range $300\text{-}500^\circ\text{C}$. It was found that the dwell time increased systematically with fuel temperature, as in dropping experiments. This may also suggest that FCIs in the injection mode of contact may be similar in nature to those in other contact modes.

5) Interactions with Na injected into stainless steel [30,31] were much less energetic than those with UO_2 and Na, possibly because of the lower fuel temperature (1800°C). Since this temperature is below the homogeneous nucleation temperature and the contact temperature very probably below the spontaneous nucleation temperature of Na, the results of these experiments cannot be explained in terms of spontaneous nucleation. Results have not been analyzed in detail so that the nature of the event is not yet clear.

6) The larger scale injection experiments (Correct 1) [28] produced rapid Na vaporization and pressurization of the gas volume. The mechanical work done was very large (100 KJ), but the pressure risetime was relatively long ($\geq 30 \text{ msec}$) suggesting that much of the work could have been due to rapid boiling rather than to an energetic FCI. Reaction forces on the crucible were relatively low (corresponding to a pressure of $\sim 10 \text{ bars}$).

SIMULATION EXPERIMENTS

Out-of-pile Experiments

Experiments at GfK Karlsruhe [85]

To simulate transient overpower (TOP) incidents, experiments have been performed in a sodium loop using electrically heated UO_2 fuel pins. A single pin or a seven-pin bundle is heated from steady-state operation in a power transient of 300 to 400 ms duration so that up to 50 g of molten UO_2 penetrate into the cooling channel. Na temperature was set at 520°C . The following results have been obtained from 12 tests with 1 pin and 6 tests with 7 pins.

- 1) Immediately after pin failure a number of narrow pressure pulses occur having half widths of about 0.1 – 0.2 ms.
- 2) The overpressure of the fuel pin filling gas influences the amplitude of the pressure pulses. At some 2 to 3 bars the pressure peak attain a maximum of about 70 bars. At 32 bars filling gas pressure no pressure pulses of this kind could be detected.
- 3) The number of pressure pulses (but not their amplitude) increase with the mass of ejected fuel.
- 4) The mechanical work on the coolant during FCI is very small. Values of the order of 0.05 Joule/g of ejected molten fuel (in addition to the expansion work of the filling gas) have been calculated from the experimental results.
- 5) Experiments performed with 7-pin bundles reveal the generation of a partial cooling channel blockage (90%).
- 6) Sodium velocity seems to have no effect on the mechanical work done during the interaction (velocity range 1 – 7.5 msec^{-1}).

JEF Experiments at Grenoble [86]

These experiments simulate a slow power excursion. Small quantities of UO_2 (7.2 g) are heated by means of the Joule effect. The fuel is in the form of a pin and is separated from the static Na by means of a thermal insulator and cladding. Fourteen tests have been carried out at Na temperatures ranging from 355°C to 765°C . All interactions were incoherent and not energetic. The maximum peak pressure measured was about 5 bars at a Na temperature of 720°C . The mechanical work reached a maximum of 12.5 Joule at this temperature. Fragmented mass of UO_2 never exceeded 50% of the total mass. A considerable part of the debris had the size of 1 – 2 μ .

CNEN Experiments [87]

These experiments are similar to the JEF experiments and have given similar results.

In-pile Experiments

RCN Petten LOC Experiments [88]

Loss of cooling experiments have been performed with fresh pins, prepressurized pins and irradiated pins. Fuel ejection was preceded by sodium expulsion, so that no direct fuel-coolant contact occurred. Fuel coolant interactions only occurred in experiments in which the power was sustained for many seconds after pin failure and were due to molten fuel dropping down to the bottom of the capsule where liquid sodium was still present.

Two pressure pulses were attributed to FCI, one of 12 bars (LOC 5), and the other of 90 bars (LOC 13), recorded in the gas space above the capsule. In the case of prepressurized or irradiated pins, large pressure pulses (~ 160 bars) were attributed to release of gas from the pins rather than to an FCI.

TREAT Tests

TREAT tests have given a great deal of very valuable information about fuel and coolant behavior in single and seven pin bundles subjected to slow transient overpower (TOP) and loss of flow (LOF) conditions. A complete critical review of all the TREAT tests goes beyond the scope of this paper but is included elsewhere in this volume. We shall limit ourselves to some specific points of particular relevance to FCI. In the case of the LOF tests (L and R series) no FCI occurred because the sodium was expelled before the fuel melted and there was no reentry while the fuel was molten [e.g., 98].

In the TOP tests E and H series, rapid Na voiding has been observed which has been attributed to fuel vapor in the case of severe transients, to gas release in the case of irradiated pins and to mild FCIs in the case of fresh fuel subjected to mild transients. For example, in the single fresh fuel pin tests H2 and E4 the rapid voiding has been attributed to FCIs of yield 10 and 50 Joules respectively [90]. In the severe TOP tests of the S series large pressure pulses (up to 200 bars) were measured, some of them occurred a significant time (0.2 to 2.4 secs.) after pin failure [91]. In test S5 with five evacuated pins, a pressure pulse of 93 bars was recorded (compared with a fuel vapor pressure of 33 bars) with an energy yield of 102 Joules. Delayed FCIs in S5 and S6 (~ 200 bars) were potentially much more energetic (1 KJ). As in all TREAT tests, the amount of fuel interacting with Na was not known so that the efficiencies of the FCIs cannot be determined. Since the interacting mass is possibly only a small fraction of the total fuel mass (~ 200 g) and the energy yields are significant (approximately 100 J), it seems possible that the local conversion efficiency could have been quite high. On the other hand, if the energy yield is compared with the total thermal energy in the pins, the overall conversion ratio is $< 0.2\%$. Extrapolating this number to a subassembly or whole core scale, however, is valid only if one can demonstrate (1) that the fraction of reacting fuel is similar and (2) that the physical nature of the interaction is not affected by the increasing scale.

Prompt Burst Excursion (PBE) Tests [89]

The power transient in these tests is much faster than that of TREAT (initial period 1.4 msec compared with 23 msec for TREAT). Nine experiments have been performed with single fresh fuel pins. The first three were conducted without sodium coolant. The energy depositions in all tests ranged up to 3200 Joule/g of fuel. In all tests large upward axial fuel motions within the cladding were observed. In the dry experiments the pressure pulses were low and the energy conversion ratios were negligible.

In contrast, the experiments with sodium showed large sharp pressure pulses (up to 600 atm), but the overall energy conversion ratios were very low ($2.1 \cdot 10^{-4}$).

It is not yet clear if a FCI occurred. A preliminary analysis shows that results are consistent with those of the ANL S-11 Treat Experiment, in which it has been suggested that fuel vapor pressure is the most likely candidate for the working fluid.

Concluding Remarks on Simulation Experiments

The tests to date have produced no efficient conversion of the total fuel thermal energy into mechanical work. They have demonstrated that FCIs can occur in some

reactor conditions but there is no tendency towards coherence in multi-pin tests. However, caution is necessary for the following reasons:

- 1) The number of pins in the tests (a maximum of 7) is so small compared to the number in a subassembly (200-300) and in reactor core ($\sim 2 \cdot 10^5$) that it is difficult to be confident about extrapolation with the present state of knowledge on the physics of FCI.
- 2) The incoherence of the pin failures in the tests (7 pins in 10 msec.) is not representative of what might be expected in the later stages of a TOP or in a prompt critical burst.
- 3) The reactivity consequences of the observed FCIs (coolant and fuel movements) require careful evaluation.

THEORETICAL

Parametric Models

Parametric models to calculate pressure transients due to FCI have been developed in various countries and the main features are summarized in [15] and [18]. All the models are characterized by a phase "A" in which the sodium remains liquid and a phase "B" in which vaporization takes place. In these models the process of fuel fragmentation and mixing is represented by an externally specified fragmentation and mixing time constant. This allows a simple analysis of the effect of the various parameters on the pressure transient. It is important, however, to point out that the results obtainable by means of these codes have a meaning only if the values of the input parameters can be justified on the basis of sound physical considerations. The use, for instance, of fragmentation and mixing time constants obtained from pressure measurements in experiments in which a significant interaction did not occur may be dangerous unless (1) the physical phenomena of fragmentation and mixing which occurred during the experiments are well understood and (2) one can demonstrate that only similar phenomena will occur in the reactor in the conditions under consideration. An extensive parametric study was carried out by Caldarola [66]. The main results are the following:

- 1) Total mechanical work strongly decreases with increasing fragmentation and mixing time constant, and increases in time constants for initial length of the sodium piston.
- 2) Vapor blanketing during the vaporization phase reduces yields only when the fragmentation and mixing is relatively slow.
- 3) Time to empty a 120 cm long channel is 15-20 msec for values of the fragmentation and/or mixing of the order of 5-10 msec.
- 4) Effects due to particle size distribution and gas content are important only for a rapid fragmentation and mixing process. However, it must be pointed out that only the cushion effect due to the compressibility of the gas was taken into account in the model. For this reason this last conclusion (as far as the gas content is concerned) has a limited value because the gas content might effect the FCI in other ways.

Incoherent Fragmentation Mechanisms

From the above parametric calculations it has been shown that the necessary conditions for an energetic vapor explosion are rapid, coherent fragmentation and mixing (with a suitable mixture ratio) and significant constraint. Therefore, the experimental observation that fine fragmentation arises in incoherent interactions of low efficiency does not necessarily imply that the fragmentation process is different from that of a coherent FCI. However, some of the proposed fragmentation mechanisms apply only to incoherent

interactions because they do not envisage any mechanism for coupling between adjacent regions.

A recent review by Cronenberg [67] considered hydrodynamic (impact) fragmentation, violent gas release, pressure forces in the coolant, and thermal stress fragmentation as possible explanations of the observed behavior of UO_2 and sodium. Cronenberg assumed that the energy required to produce the fragmentation was determined by the surface tension. We note, however, that recent calculations by Cho and Fauske [27] show that the dominant energy requirement for intermixing comes from the liquid drag forces, rather than surface tension of the fuel.

Estimates of the energy available from the various proposed mechanisms show that (1) hydrodynamic fragmentation due to the relative motion of the fuel and coolant is unable to account for the observed fragmentation unless very high relative velocities are produced by some other process, (2) the potential energy from violent gas release from pure UO_2 (solubility $\sim 10^{-6}$ moles/mole) is extremely small in comparison with that from vapor production, and (3) for thermal stress fragmentation, the maximum energy which can be stored in the drop is limited by the ultimate tensile stress. In the case of UO_2 , this value would be of the order 10^{-2} to 10^{-1} Joule/cm³. This energy would be sufficient to produce UO_2 fragmentation but it is not sufficient to produce significant rapid intermixing. Unless there is a significant energy storage, the fragmentation rate will be determined by the rate of growth of the solid crust (0.2 sec to build a 0.7 mm thick crust). Fragmentation at such a low rate cannot explain the pressure pulses and energy yields observed in the experiments.

Another proposed source of fragmentation and intermixing is vapor bubble growth and collapse. The potential energy at 1 bar is $\sim (1/10)$ J per cc of vapor. There is some direct evidence for this process, for instance, for the case of tin dropped into water [39, 83, 84, 38]. For Na coolant, the experiments of Farahat [69] in which a hot sphere made of tantalum was cooled in a pool of liquid sodium showed that bubble growth and collapse in transition boiling may be very energetic. Large vapor bubbles were formed, expelling sodium from the vessel, and producing pressure pulses reaching a maximum of 5 bars at a Na temperature of 750°C. This maximum can be understood because bubble volume increases with coolant temperature while the pressure difference to collapse the bubble decreases. Thus the energy of bubble collapse will have a maximum which was calculated by Caldarola and Kastenberg for the UO_2/Na case [68] to be at a Na temperature of about 770°C. We note that in the French JEF experiments [86] a maximum of mechanical yield was obtained at a Na temperature of 730°C. The fraction of the bubble energy which could produce intermixing cannot be predicted with confidence, because it depends on departure from radial symmetry: the simplest assumption of a single jet, based on Plesset's calculation [70] has been used, for instance by Buchanan [71] and later by Bankhoff [72], to show that the impact forces are likely to be sufficient to rupture a frozen shell of UO_2 , and by Caldarola and Kastenberg [68], who show that the fraction of the energy transmitted to the fuel as a compression wave from jet impact is small and therefore jet penetration is necessary [73]. Experimental evidence of bubble collapse suggests that only a small fraction of the energy is radiated away as a pressure pulse, so that a large fraction of the bubble energy remains localized and thus available for intermixing.

The hypothesis of vapor collapse fragmentation has the advantage over other theories (such as thermal stress fragmentation) of potentially being able to account for both the fragmentation and pressure pulses for all incoherent FCIs that occur in subcooled liquid, independently of the materials involved. It may also be relevant for coherent explosions,

even in saturated liquid, since the increase in pressure from a local interaction may cause the collapse of adjacent vapor regions.

A further development of the bubble growth and collapse model is the cyclic fragmentation model developed in turn by Board [39], Buchanan [81] and Caldarola, Todreas and Vaughan [82]. Rapid mixing due to jet penetration occurs within the fuel, and the coolant is vaporized producing another bubble. Provided sufficient hot fuel is available to vaporize enough of the coolant, successive bubbles will grow to increasingly larger radii and hence produce successively greater pressures on collapse.

The existence of a cyclic process is supported by the films of tin/water experiments of Board [39], Dulleforce [83], Bjornand [84], and Bjorkquist [38]. These all show a cyclic interaction increasing in time.

Propagating FCI Models

Theoretical modelling of large scale explosions has only been attempted since 1973. It is generally accepted that the coherence for efficient large scale FCI implies the existence of a propagation mechanism which couples the regions of explosive energy release to the adjacent unexploded regions. Explosive expansion of the coolant, due to rapid heat transfer from the fuel, produces pressures or motions of the liquids which lead to rapid heat transfer in adjacent regions. The various models differ in the initial geometry and in the mechanisms of rapid (coherent) fragmentation for producing the heat transfer.

Colgate's Explosive Self-Mixing Model [25]

Colgate (1973) suggested that local fine mixing between semi-infinite regions of fuel and coolant, on a short timescale, would release energy, which would then cause further fine mixing. Kelvin Helmholtz and Taylor instabilities of the accelerated interface would lead to turbulent mixing over a definite volume, in a manner analogous to the cratering produced by an explosive charge in the sea bed. If the volume of material intermixing is greater than the original volume releasing energy, then the explosion will escalate. Colgate somewhat overestimated the mechanical energy released by equating it to the thermal energy in the steam, and determined the likely volume of intermixing from empirical data on high explosive craters.

The mixing scale was assumed to be determined by the minimum eddy size for turbulent mixing at a liquid/liquid interface, which for the maximum liquid velocities (liquid KE = explosive energy release) was determined to be $\sim 10^{-5}$ cm for most liquids, though for molten lava, the high viscosity increased this to ~ 1 cm. For this case, Colgate suggested that thermal stresses might be responsible for the initial fracture of the material, the explosion shear stress then being sufficient to rapidly mix the already solid particles with the coolant.

The Detonation Model

Taking Colgate's concept that the explosive expansion produced its own mixing, Board, Hall and Hall [26] developed a treatment of the explosion dynamics for the simplest case of a steadily propagating one dimensional interaction. Three stages are postulated in the model. For the first stage it is assumed that fuel and coolant become coarsely intermixed (1st stage). Then an unidentified trigger mechanism is assumed to result in a shock wave (2nd stage). The model then shows that the shock wave travelling through the coarse mixture (3rd stage) causes fine fuel fragmentation and mixing, which

in its turn produces the rapid heat transfer necessary for sustaining the wave. In reference [26] it is shown that if energy transfer is completed close behind the front mechanical energy yields close to the thermodynamic maximum will be obtained. In a later paper [77], it is shown that in some circumstances detonation can also occur with partial energy transfer and therefore lower efficiency. Experimental results [51] support this model as far as the existence of the above three stages. Other experimental results [50] show clearly the existence of the propagating front and of the pressure pulse but have not yet shown whether or not it is a shock front. It must be pointed out that in all experiments coarse mixing was possible because of stable film boiling. The experiments give no definite information about the mechanism of fragmentation and energy transfer behind the propagating front. In the model [26] fine fuel fragmentation is caused by the slip behind the shock due to the different densities of the two media (hydrodynamic fragmentation). The fuel fragmentation mechanism behind the shock front is at present a matter of debate among the various specialists in the field. A discussion on hydrodynamic fragmentation is given in Appendix 2 where it is shown that recent experimental data confirm that this mechanism is likely to be effective in moderate or strong shocks. It is important to point out that three mechanisms are possible: (1) purely hydrodynamic fragmentation (such as Taylor instabilities, boundary layer stripping etc. — Board and Hall), (2) explosive boiling and (3) vapor collapse. Which mechanism is the dominant one is still an unresolved problem.

Spontaneous nucleation models

Superheated Drop Model

In 1973, Fauske [34] proposed an explanation of the Armstrong injection experiments [29], which can be stated as follows. Upon mixing of liquid sodium with molten UO_2 , some sodium will be entrained and wets the UO_2 surface. Because of the postulated lack of nucleation sites, its temperature will be raised to the limit corresponding to spontaneous nucleation. When this is reached, vaporization is rapid enough to produce shock waves. However, the assumption of a lack of nucleation sites is in marked contrast with the experimental observation of violent boiling and the ejection of UO_2 and sodium droplets prior to the explosion as reported in [29]. Results in Freon/water systems [34] demonstrate superheat explosions but do not appear to show violent boiling during the dwell.

Conditions for Explosive Boiling

Later, [24] Fauske suggested that spontaneous nucleation may also play an important role in large scale energetic FCIs. He proposed [78] that local liquid/liquid contacts above the spontaneous nucleation temperature would lead to explosive boiling which would produce further contacts, thus escalating the interaction. The following requirements must be satisfied:

- 1) Direct liquid/liquid contact is required, implying a breakdown in the vapor layer between the two fluids.
- 2) Explosive boiling immediately upon contact, implying that the interfacial temperature must exceed the spontaneous nucleation temperature. This process results in fragmentation and mixing of both the hot and cold fluid without time delay.
- 3) For the above processes to escalate on a time scale required for a large mass explosion, proper constraint is also required.

In this theory the interfacial temperature is understood to be equal to the instantaneous

contact temperature " T_c " characteristic of the system upon initial contact.

$T_c = \theta + (T - \theta)/(1 + \beta)$ where $\beta = \sqrt{(k\rho c)_{cool.}/(k\rho c)_{fuel}}$, T and θ represent respectively fuel and coolant temperatures and k , ρ , and c represent respectively thermal conductivity, density and specific heat. The main consequence of this model is that energetic FCIs cannot occur with UO_2/Na systems because condition 2 is not satisfied.

Fauske quotes as evidence the fuel temperature threshold observed in Freon/water and Freon/oil experiments [53], [56]. However, visual evidence [54] seems to suggest that this threshold is associated with film boiling allowing interpenetration (coarse mixing). It is not possible to determine in a definite way from these experiments if spontaneous nucleation is important to the fragmentation process. Experiments with metals and water also suffer from this difficulty [50].

It seems likely that some type of vigorous boiling may be important as a fragmentation mechanism. However, it is not yet clear whether or not spontaneous nucleation is necessary for this violent boiling. It also seems possible that the high value of β for UO_2/Na (~ 2) compared with the low value for metal water (~ 0.1) could lead to differences in the fragmentation behavior (due to violent boiling) without these being necessarily associated with spontaneous nucleation.

The Capture Model

Subsequently Henry and Fauske [79] developed their ideas into a more defined model evaluated in Appendix 3.

The Splash Model

Ochiai and Bankoff [80] assume that the random local contacts which occur in film boiling above the spontaneous nucleation temperature lead immediately to the growth of a large number of bubbles which coalesce into a high pressure vapor film. It is assumed that this film remains at a pressure corresponding to the saturation pressure at the spontaneous nucleation temperature until the return of a rarefaction wave from the nearest free surface. The impulse provided by this pressure is transmitted to the fuel, where it produces an annular splash around the initial contacting tongue of coolant. The splash is assumed to promote further liquid/liquid contact provided that the splash velocity is above an empirically determined threshold.

Certain aspects of this model are somewhat speculative. It is known, for instance, that rapidly propagating film breakdown can occur well below the spontaneous nucleation temperature on solid surfaces, where splashing is unlikely to enhance the contact [74]. Nevertheless the model is the first quantitative description of propagating film breakdown, a process whose occurrence is well established.

In general, the role of spontaneous nucleation in vapor explosions is clearly not completely understood. It seems more plausible that spontaneous nucleation should lead to rapid vapor production (as assumed here) than to the suppression of vapor growth with enhanced heat fluxes (as assumed in the capture model in Appendix 3), but neither model provides a sound theoretical basis for a spontaneous nucleation criterion. This criterion must be regarded, therefore, as largely empirical.

CONCLUSION

Present State of Knowledge of FCI and Identification of Unresolved Problems

1) In all the experiments to date in which fast reactor materials have been brought into contact with sodium, only low energy interactions were observed except in the case

in which sodium was injected into fuel. The basic experiments cover a very large range of conditions and modes of contact. In-pile and out-of-pile tests have covered a large spectrum of realistic situations during hypothetical reactor accidents. In some of these experiments, rapid sodium voiding due to mild FCIs has been observed.

2) The out-of-pile experimental evidence on large scale systems suggests that energetic FCIs involve the coherent interaction of the two fluids. Three successive stages can be identified, namely, (1) coarse intermixing between the two fluids producing a suitable dense dispersion, (2) triggering of the explosion and (3) coherent propagation.

3) In all large scale explosive experiments to date, the coarse mixing occurred during a period in which some kind of film boiling separated the two fluids. Energetic FCIs only occur when the film boiling occurs for a length of time (dwell time) sufficient to allow a significant coarse mixing between the two fluids.

4) A number of mechanisms to trigger the explosion are conceivable. A common requirement for all is that they must be able to produce local contact (e.g., by collapsing the vapor blanket).

5) Visual evidence suggests that energetic explosions propagate through the coarse mixture at high velocities (~ 100 m/sec). Ahead of the propagating front the material appears unfragmented.

6) It seems plausible to postulate that the propagating front and the pressure wave are coincident, though this has been demonstrated in only one experiment. In other experiments, it was not possible to demonstrate whether or not this coincidence existed.

7) As a consequence of the last point, it is probable that the propagating front is a shock wave which collapses the vapor blankets, producing fragmentation and heat transfer sufficiently rapidly that the shock is self-sustaining. However, at this stage, the possibility cannot be excluded that the propagating front is a small pressure wave which triggers the interaction (e.g., collapsing the blankets) followed by fragmentation and heat transfer at a relatively slow rate. The pressure would then increase relatively slowly behind the front (i.e., no shock front). Since pressure waves in two-phase mixtures attenuate rapidly, it seems likely that trigger waves would also need to be self-sustaining.

8) If the propagating front is a shock wave, two possibilities exist: either (1) heat transfer is completed close behind the front (complete detonation) or (2) heat transfer is not completed close behind the front (partial detonation), giving lower energy yield. Experimental evidence (efficiency less than 30% of maximum thermodynamic) seems to suggest the latter.

9) Fragmentation mechanisms behind the front are undetermined and are a matter of debate. The three conceivable candidates are: (1) vapor collapse, (2) violent boiling and (3) pure hydrodynamic breakup. Hydrodynamic fragmentation is likely to be effective only in large scale explosions with materials of different densities. Violent boiling may be either violent heterogeneous boiling following the wetting of the surface or the explosive boiling due to spontaneous nucleation postulated by Fauske. Explosion results to date seem to indicate that vapor collapse and/or violent boiling may be faster than pure hydrodynamic fragmentation. In the case of Freon/oil pure hydrodynamic fragmentation between the two liquids in the absence of vapor is highly unlikely because the two fluids have similar densities.

10) A temperature threshold for FCIs, both energetic (e.g., freon/oil) and low energy (e.g., fragmentation of tin in water) has been observed. In some cases, this is rather steep and appears to occur when the interface temperature is equal to the spontaneous nucleation temperature of the coolant (Fauske), though this cannot always be proved or disapproved, first because the interface temperature is difficult to determine and second

because the spontaneous nucleation temperature is not well defined. There is some evidence that this threshold is associated with the limit of stable film boiling. It also seems possible that it may be associated with the onset of violent boiling which would either cause rapid fragmentation or act as an energetic trigger for a self-sustaining shock wave. The behavior of UO_2 and Na (contact temperature below spontaneous nucleation temperature) is rather problematic. In fact, low energy FCIs in small scale UO_2 /Na dropping experiments have been observed and results are similar to those of systems whose contact temperature is above the spontaneous nucleation temperature. However, energetic FCIs with UO_2 and Na have not been observed in large scale dropping experiments to date.

11) The main reason why FCIs may be nonenergetic, or incoherent, in small scale fuel into coolant experiments is probably that the expansion time scale is comparable with that of the heat transfer. Both this and the observed incoherence may be expected if coarse intermixing conditions are not obtained. The fragmentation and energy transfer processes in these experiments may be similar to those operating in coherent explosions, e.g., vapor collapse and/or violent boiling. Pure hydrodynamic fragmentation is unlikely to be important in the small scale events. Thermal stress fragmentation is unlikely to be the dominant cause of fine intermixing in FCIs in UO_2 /Na systems. The details of the fragmentation and energy transfer process are not yet clear.

12) In large scale dropping experiments with UO_2 /Na there are five possible reasons why energetic FCIs do not occur.

a) The period of stable film boiling (dwell time) was too short to allow interpenetration (coarse mixing).

b) The period was too long, allowing the UO_2 to freeze.

c) The geometrical constraint was not such as to produce a suitably dense dispersion.

d) The trigger was not sufficiently energetic to trigger the interaction.

e) Propagation is not possible with these materials.

The second reason seems very unlikely since the dwell time observed was ~ 200 ms, which is too short for development of a significant crust. This leads us to the conclusion that the conditions under which we may get an adequate dwell time (high temperature sodium) and a suitable dispersion (small tank) must be investigated. If spontaneous interaction does not occur, energetic triggers should be applied.

13) For injection experiments (coolant into fuel) the evidence shows that the three stage model is applicable at least for freon/water and water/molten salt. For Na into UO_2 there is no evidence to suggest that the model does not apply. An alternative explanation based on superheated drops (Fauske) has been put forward, though this cannot explain the very similar explosion of water into salt, in which it was shown that sudden fine fragmentation of water is necessary for rapid heat transfer, and the contact temperature was above the spontaneous nucleation temperature.

14) A comparison between small scale and large scale experiments shows that FCIs are likely to be more energetic in large scale systems. To extrapolate results from small scale experiments to predict the behavior of large scale systems is not possible with the present state of knowledge.

15) The presence of noncondensable gases does not seem to inhibit energetic FCIs in systems in which they occur without gases.

16) An increase in ambient pressure seems to inhibit spontaneously triggered interactions. This could be due to inhibition of the trigger.

17) It is important to determine whether or not superheating to a nucleation limit (Fauske) is necessary for fragmentation in energetic FCIs because this would imply that UO_2 /Na systems are prohibited from exploding in most circumstances. It must be pointed

out that, if this is the case, one is compelled to postulate and demonstrate either (1) that the fragmentation mechanism which causes FCIs for UO_2 and Na is different from that for other materials such as tin/water, etc. (because experimental results show that the fragmentation for these materials allows coherence and propagation in large scale systems) or, (2) that the fragmentation mechanism in small scale systems is fundamentally different from that in large scale systems. To prove postulate 1 may be difficult (though not impossible) because the behavior of UO_2 and Na in small scale dropping experiments seems similar to that of the other materials as already noted (10). To prove postulate 2 is at this stage difficult because there is not sufficient evidence as pointed out above (11).

18) It is also important to determine whether or not film boiling is possible for UO_2 and Na in large systems, because film boiling may be necessary to allow significant coarse mixing in many contact modes. The experimental evidence with other materials (e.g., Freon/water, tin/water etc.) suggests that spontaneous nucleation on contact may be necessary for adequately stable film boiling. The UO_2 /Na systems (small and large scale droppings experiments and injection experiments), however, suggest that film boiling may occur for a limited duration (~ 200 msec). It is therefore important to determine the factors which influence film boiling in UO_2 /Na systems.

19) It is important to determine if spontaneous nucleation on contact is necessary for the triggering (and/or escalation) of energetic FCI. It is possible that energetic FCI occur only if the trigger is sufficiently energetic to generate a self-sustaining shock wave which propagates through the coarse mixture.

Suggestions for Future Work

While it has been shown that reactor materials do not react energetically in most circumstances, it has also been found that they can interact energetically in specific conditions (e.g., injection experiments). In order to demonstrate that energetic FCIs do not occur under realistic conditions during hypothetical reactor accidents, it is desirable to identify positively the limits of conditions under which an energetic FCI can occur, and to demonstrate that these conditions do not occur in a reactor and thus ease the safety arguments. The present understanding of the physics of FCI is somewhat limited. A number of crucial issues are still unresolved. Simulation experiments (in and out-of-pile tests) to date, although they have given an enormous amount of very valuable information on various aspects of reactor safety, have, however, given information of relatively limited value to the understanding of FCIs. They have demonstrated that FCIs can occur in fast reactors under realistic conditions in a hypothetical accident but that they are always incoherent and therefore of low energy yield. However, because of the severe restriction both on the type (e.g., slow transients) and scale (7 pins) of these tests coupled to the observed tendency for FCIs to become coherent and energetic only in large scale systems (coarse intermixing), it is difficult at this stage to extrapolate the results with confidence to the reactor subassembly and/or whole core scale. The extension of these tests to a subassembly scale is potentially valuable in this respect (especially prompt burst tests). However, it is important to point out that, for a full analysis of the results and a valid extrapolation to a larger scale, an understanding of the physics of FCI is required. For the above reasons the program of basic experiments should also be continued in parallel. In addition, in view of the tremendous difference in costs, it would be very unwise to perform very expensive in-pile tests without a supporting experimental program necessary to acquire basic knowledge.

Since the specification of simulation experiments involves a much wider field than just FCI, we restrict ourselves to suggestions for a basic program.

1) The injection experiments (coolant into fuel) were the only experiments in which an energetic FCI with fast reactor materials occurred, but there are relatively few results with a significant scatter. Since the mechanisms for these explosions are not yet understood, it is suggested to carry out further experiments including one in which Na is injected at several places simultaneously to determine whether or not the interaction can become coherent on a large scale.

2) In small scale dropping experiments with fast reactor materials, the Na temperature and the fuel temperature (the latter is practicable in the case of steel only) should be varied systematically to study how they affect the dwell time.

3) A special small scale dropping experiment with reactor materials should be carried out in which a sudden increase in ambient pressure is applied to the system during the dwell time. This should indicate whether or not pressure waves can initiate interactions with reactor materials. This experiment should be technically possible because dwell times as long as 200 msec. have already been observed.

4) The large scale dropping experiments with fast reactor materials to date did not have the correct geometry to ensure a suitably dense dispersion (coarse mixing) for propagation. It is suggested therefore to carry out some more of these experiments with the correct geometry. Na temperature and fuel temperature (the latter in the case of steel only) should be varied systematically to see if they influence the dwell time and the tendency for coherence.

5) Large scale dropping experiments with other materials known to be explosive (with spontaneous and induced triggers) should be continued in an attempt to define the conditions for propagation and to understand the mechanisms. In particular the following parameters should be varied:

a) Fuel to coolant volume ratio in the coarse dispersion to determine the dilution boundaries within which propagation occurs.

b) Fuel and coolant temperatures to see their influence on dwell time and on the boundaries for coherent interactions.

c) Possibly ambient pressure to determine its effect on the boundaries.

In addition, attempts should be made to determine the fragmentation and heat transfer behind the propagating front. This, however, may be technically difficult. Flash X rays may be useful.

6) Film boiling experiments on solid surfaces should be carried out to investigate the influence of the thermal properties of the hot surface on (1) film stability, (2) violence of film collapse and (3) nature of the boiling following collapse. The purpose of experiment (1) is to find out whether or not film boiling can be stable between UO_2 and Na. The purpose of experiments (2) and (3) is to investigate the potential for vapor collapse and violent boiling as fragmentation mechanisms.

7) Similar experiments as in point 6 should be carried out with molten surfaces.

8) The potential of hydrodynamic mechanisms for fuel fragmentation should be investigated. This may be done by studying the effects of shock waves on a coarse mixture of two fluids (one high density and the other low density) at room temperature.

9) Data already produced by shock tube experiments should be carefully analyzed before planning new experiments. It seems likely that the shock tube technique could be a valuable qualitative method of investigating energy transfer and fragmentation under sudden contact conditions (similar to those occurring behind the front of propagating explosion).

10) It is important to establish in a definite way whether or not propagation of explosion is possible with reactor materials and, if it is possible, under what conditions. An

in-pile one dimensional experiment in which a coarse mixture of solid UO_2 and Na is rapidly heated to get molten UO_2 before sodium boils with a pressure trigger mechanism may be a useful means to investigate this problem. The following parameters are important: fuel to coolant volume ratio, size of the fuel drops, void fraction, trigger energy and fuel energy. It is suggested that a feasibility study of this experiment should be carried out. This experiment is a basic experiment and not a simulation experiment.

11) Theoretical work to understand the physics of FCIs should be continued. In particular, the hydrodynamic effect of shock waves on dense dispersions (coarse mixing), the fragmentation due to pressure driven vapor collapse and the role of violent boiling should be investigated.

ACKNOWLEDGMENTS

This paper is published with the permission of the Central Electricity Generating Board and GFK Karlsruhe.

APPENDIX 1

MINIMUM WALL TEMPERATURE " T_{\min} " FOR STABLE FILM BOILING

In Farahat's experiments [69], a hot tantalum sphere was cooled in Na at different Na temperatures. It was found that T_{\min} decreases with increasing Na temperature (1900°C at saturation). However, there is evidence that T_{\min} also depends on the thermophysical properties of the heating surface. For example, experiments in water [92, 93, 42] demonstrate that heating surfaces (made of high conductivity materials), when coated with insulating materials, lead to an increase of " T_{\min} ". There is also evidence that T_{\min} increases with relative velocity between fuel and coolant [94, 95] and also with the roughness of the heating surface [96]. A correlation has been proposed by Henry [97] for T_{\min} as a function of the coolant temperature and of the thermophysical properties of the coolant and of the heating surface ($\sqrt{(k\rho c)_{\text{cool}}/(k\rho c)_{\text{fuel}}}$). This correlation is based on the behavior at local contacts between coolant and heating surface which occur during film boiling. The correlation was obtained by fitting some experimental results, which lie in a domain far away from the conditions of Na and UO_2 . Well validated criteria to predict whether or not stable film boiling takes place for UO_2 and Na for a given set of conditions do not yet exist. In the presence of local contacts, the definition of minimum temperature for film boiling seems to be problematic, especially in the case of molten UO_2 and Na where local contacts probably cause solidification and cracking of the UO_2 surface. Radiation may be important. Experiments and developments of more satisfactory theoretical models are therefore needed in this area.

APPENDIX 2

HYDRODYNAMIC FRAGMENTATION

If a coarse mixture of two liquids of different densities is subject to a sudden acceleration, the upwind interfaces of drops of heavy liquid may experience Taylor instability, and if interphase slip is produced, drag forces may also lead to distortion or breakup of the drops, for example, by boundary layer stripping. A review of relevant fragmentation mechanisms is given in [99]. There is little data on the effect of shocks on dense dispersions of two liquids, but the fragmentation effect of gas-liquid shocks has been well studied. Calculations by Kriebel [100] of the behavior of a shock wave in a dusty gas show that both the pressure and gas velocity jump suddenly to some fraction of their final equilibrium values, and then increase slowly. The dust particles are unaffected by the initial shock and are accelerated to the final equilibrium velocity by gas drag forces. Qualitatively similar behavior might be expected of a dispersion of fuel drops in coolant subjected to a shock wave from a propagating explosion. An exact calculation requires a numerical solution of the two component conservation relations, but we may approximate to the solution by assuming that the coolant jumps to the final equilibrium velocity, and is maintained there by the pressure field while the fuel drops are accelerated to this velocity by coolant drag. We note incidentally the approximation used by Bankoff [75] and independently by Williams [76] neglects the pressure field and considers deceleration of the coolant by the fuel, but assumes that it starts from the equilibrium mixture velocity, and thus leads to a final mixture velocity much lower than that required by the conservation laws. Empirical relations for breakup time and drag coefficient for liquid drops in gas shocks [103] suggest that shocks with a final equilibrium velocity (in the lab frame) of 200-500 m sec⁻¹ characteristic of complete detonations [26], give drop Weber numbers approximately 10⁵ which will give fine fragmentation by Taylor breakup.

However, recent experimental data [99] on behavior of coarse mixtures (dense dispersions) and single drops and of mercury in water, subjected to lower velocity jumps (10-100 msec⁻¹), suggest that hydrodynamic fragmentation may also be effective for much weaker shocks, (Weber numbers approximately 10⁵) where the dominant mechanism is boundary layer stripping. The nondimensional breakup time was similar to that for gas/liquid systems, remaining roughly constant at a value between 3 and 5 over a very wide range of Weber numbers (10² - 10⁵).

The drag coefficient in these experiments (approximately 2) was also similar to that in gas liquid systems.

APPENDIX 3

THE CAPTURE MODEL [79]

The following four stages can be identified:

1) Coarse mixing with large droplets of coolant separated by their vapor from the fuel.
2) Capture of a few small drops of coolant ($\sim 100 \mu$ diameter) by the surface of the fuel. A drop is said to be captured when microscopic vapor bubbles ($\sim (1/10) \mu$ diameter) attempt to grow at the interface with the fuel but cannot coalesce. In this situation, heat is transferred rapidly through the vapor bubble by evaporation at the contact interface and condensation on the opposite face of the bubble. Capture can only occur when the following two conditions are satisfied.

a) contact temperature is higher than the spontaneous nucleation temperature but lower than the critical temperature of the coolant

b) the thermal boundary layer at the time of acoustic relief must be sufficiently thick to support a vapor cavity of the critical size but not thick enough to allow the bubbles to grow into the saturated liquid. If the boundary layer is between these two limits, the bubble will grow to a maximum radius given by "the intersection of the mechanical stability line and the thermal boundary layer." Since the acoustic relief time increases with drop size, only small drops can be captured. In support of this, data on Freon 12 drops on mineral oil are quoted [56].

3) Individual captured drops are heated up to the spontaneous nucleation temperature and explode, producing shock waves which lead to incoherent fragmentation of the adjacent coolant drops.

4) The mixture is then assumed to be uniformly fragmented at the capture diameter ($\sim 100 \mu$). The subsequent explosion of one or several drops causes the capture of all the other drops therefore producing a coherent explosion.

As a comment on this model the following must be said:

a) A consequence of this model is that fine fragmentation of coolant must be achieved *before* a large scale vapor explosion can occur. This is in contrast with experimental visual evidence [51] and [50] which showed only coarse mixing ahead of the interaction front.

b) The model cannot explain explosions at a contact temperature higher than the critical temperature like tin, aluminum, silver/water, molten metal/water, steel and water [50].

c) The hypothesis that the microscopic bubble cannot grow beyond its maximum value during the heating of the captured drop, which takes about $500 \mu\text{sec}$, is not self consistent. In fact, according to the model, after only $10 \mu\text{secs}$. the bubble should grow without limit because there is no intersection between the mechanical stability line and the boundary layer.

d) In the model, it is said that the vapor bubble cannot grow until acoustic relief takes place. However, it can easily be shown that by applying a simple acoustic constraint, bubble growth is possible before acoustic relief.

e) Incoherent fragmentation is unlikely to produce mixture uniformly fragmented at the capture diameter (stage 3 to stage 4). In fact, according to the model, the drops should explode as soon as they reach the capture diameter.

REFERENCE

- [1] Lipsett, S. G., "Explosion From Molten Materials and Water," *Fire Technology*, vol. II, 2, 1966, pp. 118-126.
- [2] Epstein, L. F., "Reactor Safety Aspects of Metal Water Reactions," GEAP 3335, Jan. 1960.
- [3] Sallack, J. A., "On Investigation of Explosion in the Soda Smelt Dissolving Operation," Meeting of the Canadian Pulp and Paper Association, Quebec, Canada, June 6-8, 1955.
- [4] Burgess, D. S., Murphy, J. N., and Zabetakis, M. G., "Hazards Associated with the Spillage of Liquefied Natural Gas on Water," U.S. Bureau of Mines RI 7448, 1970.
- [5] Miller, R. W. et al., "Experimental Results and Damage Effects of Destructive Tests," *ANS Trans.*, vol. VI, 1963, pp. 138.
- [6] Witte, L. C., Cox, J. E., and Bouvier, J. E., "The Vapour Explosion," *Journal of Metals*, Feb. 1970, pp. 39-44.
- [7] Hicks, E. P., and Menzies, D. C., "Theoretical Studies on the Fast Reactor Maximum Accident," *ANL-7120*, 1965, pp. 654-670.
- [8] Long, G., "Explosions of Molten Aluminum in Water. Cause and Prevention," *Metal Progress*, May 1957, pp. 107-112.
- [9] Wright, R. W. et al., "Kinetic Studies of Heterogeneous Water Reactors," USAEC Rep. STL 372-22, July 1965 and STL-30 December 1965.
- [10] Ivins, R. O., "Interactions of Fuel, Cladding and Coolant," *ANL-7399*, November 1967, pp. 162-165.
- [11] Swift, D. L. and Baker, L., Jr., "Experimental Studies of the High Temperature Interaction of Fuel and Cladding Materials with Liquid Sodium," *Proc. of the Conf. on Safety, Fuels and Core Design in Large Fast Power Reactors*, ANL-7120, October 1965.
- [12] Hsiao, K. H. et al., "Pressurization of a Solidifying Sphere," *J. of Appl. Mech.*, vol. 39, March 1972, pp. 71-77.
- [13] Hoskins, N. E., and Morgan, K., "Studies of Pressure Generation by Water Impact Upon Molten Aluminum With Reference to Fast Reactor Subassembly Accidents," *Proc. of Int. Conf. on Eng. of Fast Reactors for Safe and Reliable Operation*, Karlsruhe, October 1972, pp. 870-883.
- [14] Cho, D. H., Ivins, R. O., and Wright, R. W., "Pressure Generation by Molten Fuel-Coolant Interactions under LMFBR Accident Conditions," *Proc. of Conf. on New Develop. in Reactor Math. and Applications*, Idaho Falls, March 71, pp. 25-49.
- [15] Jakemann, D., "A Review of the Meeting of the Working Group on the Comparison of Calculated Models," *PNC N251 76-12*, vol. 2, pp. 733-750, March 1976.
- [16] "Sodium Fuel Interaction in Fast Reactor Safety," *Proc. of the symposium held in Grenoble*, January 1972.
- [17] "Second Specialist Meeting on Sodium/Fuel Interaction in Fast Reactors," Ispra, November 1973, EUR 5309 e.
- [18] "Third Specialist Meeting on Sodium/Fuel Interaction in Fast Reactors," Tokyo, March 1976, *PNC N251 76-12* (2 volumes)
- [19] Teague, H. J., "Summary of the Papers Presented on the CREST Meeting on Fuel-Sodium Interaction at Grenoble in January 1972 and Report of Conference Papers 38 a-k on Fuel Sodium Interaction," *Proc. of Int. Conf. on Eng. of Fast Reactors for Safe and Reliable Operation*, Karlsruhe, October 1972, pp. 812-838
- [20] Caldarola, L., "Current Status of Knowledge of Molten Fuel/Sodium Thermal Interactions," *KFK 1944*, February 1974.
- [21] Fauske, H. K., "CSNI Meeting on Fuel-Coolant Interactions," *Nuclear Safety*, vol. 16, No. 4, July-August 1975.
- [22] Buxton, L. D., and Nelson, L. S., "Core-meltdown Experimental Review - Steam explosion," *SAND 74-0382*, August 1975.
- [23] Benz, R., Fröhlich, G., and Unger, "Literaturstudie zur Dampfexplosion," *IKE, BMFT-QS-76*, February 1976.
- [24] Fauske, H. K., "Mechanisms of Liquid-liquid Contact and Heat Transfer Related to Fuel-coolant Interactions," *EUR 5309 e*, pp. 201-209, November 1973.

- [25] Colgate, S. A., and Sigurgeirsson, T., "Dynamic Mixing of Water and Lava," *Nature*, vol. 244, pp. 552-555, August 1973.
- [26] Board, S. J., Hall, R. W., and Hall, R. S., "Detonation of Fuel Coolant Explosions," *Nature*, vol. 254, No. 5498, pp. 319-321, March 1975.
- [27] Cho, D. H., Fauske, H. K., and Grohms, M. A., "Some Aspects of Mixing in Large Mass, Energetic Fuel-coolant Interactions," *ANS/ENS meeting*, Chicago, October 1976.
- [28] Amblard et al., "Experience CORRECT-1 Resultats Experimentaux," Note T.T. N^o 480 CEA-CENG, Department de Transfer et Conversion d'Energie (November 1974).
- [29] Armstrong et al., "Explosive Interaction of Molten UO₂ and Liquid Sodium," *ANL 76-24*, March 1976.
- [30] Asher et al., "Experimental Work at Harwell on the Injection of Sodium into Liquid Steel," *AERE M2770*, February 1976.
- [31] Abbey et al., "The Injection of Sodium into Liquid Stainless Steel: a Report of the Second Experiments NA-SS/1," *AERE M2771*, February 1976.
- [32] Asher et al., "Vapour Explosions (fuel coolant interactions) Resulting from the Sub-Surface Injection of Water into Molten Metals: Preliminary Results," *AERE M2772*, March 1976.
- [33] Anderson, R. P., and Bova, L., "Final Report on the Small Scale Vapour Explosion Experiments with NaCl-H₂O system," *ANL 76-57 (1976)*.
- [34] Fauske, H. K., "On the Mechanism of Uranium Dioxide-Sodium Explosive Interactions," *Nuclear Science and Engineering*, vol. 51, pp. 95-101 (1973).
- [35] Armstrong et al., "Interaction of Sodium with Molten UO₂ and Stainless Steel Using a Dropping Mode of Contact," *ANL 7890 (1971)*.
- [36] Dullforce, et al., "Self Triggering of Small Scale Fuel Coolant Interactions," *CLM-P 424 (1975)*.
- [37] Cho et al., "Fragmentation of Molten Materials Dropped into Water," *ANL 8155 (1974)*.
- [38] Bjorkquist, G. M., "Experimental Investigation of the Fragmentation of Molten Metals in Water," *TID-26826 (June 1975)*.
- [39] Board et al., "Fragmentation in Thermal Explosions," *CEGB RD/B/N 2423 (October 1972)*.
- [40] Board, S. J., and Hall, R. W., *An Explosion Propagation Mechanism*, Crest Second Specialist Meeting on SFI in Fast Reactors, Ispra November 1973, EUR 5309 e.
- [41] Arakeri et al., "An Experimental Study of the Thermal Interaction for Molten Tin Dropped into Water," *UCLA-ENG-7592 (December 1975)*.
- [42] Zyszwowski, "Results of Measurements of Thermal Interaction Between Molten Metal and Water," *KFK 2193 (October 1975)*.
- [43] Fröhlich, G. et al., "Experiments with Water and Hot Melts of Lead," *Journal of Non-Equil. Thermodyn.* vol. 1 (1976).
- [44] Bradley, R. H., and Witte, L. C., "Explosive Interaction of Molten Metals Injected into Water," *Nuclear Science and Engineering* 48, 387-396 (1972).
- [45] Henry, R. H. et al., "Vapour Explosion Experiments with Simulant Fluids," *ANS/ENS meeting*, Chicago, October 1976.
- [46] Mizuta, H., *Progress Report on the Molten UO₂ Experiments*, Crest Second Specialist Meeting on SFI in Fast Reactors, Ispra, November 1973, EUR 5309 e.
- [47] Yasin, J., "A Simulation of Thermal Phenomenon Expected in Fuel Coolant Interaction in LMFBR's," *UCLA-ENG 76100*, September 1976.
- [48] Ivins, R. O., *ANL 7152*, January 1966.
- [49] Hess, P. O., and Brondyke, K. J., "Causes of Molten Aluminum-water Explosions and Their Prevention," *Metal Progress* 95, April 1969, pp. 93-110.
- [50] Briggs, A. J., *Experimental Studies of Thermal Interactions at AEE Winfrith*, Third Specialist Meeting on Sodium Fuel Interactions, Tokyo 1976, PNC N251, 76-12, vol. 1, pp. 75-96.
- [51] Board, S. J., and Hall, R. W., *Recent Advances in Understanding Large Scale Vapour Explosions*, Third Specialist Meeting on Sodium Fuel Interactions, Tokyo, PNC N251, 76-12, 1976, pp. 249-283.
- [52] Briggs, A. J., unpublished.
- [53] Henry, R. E. et al., *Large Scale Vapour Explosion*, Fast Reactor Safety Meeting, Beverly Hills, April 1974, CONF-740401-P3, pp. 922-934
- [54] Board, S. J., Hall, R. W., and Brown, G. I., *The Role of Spontaneous Nucleation in Thermal Explosions - Freon/water Experiments*, Fast Reactor Safety Meeting, Beverly Hills, April 1974, CONF-740401-P3, pp. 935-946.

- [55] Armstrong, D. R., and Anderson, R. P., ANL-RDP 49, 1976.
- [56] Henry, R. E., Fauske, H. K., and McUnker, L. M., "Vapour Explosions and Simulant Fluids," ANS/ENS, Chicago Conference, October 1976.
- [57] Holtbecker et al., EUR/C-15/733/74.d.
- [58] Alexander, unpublished.
- [59] Clerici, C. et al., "Interactions with Small and Large Sodium and UO_2 Mass Ratios," PNC N251, 1976, pp. 507-543.
- [60] Johnson, T. R., Baker, L., and Pavlik, J. R., *Large Scale Molten Fuel-sodium Interaction Experiments*, Proceedings of the Fast Reactor Safety Meeting, Beverly Hills, CONF-740401-P3, 1976, pp. 883-896.
- [61] Guest, J. N., Turner, R. G., and Reis, N. J., "Al/water Shock Tube Experiments at AERE Foulness since Jan. 1972," EUR-5309 e, pp. 1-21.
- [62] Winscale report unpublished.
- [63] Goldammer, H., and Kottowski, H. M., "Theoretical Experiments Investigation of FCI in a Shock Tube Configuration," ANS/ENS, Chicago Conference, 1976.
- [64] Kottowski, H. M., Private Communication.
- [65] Amblard, M., "Preliminary Results on a Contact Between 4 kg UO_2 and Liquid sodium," PNC N251, 76-12, 1976, pp. 545-560.
- [66] Caldarola, L., "A Theoretical Model with Variable Masses for the Molten Fuel Sodium Interaction in a Fast Reactor," *Nuclear Engineering and Design* 34, 1975, pp. 181-201.
- [67] Croneberg, A. W., and Grolmes, M. A., "A Review of Propagation Models Relative to Molten UO_2 Breakup When Quenched in Sodium," PNC N251, 76-12, 1976, pp. 623-650.
- [68] Caldarola, L., and Kastenberg, W. E., "On the Mechanism of Fragmentation During Molten Fuel Coolant Interactions," CONF-740401-P3, April 1974, pp. 937-954
- [69] Farahat, M. K., and Egges, D. T., "Pool Boiling Subcooled Sodium," *Nuclear Science and Engineering*, vol. 53, 1974, pp. 240-253.
- [70] Plesset, M. S., and Chaprin, R. B., "Collapse of an Initially Spherical Bubble Near the Wall," *J. Fluid Mech.*, vol. 47, 1971, pp. 283-290.
- [71] Buchanan, D. J., "Penetration of a Solid Layer by a Liquid Jet," *J. Phys. D. Applied Physics*, vol. 6, 1973, pp. 1762-1771.
- [72] Bankoff, S. G., and Ganguli, A., "Mechanism of Vapour Explosions," ANS/ENS, Chicago Conference 1976.
- [73] Buchanan, D. J., "Fuel-coolant Interactions: Small Scale Experiments and Theory," EUR 5309 e (1973).
- [74] Caldarola, L., "A Theoretical Model for the Molten Fuel-Sodium Interaction in a Nuclear Fast Reactor," *Nuclear Engng. and Des.*, vol. 22, No. 2, pp. 175-211, Oct. 1972.
- [75] Bankoff, S. G., and To, J. H., "On the Existence of Steady State Fuel-coolant Detonation Waves," PNC N251, 76-12, 1976, pp. 53-128.
- [76] Williams, D. C., "A Critique of the Board-Hall Model for Thermal Detonations in UO_2 -Na Systems," ANS/ENS, Chicago Conference, 1976.
- [77] Hall, R. W., to be published.
- [78] Fauske, H. K., "Some Aspects of Liquid-liquid Heat Transfer and Explosive Boiling," CONF-740401-P3, April 1974, pp. 992-1005.
- [79] Henry, R. E., and Fauske, H. K., "Nucleation Characteristics in Physical Experiments," PNC N251, 76-12, 1976, pp. 595-622.
- [80] Ochiai, M., and Bankoff, S. G., "Liquid-liquid Contact in Vapour Explosions," ANS/ENS, Chicago Conference, 1976.
- [81] Buchanan, D. J., and Dullforce, T. A., "Fuel-coolant Interaction: Small Scale Experiment and Theory," EUR 5309 e, 1973, pp. 143-176.
- [82] Vaughan, G. J., Caldarola, L., and Todreas, N., "A Model for Fuel Fragmentation During Molten Fuel-coolant Interactions," ANS/ENS, Chicago Conference, 1976.
- [83] Dullforce, T. A., Buchanan, D. J., and Pechover, R. S., *J. Phys. D. Appl. Phys.*, Vol. 9, 1976, pp. 1295.
- [84] Bjornard, T. A., MITNE-163, 1974.
- [85] Bojarski et al., "Effects of Fuel Sodium Interaction in TOP Tests with Electrically Heated Fuel Pins," ANS/ENS Meeting Chicago, October 1976.
- [86] Amblard, M. et al., "Interaction UO_2 /Na Experience JEF," CEA-CENG Note TT No. 472 (1974).

- [87] Martini, M. et al., *Out-of-pile Tests on UO₂ Pins*, Crest 2nd Specialist Meeting on SFI in Fast Reactors (Ispra Nov. 1973), EUR 5309 e.
- [88] Kwast, H., "Loss of Cooling Experiments with Single Fuel Pins," ECN-76-132, November 1976.
- [89] Schmidt, T. R., "LMFBR Prompt Burst Excursion (PBE) Experiments in the Annular Core Pulse Reactor (ACPR)," *ANS/ENS* meeting, Chicago, October 1976.
- [90] Doerner, R. C. et al., "Final Summary Report of Fuel Dynamics Tests H2 and E4, ANL 76-16.
- [91] Wright, R. W. et al., "Summary of Autoclave Treat Tests on Molten Fuel Coolant Interactions," CONF-740401, 1974, pp. 254-267.
- [92] Moreaux, Chevier, and Beck, "Destabilisation of Film Boiling by Means of a Thermal Resistance," *Int. J. Multiphase Flow* 2, pp. 183-190 (1975).
- [93] Zhakov, Kazakov, Kovalov, and Kuzma Kichta, "Heat Transfer in Boiling of Liquids on Surfaces Coated with Low Conductivity Films," *Heat Transfer Sov. Research* 7 No. 3, May-June 1975.
- [94] Walford, "Transient Heat Transfer from Nickel Spheres," *Int. Jnl. Heat Mass Transfer* 23, pp. 1621 (1969).
- [95] Stevens, J. W., and Witte, L. C., "Destabilisation of Vapour Film Boiling Around Spheres," *Int. J. Heat Mass Transfer* 16, pp. 669-678 (1973).
- [96] Fröhlich and Oswald, "Aufbau and Abbau des Leidenfrost Phänomens in Wasser an kugelförmigen Flächen mit und ohne Störstellen," IKE-Bericht Nr. 2-15 Juni 1975.
- [97] Henry, R. E., "A Correlation for the Minimum Film Boiling Temperature," Heat transfer research design, *AIChE Symposium series* 1970, pp. 138.
- [98] Barts, E. W., et al., "Summary and Evaluation — Fuel Dynamics Loss of Flow Experiments," (Tests L2, L3, L4), ANL 75-57.
- [99] Buttery, N. E., to be published.
- [100] Kriebal, A. R., *J. Basic Engineering* 86, pp. 655 (1964).
- [101] Bankoff, S. G., and Jo, T. H., *Paper SNI 6/30*, 3rd SFI Meeting, Tokyo 1976, PNC N252, 76-12, pp. 153-177.
- [102] Williams, D. C., "A Critique of the Board-Hall Model," Paper 18-1, *Int. Conference on Fast Reactor Safety*, Chicago 1976.
- [103] Simpkins and Bales, *J. Fluid Mech.* 55, pp. 629, 1972.
- [104] Davies, D., Kelly, J. C., and Sangwine, S. J., "Injection of Water into Liquid Tin—Occurrence of Explosions and Measurements of Dwell Times," unpublished.

Der folgende Artikel

L. Caldarola

Coherent Systems with Multistate Components

aus

Nuclear Engineering and Design,

58 (1980) pp 127-139

wurde mit freundlicher Genehmigung der
North-Holland Physics Publishing, Amsterdam,
nachgedruckt



COHERENT SYSTEMS WITH MULTISTATE COMPONENTS

L. CALDAROLA *

*Kernforschungszentrum Karlsruhe GmbH, Institut für Reaktorentwicklung 7500 Karlsruhe 1,
Federal Republic of Germany*

Received 12 December 1979

The basic rules of the Boolean algebra with restrictions on variables are briefly recalled. This special type of Boolean algebra allows one to handle fault trees of systems made of multistate (two or more than two states) components.

Coherent systems are defined in the case of multistate components. This definition is consistent with that originally suggested by Barlow in the case of binary (two states) components. The basic properties of coherence are described and discussed. Coherent Boolean functions are also defined. It is shown that these functions are irredundant, that is they have only one base which is at the same time complete and irredundant. However, irredundant functions are not necessarily coherent.

Finally a simplified algorithm for the calculation of the base of a coherent function is described. In the case that the function is not coherent, the algorithm can be used to reduce the size of the normal disjunctive form of the function. This in turn eases the application of the Nelson algorithm to calculate the complete base of the function. The simplified algorithm has been built in the computer program MUSTAFA-1. In a sample case the use of this algorithm caused a reduction of the CPU time by a factor of about 20.

1. Introduction

The evaluation of the occurrence probability of the top event of a fault tree can be carried out by means of simulation methods (Monte-Carlo-type methods) or by means of analytical methods. Numerical simulation allows reliability information to be obtained for systems of almost any degree of complexity. However, this method provides only estimates and no parametric relation can be obtained. In addition, since the failure probability of a system is usually very low, precise results can be achieved only at the expense of very long computational times.

Analytical methods give more insight and understanding because explicit relationships are obtainable. Results are also more precise because these methods usually give the exact solution of the problem.

In 1970 Vesely [1] gave the foundations of the analytical method for fault tree analysis.

Vesely's theory was improved by the author. A

computer program for fault tree analysis was developed based on this theory [2,3]. This computer program proved to be the best analytical program for fault tree analysis in the Federal Republic of Germany [4]. Vesely's method can be applied only to coherent systems with binary (two states) components. Another important limitation of the method is that the Boolean function which describes the top variable of the fault tree must not contain negated variables. Finally the theory does not give any indication on how to handle statistically dependent components.

Since there are components (e.g. a switch) which have more than two states, a theory was developed by the author in 1977 [5] to handle systems with multistate components. Here the basic idea to associate the primary variables with the states of the primary components instead than with the primary components was introduced. In addition the basic Boolean algorithms were described. In 1978 the author [6] showed that the technique of multistate super-components can be used to remove statistical dependencies from a fault tree.

An interesting feature of the method proposed in [5] and [6] is that the Boolean function which de-

* Principal Scientific Officer of the Commission of the European Community; delegated to the Kernforschungszentrum Karlsruhe.

scribes the top variable of the fault tree does not necessarily need to be coherent. In addition Boolean functions containing negated variables can be treated.

A formalization of the theory by means of the so called 'Boolean algebra with restriction on variables' has been developed by the author in [7], [8] and [12].

The coherent systems constitute a very important class of technical systems. Barlow [9] gives the definition of a coherent system in the case of a system made of binary primary components. Here we want to define a coherent system in the more general case of multistate primary components and to describe and discuss its properties.

2. Generalities on the Boolean algebra with restrictions on variables

According to what is said in the introduction, the basic idea of the Boolean algebra with restrictions on variables is that of associating the primary variables (literals) with the states of the primary components instead of with the primary components.

A primary component will be indicated by the small letter c followed by an integer positive number (c_1, c_2, c_3 , etc.). In general we shall have c_j with $j = 1, 2, \dots, m$, where ' m ' is the total number of primary components contained in the system.

A state of a primary component will be indicated by the same notation of the primary component to which it belongs followed by a positive integer number as an index ($c_{j_1}, c_{j_2}, c_{j_3}$, etc.). In general we shall have c_{j_q} with $q = 1, 2, \dots, n_j$, where n_j is the total number of states belonging to primary component c_j .

We now associate with each state c_{j_q} a Boolean variable C_{j_q} which takes the value 1 (true) if primary component c_j occupies state c_{j_q} and the value 0 (false) if c_j does not occupy c_{j_q} .

The event

$$\{C_{j_q} = 1\} \equiv c_{j_q}, \quad (1.1)$$

indicates that primary component c_j occupies state c_{j_q} .

Conversely, the event

$$\{C_{j_q} = 0\} \equiv \bigcup_{k=1}^{n_j} c_{j_k}, \quad k \neq q, \quad (1.2)$$

indicates that primary component c_j does not occupy state c_{j_q} and therefore occupies one of its other possible states.

Note the one to one correspondence between state c_{j_q} (small c) and Boolean variable C_{j_q} (capital C) associated with it. We have

$$c_{j_q} \equiv \{C_{j_q} = 1\}, \quad (1.3)$$

and

$$\bar{c}_j \equiv \{\bar{C}_{j_q} = 1\} \equiv \{C_{j_q} = 0\}. \quad (1.4)$$

The binary variables C_{j_q} are the primary variables (literals). They are not pairwise mutually independent.

Since a primary component *must* occupy one of its states and *can* occupy only one state at a time, the variables C_{j_q} must obviously satisfy the following two types of restrictions.

Restriction type 1. The disjunction of all binary variables associated with the same primary component is *always* equal to 1.

$$\bigvee_{q=1}^{n_j} C_{j_q} = 1. \quad (1.5)$$

Restrictions type 2. The conjunction of two different binary variables associated with the same primary component is *always* equal to 0.

$$C_{j_q} \wedge C_{j_k} = 0, \quad q \neq k. \quad (1.6)$$

Note that there is only one Restriction type 1 and $n_j(n_j - 1)/2$ Restrictions type 2.

The following rule is also important.

Rule 1 (Complement rule). A negated (complemented) literal is equal to the disjunction of all remaining literals belonging to the same primary component, that is,

$$\bar{C}_{j_q} = \bigvee_{k=1}^{n_j} C_{j_k}, \quad k \neq q. \quad (1.7)$$

It has been shown in [7], [8] and [12] that the Boolean algebra with restriction on variables allows one to operate on Boolean variables in a way similar to the traditional Boolean algebra, but with the additional rules given by eqs. (1.5)–(1.7).

The following definitions have already been partially introduced in [7], [8] and [12] and will be used throughout this paper.

Definition 1. A *monomial* is a conjunction of literals. Note that by definition a monomial does not contain negated literals.

Definition 2. A *zero monomial* is a monomial which is always equal to zero. A monomial is identical with zero if it contains at least two different literals of the same primary component. If B is a primary component and B_j and B_k are two different literals of B , we have

$$B_j \wedge B_k \equiv 0, \quad j \neq k. \quad (1.8)$$

Definition 3. A literal is said to be *obligatory* if its deletion in a given monomial alters the truth table of the monomial. Repeated literals are not obligatory.

$$B_i \wedge B_i = B_i. \quad (1.9)$$

Definition 4. An *irredundant monomial* is a non zero monomial which contains only obligatory literals.

Definition 5. A *complete monomial* (minterm) is an irredundant monomial which has a number of literals equal to the number of primary components present in the system.

Definition 6. Two monomials (say X_j and X_k) are said to be *mutually exclusive* if the monomial resulting from their conjunction is a zero monomial

$$X_j \wedge X_k \equiv 0. \quad (1.10)$$

Definition 7. If two irredundant monomials are such that the first (say X_j) contains all literals of the second one (say X_k), the first monomial implies the second one. The first monomial (X_j) is called *subsuming monomial* and the second one (X_k) *subsumed monomial*.

Definition 8. A *disjunctive form* of a Boolean function is any disjunction of monomials which is equivalent to the function.

Definition 9. The *disjunctive canonical form* of a Boolean function is that disjunctive form of the function in which every monomial is complete.

Definition 10. A monomial belonging to a disjunctive form of a Boolean function is said to be *obligatory* if

its deletion in the disjunctive form alters the truth table of the function.

A monomial is not obligatory if (1) it is a zero monomial, or (2) it subsumes another monomial of the disjunctive form, or (3) it is implied by the disjunction of two or more other monomials of the disjunctive form.

Definition 11. A disjunctive form of a Boolean function is called a *normal disjunctive form* if (1) all monomials are irredundant and (2) no subsuming monomial is contained in it.

Definition 12. An *irredundant disjunctive form* of a Boolean function is a normal disjunctive form of the function which ceases to be a disjunctive form of the function if one of its monomials is removed (deleted).

Definition 13. An irredundant monomial (say X) is said to be a *prime monomial* (or *prime implicant*) of a Boolean function (say TOP) if (1) X implies the TOP and (2) every subsumed monomial Y obtained from X by replacing one of its literals with 1 does not imply the TOP.

Definition 14. A *base* of a Boolean function is any disjunction of prime monomials which is equivalent to the function.

Definition 15. The *complete base* of a Boolean function is the disjunction of all its prime monomials.

Definition 16. An *irredundant base* of a Boolean function is a base which ceases to be a base if one of its prime monomials is removed (deleted).

Definition 17. The *three simplification rules*, which allow one to get a normal disjunctive form from a disjunctive form of a Boolean function, are the following:

- (1) Delete the repeated literals of a monomial (idempower law).
- (2) Delete zero monomials (exclusion law).
- (3) Delete subsuming monomials (absorption law).

Definition 18. The *complement* (negation) of a Boolean function is obtained by replacing in the function (1) each literal by its complement (that is

by the disjunction of all other literals belonging to the same primary component), (2) each disjunction (\vee) by a conjunction (\wedge) and (3) each conjunction (\wedge) by a disjunction (\vee).

Definition 19. The *Nelson algorithm* is a special algorithm which allows one to calculate the complete base of a Boolean function from any one of the normal disjunctive forms.

The algorithm consists simply in complementing a normal disjunctive form of a Boolean function and then in complementing its complement. After each complement operation the three simplification rules are applied to the result.

The Nelson algorithm is described in [7] and [8].

In the following we shall use indifferently both notations ‘ \cdot ’ and ‘ \wedge ’ to indicate the operation of conjunction.

3. Coherent systems

In the literature great importance is given to the concept of coherence. Some authors argue that most technical systems are coherent. Barlow [9] claims that coherence is synonymous of good design.

“A physical system would be quite unusual (or perhaps poorly designed) if improving the performance of a component (that is, replacing a failed component by a functioning component) caused the system to deteriorate (that is, to change from the functioning state to the failed state). Thus we restrict consideration to structure functions that are monotonically increasing in each argument. Also, to avoid trivialities we will, wherever possible, eliminate consideration of any system whose state does not depend on the state of its components.

Definition. A system of components is *coherent* if (a) its structure function is increasing and (b) each component is relevant, [9].”

Note that in [9] the structure function of a system takes the value 1 if the system is intact and the value 0 if it is failed.

The author [8] has shown the relationship between a Boolean function, and its associated structure function and that one can operate with Boolean functions instead of structure functions. Kuntzmann [10] defines also increasing and decreasing Boolean functions. We

shall refer here to Boolean functions and we shall adopt the following conventions.

(i) Each primary component is given a Boolean binary variable which takes the value 1 if the component is failed and the value 0 if it is intact.

(ii) The complete set of all elementary failed states of a system is called the failed state of the system.

(iii) The Boolean binary variable associated with the failed state of the system is called TOP.

(iv) If the system is in its failed state the variable TOP takes the value 1. If the system is not in its failed state the variable TOP takes the value 0.

(v) The value 1 is larger than 0 ($1 > 0$).

Taking into account the above conventions, Barlow’s definition [9] can be written as follows

Definition. A system of components is *coherent* if (a) its Boolean function TOP is increasing and (b) each component is relevant.

A Boolean function (with binary primary components) which is monotonic (increasing or decreasing) in each literal has the following two properties [10].

(1) Each prime implicant of an increasing Boolean function contains only literals but not negated literals (i.e. only the failed state and not the intact state of the primary components) and conversely each prime implicant of a decreasing Boolean function contains only negated literals.

(2) The function has only one base which is complete and irredundant at the same time.

Note that the second property can be shown to be a consequence of the first one [10].

An interesting feature of coherent systems with binary primary components is that the two above properties are *symmetric*, that is they hold for both Boolean functions: that associated with the failure of the system (TOP) as well as that associated with its success ($\overline{\text{TOP}}$). For this reason the definition of coherence based on the $\overline{\text{TOP}}$ (Barlow [9]) is perfectly equivalent to that based on the TOP. We shall see later that this does not hold in general in the case of systems with multistate components.

The problem of defining a monotonic Boolean function in the case of systems with multistate components is not straight forward, and is perhaps unnecessary.

Some authors [11] extend the concept of a

monotonic Boolean function to the case of multi-state components by introducing an ordered set of values for each primary component. This approach can be applied only to problems in which a decreasing (or increasing) scale of values can be assigned to the states of the primary components (from the intact state which is the least failed to the complete failed state which is the most failed). Many technical systems however cannot be treated by using an *ordered logic*. It would be in fact very hard to decide whether or not the state ‘failed closed’ of a circuit breaker is more failed than the state ‘failed open’. In addition for a given component the ordered scale of values may depend upon the system to which the component belongs and may therefore change from system to system.

We have used in our paper a *non-ordered logic* which can be applied in principle to any type of problem. For this reason it is difficult to extend the concept of monotonic Boolean function to the case of the Boolean algebra with restrictions on variables.

We can however define a coherent system by referring to some physical properties of the system. The following definition is proposed.

Definition 20. A system is said to be *coherent* (a) if each primary component is relevant and (b) if deterioration of the performance of an intact primary component (that is replacing the intact component by the same component in anyone of its possible failed states) causes the system to deteriorate (that is the system remains failed if it was originally failed, and it becomes failed or it remains intact if it was originally intact).

Conversely one could also propose the following definition which is fully equivalent to the one given above.

Definition 21. A system is said to be *coherent* (a) if each primary component is relevant and (b) if improving the performance of a failed primary component (that is replacing the failed component in anyone of its possible failed states by the same component in *the* intact state) causes the system to improve (that is the system remains intact if it was originally intact and it becomes intact or it remains failed if it was originally failed).

We introduce also the definition of an irredundant Boolean function.

Definition 22. A Boolean function is said to be *irredundant* if it has only one base which is at the same time complete and irredundant.

According to Theorem 2 of Appendix A, the following rule can be stated.

Rule 2. A sufficient condition for a Boolean function to be irredundant is that at least one literal of each primary component does not appear in the complete base of the function.

The following two properties hold in the case of coherent systems.

Property 1. No prime implicant of the Boolean function TOP associated with the failed state of a coherent system contains an intact literal (that is a literal associated with the intact state of the primary components).

Property 2. A Boolean function which satisfies Property 1 is irredundant.

Property 1 is proved by Theorem 1 in Appendix A. Property 2 is proved by Step 2 and 3 of Theorem 2 in Appendix A.

We shall assign the attribute ‘coherent’ also to the Boolean function TOP which is associated with the failed state of a coherent system and which therefore satisfies the two above properties.

Since the Boolean functions which satisfy Property 1 satisfies also Property 2, one could define a coherent function by referring to Property 1 only.

Definition 23. A Boolean function is said to be *coherent* if the intact literal of each primary component relevant to the function does not appear in the complete base of the function.

It is important to point out that a coherent function is irredundant but that an irredundant function is not necessarily coherent.

An important feature of coherent Boolean functions is the following:

If a Boolean function (TOP) is coherent, its complement ($\overline{\text{TOP}}$) is not necessarily coherent (*no symmetry in general*). However, if all primary components are binary, the complemented function $\overline{\text{TOP}}$ is also coherent because all its prime implicants do not contain any failed literal (that is any literal associated with the failed state of the binary primary components).

The concepts of coherence and irredundance are very useful, because they allow one to apply some rules which may enormously simplify the calculation of the complete base of a Boolean function.

Rule 3. If a normal disjunctive form of a Boolean function is such that at least one literal of each primary component relevant to the function does not appear in it, the function is irredundant, and the normal disjunctive form is the only base of the function.

For the proof of Rule 3 see Theorem 2 in Appendix A. Here we apply Rule 3 to an example.

We consider the following Boolean function, which is obtained by solving the fault tree of fig. 1. This

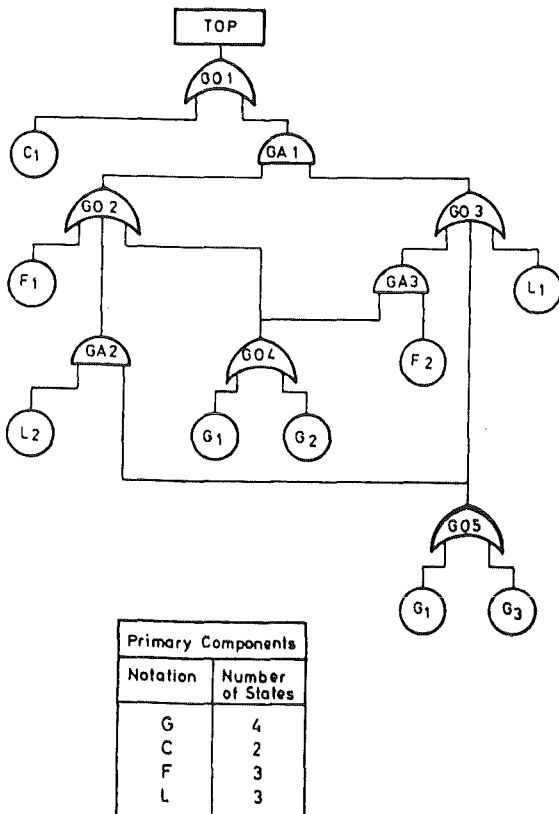


Fig. 1. Fault tree.

fault tree (which refers to a simplified electric power supply system) has been constructed and solved in [7] and in [8].

$$\text{TOP} = C_1 \vee L_1 \cdot F_1 \vee F_1 \cdot G_3 \vee G_3 \cdot L_2 \vee L_1 \cdot G_2 \vee G_1 \vee F_2 \cdot G_2. \tag{2.1}$$

In eq. (2.1) the primary components are G, C, F and L have respectively 4, 2, 3 and 3 states. The literals associated with the intact states are respectively G_4 , C_2 , F_3 and L_3 .

Since the literals associated with the intact states of all primary components do not appear in eq. (2.1), the function TOP is coherent and, according to Rule 3, eq. (2.1) is the only base of the function.

Definition 24. The coherent function Φ associated with the Boolean function TOP is that function generated from any normal disjunctive form of the TOP by replacing all intact literals by 1 and by applying the absorption rule among the monomials.

$$\Phi = [\text{TOP}]_{\text{all intact literals replaced by 1 + absorption rule.}} \tag{2.2}$$

We point out that, due to Rule 3, eq. (2.2) is already the only base of Φ .

Due to the way in which the function has been generated, one can easily verify that TOP implies Φ , that is

$$\text{TOP} \wedge \Phi = \text{TOP}. \tag{2.3}$$

Since TOP implies Φ , we obviously have

$$E\{\text{TOP}\} \leq E\{\Phi\}. \tag{2.4}$$

Eq. (2.4) is Rule 4.

Rule 4. The expected value of the coherent function Φ associated with a Boolean function TOP is an upper bound of the expected value of the latter.

Let us now consider a generic prime implicant of Φ . Due to the fact that the TOP is an implicant of Φ [eq. (2.3)], we can state the following rule (see Theorem 3 of Appendix A).

Rule 5. Any implicant of the Boolean function TOP, which is also a prime implicant of its associated coherent function Φ , is a prime implicant of the TOP.

An important corollary follows straightforwardly from the above rule.

Corollary. If all prime implicants of the coherent function Φ associated with a given Boolean function TOP are also implicants of the TOP, the two functions Φ and TOP are identical.

The above definitions, rules and corollaries allow us to identify a simplified algorithm for the calculation of the base of a coherent Boolean function.

Algorithm (Calculation of the complete base of a coherent Boolean function).

Step 1. Calculate complete base of the coherent function Φ associated with a given Boolean function TOP from the associated normal disjunctive form of the latter by replacing all intact literals by 1 and by applying the absorption rule among the monomials.

Step 2. Check that each prime implicant of Φ is also an implicant of the TOP. If the result of the test is positive, the two functions TOP and Φ are identical.

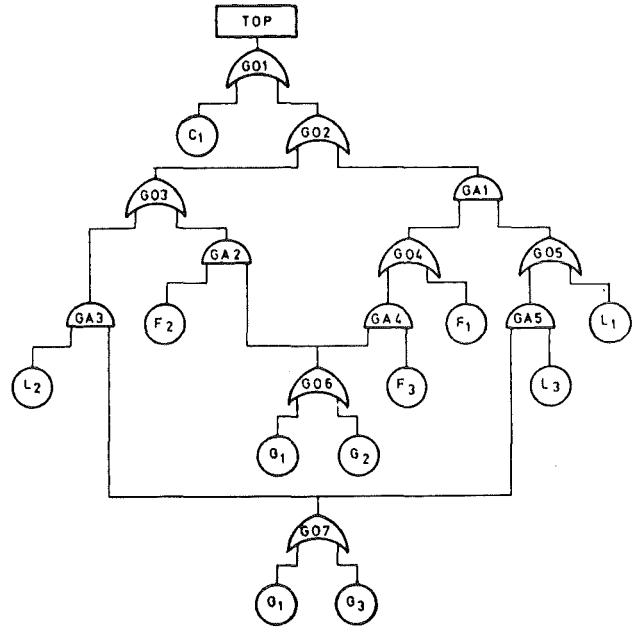
The test of Step 2 is described in Appendix B.

Note that the above algorithm allows one to calculate the only base of the TOP if and only if the TOP is coherent. It is important to point out that, whilst most technical systems appear to be coherent, to the best knowledge of the author there exist no general mathematical rules which allow one to establish a priori the coherence of any system. Step 2 of the algorithm can therefore be understood as a test for finding out a posteriori whether or not the system is coherent.

We apply now the simplified algorithm to the following Boolean function which is obtained by solving the fault tree of fig. 2. This fault tree refers to the same simplified electric power supply system of the fault tree of fig. 1. The fault tree of fig. 2 has also been constructed and solved in [7] and in [8].

$$\begin{aligned} \text{TOP} = & C_1 \vee F_2 \cdot G_1 \vee F_2 \cdot G_2 \vee L_2 \cdot G_1 \vee L_2 \cdot G_3 \\ & \vee G_1 \cdot F_3 \cdot L_1 \vee G_2 \cdot F_3 \cdot L_1 \vee F_1 \cdot G_1 \cdot L_3 \\ & \vee F_1 \cdot G_3 \cdot L_3 \vee F_1 \cdot L_1 \vee G_1 \cdot F_3 \cdot L_3. \end{aligned} \quad (2.5)$$

The literals associated with the intact states of the primary components are: G_4, F_3, L_3 and C_2 . We



Primary Components	
Notation	Number of States
G	4
C	2
F	3
L	3

Fig. 2. Fault tree.

replace now by 1 the above literals in eq. (2.5) (Step 1).

We get

$$\begin{aligned} \Phi = & C_1 \vee F_2 \cdot G_1 \vee F_2 \cdot G_2 \vee L_2 \cdot G_1 \vee L_2 \cdot G_3 \\ & \vee G_1 \cdot 1 \cdot L_1 \vee G_2 \cdot 1 \cdot L_1 \vee F_1 \cdot G_1 \cdot 1 \\ & \vee F_1 \cdot G_3 \cdot 1 \vee F_1 \cdot L_1 \vee G_1 \cdot 1 \cdot 1. \end{aligned} \quad (2.6)$$

Eq. (2.6) can be written as follows

$$\begin{aligned} \Phi = & C_1 \vee F_2 \cdot G_1 \vee F_2 \cdot G_2 \vee L_2 \cdot G_1 \vee L_2 \cdot G_3 \\ & \vee G_1 \cdot L_1 \vee G_2 \cdot L_1 \vee F_1 \cdot G_1 \vee F_1 \cdot G_3 \\ & \vee F_1 \cdot L_1 \vee G_1. \end{aligned} \quad (2.7)$$

Eq. (2.7) contains the monomial G_1 which is implied by the monomials $F_2 \cdot G_1, L_2 \cdot G_1, G_1 \cdot L_1$ and $F_1 \cdot G_1$. These monomials can therefore be deleted (absorption

rule). Eq. (12.7) becomes finally

$$\Phi = C_1 \vee F_2 \cdot G_2 \vee L_2 \cdot G_3 \vee G_2 \cdot L_1 \vee F_1 \cdot G_3 \vee G_1 \vee F_1 \cdot L_1, \quad (2.8)$$

which is identical with eq. (2.1).

By applying the test described in Appendix B (Step 2), it is easy to show that each monomial of eq. (2.8) is an implicant of the TOP. We can therefore conclude that eq. (2.8) is the only base of the TOP.

The complete base of TOP (eq. (2.8)) can be obtained from eq. (2.5) by applying the Nelson algorithm. This has been shown in [7] and in [8]. The simplified algorithm described in this paper is less general than the Nelson algorithm because it can be applied only to coherent Boolean functions. However the simplified algorithm, if applicable, is much simpler than the Nelson algorithm and requires much less computing time.

Before closing this chapter we want to show by means of an example that the property of coherence is not necessarily symmetric.

We complement eq. (2.5) and we reduce the result to a normal disjunctive form, which is the complete base of $\overline{\text{TOP}}$. We get

$$\begin{aligned} \overline{\text{TOP}} = & \overline{C}_1 \cdot (F_2 \vee \overline{G}_1) \cdot (F_2 \vee \overline{G}_2) \cdot (L_2 \vee \overline{G}_1) \cdot (\overline{L}_2 \vee \overline{G}_3) \\ & \cdot (\overline{G}_1 \vee \overline{F}_3 \vee L_1) \cdot (\overline{G}_2 \vee \overline{F}_3 \vee L_1) \cdot (F_1 \vee \overline{G}_1 \vee L_3) \cdot \\ & \cdot (F_1 \vee \overline{G}_3 \vee L_3) \cdot (F_1 \vee L_1) \cdot (\overline{G}_1 \vee \overline{F}_3 \vee L_3). \end{aligned} \quad (2.9)$$

Now we have

$$\overline{C}_1 = C_2, \quad (2.10)$$

$$\overline{G}_k = \bigvee_{q=1}^4 G_q, \quad k \neq q, \quad k = 1, 2, 3, 4, \quad (2.11)$$

$$\overline{F}_k = \bigvee_{q=1}^3 F_q, \quad k \neq q, \quad k = 1, 2, 3, \quad (2.12)$$

and

$$\overline{L}_k = \bigvee_{q=1}^3 L_q, \quad k \neq q, \quad k = 1, 2, 3, \quad (2.13)$$

By taking into account eqs. (2.10) to (2.13), eq. (2.9)

becomes

$$\begin{aligned} \overline{\text{TOP}} = & C_2 \cdot (F_1 \vee F_3 \vee G_2 \vee G_3 \vee G_4) \cdot (F_1 \vee F_3 \vee G_1 \\ & \vee G_3 \vee G_4) \cdot (L_1 \vee L_3 \vee G_2 \vee G_3 \vee G_4) \\ & \cdot (L_1 \vee L_3 \vee G_1 \vee G_2 \vee G_4) \\ & \cdot (G_2 \vee G_3 \vee G_4 \vee F_1 \vee F_2 \vee L_2 \vee L_3) \\ & \cdot (G_1 \vee G_3 \vee G_4 \vee F_1 \vee F_2 \vee L_2 \vee L_3) \\ & \cdot (F_2 \vee F_3 \vee G_2 \vee G_3 \vee G_4 \vee L_1 \vee L_2) \\ & \cdot (F_2 \vee F_3 \vee G_1 \vee G_2 \vee G_4 \vee L_1 \vee L_2) \\ & \cdot (F_2 \vee F_3 \vee L_2 \vee L_3) \\ & \cdot (G_2 \vee G_3 \vee G_4 \vee F_1 \vee F_2 \vee L_1 \vee L_2). \end{aligned} \quad (2.14)$$

We execute the operations of eq. (2.14) and we apply the three simplification rules. We get

$$\begin{aligned} \overline{\text{TOP}} = & C_2 \cdot G_2 \cdot F_1 \cdot L_2 \vee C_2 \cdot G_2 \cdot F_1 \cdot L_3 \\ & \vee C_2 \cdot G_2 \cdot F_3 \cdot L_2 \vee C_2 \cdot G_2 \cdot F_3 \cdot L_3 \\ & \vee C_2 \cdot G_3 \cdot F_2 \cdot L_1 \vee C_2 \cdot G_3 \cdot F_2 \cdot L_3 \\ & \vee C_2 \cdot G_3 \cdot F_3 \cdot L_1 \vee C_2 \cdot G_3 \cdot F_3 \cdot L_3 \\ & \vee C_2 \cdot G_4 \cdot F_2 \vee C_2 \cdot G_4 \cdot F_3 \\ & \vee C_2 \cdot G_4 \cdot L_2 \vee C_2 \cdot G_4 \cdot L_3. \end{aligned} \quad (2.15)$$

The function $\overline{\text{TOP}}$ is not coherent because all literals of the primary components F and L appear in its complete base [eq. (2.15)].

By properly applying the implication test described in Appendix B (see Appendix B) it is possible to show that each monomial of eq. (2.15) is obligatory. The function $\overline{\text{TOP}}$ is therefore irredundant but not coherent.

4. Conclusions

Coherent systems have been defined in the case of systems made of multistate (two or more than two states) primary components.

This definition is consistent with that originally suggested by Barlow [9] in the case of systems with binary components.

Irredundant and coherent Boolean functions have also been defined. The properties of coherence have been described and discussed. This has led to a simplified algorithm which allows one to calculate the base of a coherent Boolean function.

In addition the algorithm may contribute to reduce the size of a normal disjunctive form of a Boolean function (TOP) also in the case in which the function is not coherent. In fact, whenever a prime implicant X of the associated coherent function Φ is found to be an implicant of the TOP (Step 2 of the algorithm), X can be written in the list of the monomials of the TOP. All monomials of the TOP which subsume X can be deleted (absorption rule). The Nelson algorithm is then applied to the reduced normal disjunctive form of the TOP and the complete base is calculated.

The algorithm has been built in the Karlsruhe computer program MUSTAFA-1, which can handle fault trees of systems with multistate components ([7] and [8]). In a sample case the algorithm reduced the computing (CPU) time of the complete base by a factor of about twenty.

Appendix A

Theorem 1. *No prime implicant of the Boolean function TOP associated with the failed state of a coherent system contains an intact literal.*

Proof. We argue ad absurdum. Let us consider a prime implicant (say X) of the TOP. If X were to contain an intact literal (say A_1), we could write

$$X = M \wedge A_1, \quad (\text{A.1})$$

where M is a monomial and A is a primary component with n_A literals. All other monomials

$$M \wedge A_i, \quad i = 2, 3, \dots, n_A,$$

would necessarily all be implicants of the TOP, because otherwise deterioration of the performance of primary component A could cause (in some system configurations) the system to improve. This would be in contrast with the definition of coherent system

(see Definition 20). Since

$$M \wedge \left(\bigvee_{i=1}^{n_A} A_i \right) = M, \quad (\text{A.2})$$

monomial M would be an implicant of the TOP and X (eq. A.1) could not therefore be a prime implicant of the TOP. This is in contrast with the initial assumption, that X is a prime implicant of the TOP.

Theorem 2. *If a normal disjunctive form of a Boolean function is such that at least one literal of each primary component relevant to the function does not appear in it, the Boolean function is irredundant, i.e., the normal disjunctive form is the only base of the function.*

Let us indicate with TOP the Boolean function and with X_i a generic monomial of a normal disjunctive form of the TOP. We can write

$$\text{TOP} = \bigvee_{i=1}^n X_i, \quad (\text{A.3})$$

where n is the total number of monomials. Let us indicate with A, B, C , etc. the primary components. Without any loss of generality we can assume that the first literal of each component (A_1, B_1, C_1 , etc.) does not appear in the normal disjunctive form of the TOP.

Proof. The proof is carried out in three steps and we argue ad absurdum throughout.

Step 1. The normal disjunctive form is a base of the function i.e., each monomial X_i is a prime implicant.

Step 2. The base is irredundant, i.e., each prime implicant is obligatory.

Step 3. The base is complete, i.e., no other prime implicant of the function exists.

Ad Step 1

We select a primary component (say A). By grouping together all monomials which contain the same literal A_q , we can write the TOP (eq. (A.3)) as follows

$$\text{TOP} = \bigvee_{q=2}^{n_A} (A_q \wedge \Phi_q) \vee \Psi, \quad (\text{A.4})$$

where n_A is the total number of literals belonging to

A and Φ_q, Ψ are Boolean functions (in normal disjunctive form) which do not contain any literal of A .

We consider now a monomial X_j of eq. (A.3) which contains the literal A_k . We can write X_j as the conjunction of A_k and of the monomial M_{kj} which contains no literal of A . The monomial M_{kj} is therefore subsumed by X_j . In addition M_{kj} is a monomial which implies Φ_k because of eq. (A.4).

We have therefore

$$X_j = M_{kj} \wedge A_k, \quad (\text{A.5})$$

and

$$M_{kj} \wedge \Phi_k = M_{kj}. \quad (\text{A.6})$$

If M_{kj} were also an implicant of the TOP, we could write

$$M_{kj} \wedge \text{TOP} = M_{kj}. \quad (\text{A.7})$$

Eqs. (A.4), (A.6) and (A.7) obviously require M_{kj} to be also an implicant of Ψ , that is

$$M_{kj} \wedge \Psi = M_{kj}. \quad (\text{A.8})$$

Since Ψ does not contain at least one literal of each relevant primary component and M_{kj} is an implicant of Ψ , M_{kj} should necessarily either appear directly in the expression of Ψ or subsume a monomial of Ψ . In both cases the subsuming monomial X_j would be deleted because of the absorption rule. Since this result would be in contrast with the original assumption that the disjunction form of the TOP is normal, the monomial M_{kj} cannot be an implicant of the TOP. By repeating the above procedure for all other literals of X_j , we would come to the conclusion that no subsumed monomial of X_j can be an implicant of the TOP. This is equivalent to saying that X_j is a prime implicant.

Since each monomial X_j is a prime implicant, eq. (A.3) is a base of the TOP.

Ad Step 2

We consider the Boolean function α_j which one obtains from the base of the TOP (eq. (A.3)) by deleting the arbitrarily selected prime implicant X_j .

We consider now the Boolean function β_j obtained from α_j by deleting all monomials which are

mutually exclusive with X_j and by replacing by 1 (in each surviving prime implicant) all literals which are contained in X_j . This is equivalent to writing

$$\beta_j = [\alpha_j]_{X_j=1}. \quad (\text{A.9})$$

We point out that no intact literal is present in β_j .

We expand now β_j into its canonical form. We point out that the complete monomial resulting from the conjunction of all first literals of the primary components relevant to β_j is not contained in the canonical form of β_j . This is equivalent to writing that β_j is not identical with 1.

$$\beta_j \neq 1. \quad (\text{A.10})$$

If X_j were *not* an obligatory prime implicant of the TOP, we would have

$$\alpha_j \equiv \text{TOP}, \quad (\text{A.11})$$

and therefore

$$\beta_j = [\alpha_j]_{X_j=1} \equiv [\text{TOP}]_{X_j=1} \equiv 1 \quad (\text{A.12})$$

Since eq. (A.10) does not agree with eq. (A.12), X_j must be an obligatory prime implicant.

By repeating the above procedure for each prime implicant, one shows that all prime implicants are obligatory.

Since all prime implicants are obligatory, the base of the TOP [eq. (A.3)] is irredundant.

Ad Step 3

We consider a monomial Y which subsumes none of the prime implicants of the irredundant base of the TOP (eq. (A.3)).

We consider now the Boolean function γ obtained from the TOP by deleting all prime implicants which are mutually exclusive with Y and by replacing by 1 (in each surviving prime implicant) all literals which are contained in Y . This is equivalent to writing

$$\gamma = [\text{TOP}]_{Y=1}. \quad (\text{A.13})$$

We point out that no intact literal is present in γ .

We expand now γ into its disjunctive canonical form. We observe that the complete monomial resulting from the conjunction of all the first literals of the

primary components which are relevant to γ is not contained in the disjunctive canonical form of γ . This is equivalent to writing that γ is not identical with 1.

$$\gamma \neq 1. \quad (\text{A.14})$$

On the other hand, if Y were a prime implicant of the TOP, we should have, according to eq. (A.15),

$$\gamma \equiv 1. \quad (\text{A.15})$$

Since eq. (A.15) obviously does not agree with eq. (A.14), we conclude that Y cannot be an implicant of the TOP and therefore the irredundant base (eq. (A.3)) is also complete.

Theorem 3. Any implicant of the Boolean function TOP, which is also a prime implicant of its associated coherent function Φ , is a prime implicant of the TOP.

Proof. We argue ad absurdum. We can write

$$\Phi = \text{TOP} \vee \Psi, \quad (\text{A.16})$$

where Ψ is a Boolean function which implies Φ but not TOP. Let us indicate with X a prime implicant of Φ which is also an implicant of TOP. We can write therefore

$$X \wedge \Phi = X, \quad (\text{A.17})$$

and

$$X \wedge \text{TOP} = X. \quad (\text{A.18})$$

Let us indicate with Y any one of the monomials which are subsumed by X . Since X is a prime implicant of Φ , we must have

$$Y \wedge \Phi \neq Y. \quad (\text{A.19})$$

We consider now the Boolean function $Y \wedge \Phi$. Taking into account eq. (A.16), we can write

$$Y \wedge \Phi = (Y \wedge \text{TOP}) \vee (Y \wedge \Psi). \quad (\text{A.20})$$

If X were not a prime implicant of TOP, there would exist at least one monomial Y subsumed by X for which the following equation would hold

$$Y \wedge \text{TOP} = Y. \quad (\text{A.21})$$

Taking into account eq. (A.21), eq. (19) would become

$$Y \wedge \Phi = Y \vee (Y \wedge \Psi) = Y, \quad (\text{A.22})$$

which does not agree with eq. (A.21). We conclude

that eq. (A.21) does not hold and that we must have

$$Y \wedge \text{TOP} \neq Y. \quad (\text{A.23})$$

Since X is an implicant of TOP (eq. (A.18)) and every monomial subsumed by X is not an implicant of TOP (eq. (A.23)), X is a prime implicant of TOP.

Appendix B

Implication test for monomials

Given two functions (say TOP and X), we say that X implies TOP if

$$X \wedge \text{TOP} = X, \quad (\text{B.1})$$

eq. (B.1) can be used as a test to verify that X implies the TOP.

Another possible way of testing that X is an implicant of the TOP is based on the following statement.

If (1) X implies TOP and (2) X takes the value 1, TOP takes the value 1

$$[\text{TOP}]_{X=1} = 1. \quad (\text{B.2})$$

The following equation is obtained by complementing both sides of eq. (B.2).

$$\overline{[\text{TOP}]_{X=1}} = 0. \quad (\text{B.3})$$

The above statement can be changed into the following, by making use of eq. (B.3).

If (1) X implies TOP, and (2) X takes the value 1, the complement of TOP ($\overline{\text{TOP}}$) takes the value 0.

The last statement suggests the following implication test in the case that the function TOP is given in a disjunctive form and the function X is a monomial.

The test is carried out in five steps:

Step 1. Delete all monomials of TOP which are mutually exclusive with X . Call result α .

Step 2. Replace by 1 in each monomial of α every literal which is also present in X . Call result β .

Step 3. Delete in β every subsuming monomial (absorption rule). Call result γ .

Step 4. Complement γ and reduce it to a normal disjunctive form. Call result $\bar{\gamma}$.

Step 5. If $\bar{\gamma} \equiv 0$, X is an implicant of TOP.

We apply now the test to eq. (2.5) (TOP) and to

the monomial G_1 . We have

$$\begin{aligned} \text{TOP} = & C_1 \vee F_2 \cdot G_1 \vee F_2 \cdot G_2 \vee L_2 \cdot G_1 \vee L_2 \cdot G_3 \\ & \vee G_1 \cdot F_3 \cdot L_1 \vee G_2 \cdot F_3 \cdot L_1 \vee F_1 \cdot G_1 \cdot L_3 \\ & \vee F_1 \cdot G_3 \cdot L_3 \vee F_1 \cdot L_1 \vee G_1 \cdot F_3 \cdot L_3, \end{aligned} \quad (\text{B.4})$$

$$X = G_1. \quad (\text{B.5})$$

The test is carried out as follows.

Ad Step 1:

$$\begin{aligned} \alpha = & C_1 \vee F_2 \cdot G_1 \vee L_2 \cdot G_1 \vee G_1 \cdot F_3 \cdot L_1 \\ & \vee F_1 \cdot G_1 \cdot L_3 \vee F_1 \cdot L_1 \vee G_1 \cdot F_3 \cdot L_3; \end{aligned} \quad (\text{B.6})$$

Ad Step 2:

$$\begin{aligned} \beta = & C_1 \vee F_2 \cdot 1 \vee L_2 \cdot 1 \vee 1 \cdot F_3 \cdot L_1 \\ & \vee F_1 \cdot 1 \cdot L_3 \vee F_1 \cdot L_1 \vee 1 \cdot F_3 \cdot L_3; \end{aligned} \quad (\text{B.7})$$

Ad Step 3:

$$\begin{aligned} \gamma = & C_1 \vee F_2 \vee L_2 \vee F_3 \cdot L_1 \vee F_1 \cdot L_3 \vee F_1 \cdot L_1 \vee F_3 \cdot L_3; \\ & \end{aligned} \quad (\text{B.8})$$

Ad Step 4:

$$\begin{aligned} \bar{\gamma} = & C_2 \cdot (F_1 \vee F_3) \cdot (L_1 \vee L_3) \cdot (F_1 \vee F_2 \vee L_2 \vee L_3) \\ & \cdot (F_2 \vee F_3 \vee L_1 \vee L_2) \cdot (F_2 \vee F_3 \vee L_2 \vee L_3) \\ & \cdot (F_1 \vee F_2 \vee L_1 \vee L_2) \equiv 0; \end{aligned} \quad (\text{B.9})$$

Ad Step 5:

Since $\bar{\gamma} \equiv 0$, the monomial G_1 is an implicant of TOP (eq. (B.4)).

The implication test can be used to prove whether or not a monomial is obligatory. We consider the function TOP_j obtained from the function TOP by removing the monomial X_j which is intended to be tested. If X_j is not an implicant of TOP_j , X_j is an obligatory monomial of the TOP.

As an example we apply the test to the function

$\overline{\text{TOP}}$ of eq. (2.15). We have

$$\begin{aligned} \overline{\text{TOP}} = & C_2 \cdot G_2 \cdot F_1 \cdot L_2 \vee C_2 \cdot G_2 \cdot F_1 \cdot L_3 \\ & \vee C_2 \cdot G_2 \cdot F_3 \cdot L_2 \vee C_2 \cdot G_2 \cdot F_3 \cdot L_3 \\ & \vee C_2 \cdot G_3 \cdot F_2 \cdot L_1 \vee C_2 \cdot G_3 \cdot F_2 \cdot L_3 \\ & \vee C_2 \cdot G_3 \cdot F_3 \cdot L_1 \vee C_2 \cdot G_3 \cdot F_3 \cdot L_3 \\ & \vee C_2 \cdot G_4 \cdot F_2 \vee C_2 \cdot G_4 \cdot F_3 \vee C_2 \cdot G_4 \cdot L_2 \\ & \vee C_2 \cdot G_4 \cdot L_3. \end{aligned} \quad (\text{B.10})$$

We want to test the ninth monomial, that is

$$X_9 = C_2 \cdot G_4 \cdot F_2. \quad (\text{B.11})$$

By deleting the ninth monomial in eq. (B.10), we get

$$\begin{aligned} \overline{\text{TOP}}_9 = & C_2 \cdot G_2 \cdot F_1 \cdot L_2 \vee C_2 \cdot G_2 \cdot F_1 \cdot L_3 \\ & \vee C_2 \cdot G_2 \cdot F_3 \cdot L_2 \vee C_2 \cdot G_2 \cdot F_3 \cdot L_3 \\ & \vee C_2 \cdot G_3 \cdot F_2 \cdot L_1 \vee C_2 \cdot G_3 \cdot F_2 \cdot L_3 \\ & \vee C_2 \cdot G_3 \cdot F_3 \cdot L_1 \vee C_2 \cdot G_3 \cdot F_3 \cdot L_3 \\ & \vee C_2 \cdot G_4 \cdot F_3 \vee C_2 \cdot G_4 \cdot L_2 \vee C_2 \cdot G_4 \cdot L_3. \end{aligned} \quad (\text{B.12})$$

We apply now the implication test to the function given by eq. (B.12). We have

$$\text{Step 1. } \alpha = C_2 \cdot G_4 \cdot L_2 \vee C_2 \cdot G_4 \cdot L_3. \quad (\text{B.13})$$

$$\text{Step 2. } \beta = L_2 \vee L_3. \quad (\text{B.14})$$

$$\text{Step 3. } \gamma = L_2 \vee L_3. \quad (\text{B.15})$$

$$\text{Step 4. } \bar{\gamma} = L_1.$$

Step 5. Since $\bar{\gamma} \neq 0$, the monomial $C_2 \cdot G_4 \cdot F_2$ is not an implicant of $\overline{\text{TOP}}_9$ (eq. (B.12)).

Since the monomial $C_2 \cdot G_4 \cdot F_2$ is not an implicant of $\overline{\text{TOP}}_9$, it is an obligatory monomial of $\overline{\text{TOP}}$ (eq. (B.10)).

By applying the test to each monomial of the $\overline{\text{TOP}}$ (eq. (B.10)), it is possible to show that each monomial is obligatory.

References

- [1] W.E. Vesely, Nucl. Engrg. Des. 13 (1970) 337–360.
- [2] L. Caldarola, Nucl. Engrg. Des. 44 (1977) 147–162.
- [3] L. Caldarola and A. Wickenhäuser, Nucl. Engrg. Des. 43 (1977) 463–470.
- [4] K. Kotthoff and W. Otto, Vergleich von Rechenprogrammen zur Zuverlässigkeitsanalyse von Kernkraftwerken, IRS-RS 172 (1976).
- [5] L. Caldarola and A. Wickenhäuser, Recent advancements in fault tree methodology at Karlsruhe, Internat. Conf. Nucl. Systems Reliability Engrg. and Risk Assessment, Gatlinburg, SIAM, 518–542 (June 1977).
- [6] L. Caldarola, ANS Topical Meeting on Probabilistic Analysis of Nuclear Reactor Safety, Los Angeles, CA, Paper VIII.1 (May 1978).
- [7] L. Caldarola, Fault tree analysis with multistate components, KFK 2761 (1979).
- [8] L. Caldarola, Generalized fault tree analysis combined with state analysis, KFK 2530 (1980).
- [9] R.E. Barlow, Statistical Theory of Reliability and Life Testing: Probability Models (Holt Rinehart and Winston, 1975, New York).
- [10] J. Kuntzmann, Fundamental Boolean Algebra (Blackie and Sons, 1967).
- [11] R.E. Barlow and A.S. Wu, Math. Operations Res. 3 (4) (1978) 275–281.
- [12] L. Caldarola, Grundlagen der Booleschen Algebra mit beschränkten Variablen, KFK 2915 (1980).



VERÖFFENTLICHUNGSLISTE

1. L. Caldarola
Regolazione automatica per un impianto di laminazione a freddo,
Thesis, 1957
2. L. Caldarola
Transitori termici in simmetria cilindrica
Rendiconti A.E.I., 1959
3. L. Caldarola
Transitori termici in un reattore nucleare
Rendiconti A.E.I., 1959
4. L. Caldarola
Design Principles for Control Mechanisms
Dragon Project Report No. 145, March 1963
5. L. Caldarola
Dragon Reactor Automatic Control
Dragon Project Report No. 174, April 1963
6. L. Caldarola
Absorber Rod Control Circuit
Dragon Project Report No. 122, October 1963
7. L. Caldarola
Control Circuit for By-Pass Valves in the Primary Gas Circuit
Dragon Project Report No. 238, November 1963
8. L. Caldarola, E.G. Schlechtendahl
Reactor Temperatur Transients with Spatial Variables
First Part: Radial Analysis
KfK-223 (Mai 1964)
EUR-2403 (1965)
9. W. Häfele, K. Ott, L. Caldarola, W. Schikarski, K.P. Cohen,
B. Wolfe, P. Greebler, A.B. Reynolds
Static and Dynamic Measurements on the Doppler Effect in an Experimental
Fast Reactor
3rd United Nations International Conference on the Peaceful Uses
of Atomic Energy, Geneva Conf. 1964A/28/P/644
EUR-2484e
10. L. Caldarola
The Balanced Oscillator Experiment to Measure Doppler Reactivity
Coefficient and Thermal Parameters of Fuel Rod in Fast Reactors
Nukleonik 7, Bd. 3 (1965), S. 120-27
KfK-253
11. L. Caldarola, W. Häfele, W. Schikarski
Experiments to Evaluate Reactivity Coefficients with Reactor
Operating at Steady State Conditions
KfK-260 (Febr. 1966)

12. L. Caldarola, R.G. Pflasterer
SEFOR Experimental Program
Part 2: Test Description and Requirements
General Electric Report No. 5092 (1966)
13. L. Caldarola, M. Tavosanis
Design Criteria and Preliminary Calculations
of SEFOR Second and Third Cores
KfK-467 (1966)
14. L. Noble, G.R. Pflasterer, C.D. Wilkinson, L. Caldarola
Recent Developments in the SEFOR Experimental Program
Int. Conf. on Critical Experiments and their Analysis,
Argonne Nat. Labs., Argonne, Ill. Oct. 1966
KfK-649
ANL-7320, S. 746-58
15. M. Audoux, L. Caldarola, P. Giordano, H. Rohrbacher, C. Russel
The Balanced Oscillator Tests in SEFOR - Manual and Automatic Control -
Int. Conf. on Critical Experiments and their Analysis,
Argonne, Ill. (Oct. 1966)
KfK-650
EUR-3686e
16. L. Caldarola
Analysis of Reactor Power Excursions by Means of Solutions with
Asymptotic Expansions
Nukleonik 9 (1967), Bd. 7, S. 129-38
17. L. Caldarola, C. Russel
The Second Balanced Oscillator Experiment
Nukleonik 9, Bd. 7 (1967), S. 323-29
18. L. Caldarola, W. Niedermeyr, J. Voit
Reactor Temperature Transients with Spatial Variables
Second Part: Axial Analysis
KfK-618 (1967)
EUR-2403e
19. M. Audoux, L. Caldarola, P. Giordano, H. Rohrbacher
Automatic Control System for Balanced Oscillator Tests
KfK-667 (1967)
EUR-3700e
20. L. Caldarola, G. Weber
General Criteria to Optimize the Operations of a Power Plant with
Special Consideration to the Safety Requirements
KfK-640 (1967)
EUR-3685e

21. L. Caldarola
Il modello a uovo. Un nuovo modello per una trattazione piu generale del transitorio di pressione dovuto alla formazione della bolla di gas durante la reazione Sodio/Acqua
Rapporto PMN TNA (70) 402 C), 1970
22. L. Caldarola
Metodo di calcolo dello spessore di un contenitore cilindrico sottoposto ad un transitorio di pressione per un valore assegnato di deformazione massima in campo plastico
Rapporto PMN TNA (70), 1970
23. L. Caldarola
Rapporto aggiuntivo sul metodo di calcolo dello spessore di un contenitore cilindrico sottoposto ad un transitorio di pressione per un valore assegnato di deformazione massima in campo plastico
Rapporto PMN TNA (70) 403 C, 1970
24. L. Caldarola
A Theoretical Model for the Molten Fuel/Sodium Interaction in a Nuclear Fast Reactor,
Nucl. Eng. and Design, Vol. 22, No. 2, Oct. 1972, S. 175-211
25. L. Caldarola, P. Giordano
Verfahren und Regelanordnung zur Regelung einer physikalischen Größe in einer Regelstrecke, die einer periodischen Störgröße ausgesetzt ist
DAS 1 588 234 (13. 11. 1970)
26. G.R. Pflasterer, D.D. Freeman, P. Greebler, L.D. Noble, G. Kußmaul, F. Mitzel, L. Caldarola, W.J. Oosterkamp, D. Wintzer
SEFOR Experimental Results and Application to LMFBR's
Int. Conf. on Engineering of Fast Reactors for Safe and Reliable Operation, Karlsruhe Oktober 1972
27. L. Caldarola, G. Koutsouvelis
Theoretical Models for the Molten Fuel-Sodium Interaction,
Internat. Conf. on Engineering of Fast Reactors for Safe and Reliable Operation, Karlsruhe, Oktober 1972
28. L. Caldarola
New Definition of Reliability, Continuous Lifetime Prediction and Learning Processes
Int. Conf. on Reliability, Liverpool, July 1973
KfK-1847 (Juli 1973)
EUR-4969e
29. L. Caldarola
Considerations for an European Centralized Reliability Data Bank System
Int. Seminar on Reliability Data Banks, Stockholm, Oktober 1973
KfK-1929 (Okt. 1973)
EUR-4972
30. L. Caldarola, W.E. Kastenberg
A Model and Conditions for Fragmentation During Molten Fuel/Coolant Thermal Interactions
2nd Internat. Conf. on Structural Mechanics in Reactor Technology, Berlin, Sept. 1973

31. L. Caldarola
Balanced Oscillator Experiments in SEFOR
ANS Winter Meeting, San Francisco, USA, Nov. 1973
32. L. Caldarola
The Karlsruhe Variable Mass Model for the Description of the
Fuel/Coolant Interaction
2nd Specialists' CREST Meeting on Sodium Fuel Interaction in
Fast Reactors, Ispra, Italy, Nov. 1973
33. L. Caldarola
A Theoretical Model with Variable Masses for Fuel-Sodium Thermal
Interactions,
ANS Fast Reactor Safety Meeting, Beverly Hills, Calif., USA, Apr. 1974
34. L. Caldarola
On the Mechanisms of Fragmentation During Molten Fuel/Coolant Thermal
Interactions
ANS Fast Reactor Safety Meeting, Beverly Hills, Calif., USA, Apr. 1974
35. L. Caldarola
Reliability of Non-Deteriorating Devices
IEEE Transactions on Reliability 23 (1974), S. 219-23
36. L. Caldarola
Current State of Knowledge of Molten Fuel/Sodium Thermal Interactions
Meeting of the European Safety Working Group, Brüssel, Febr. 1974
KfK-1944 (Febr. 1974)
EUR-4973e
37. L. Caldarola
Stand der quantitativen Risikoanalyse
Jahreskolloquium 1974 des Projektes Nukleare Sicherheit, Karlsruhe, Nov. 1974
KfK-2101, S. 167-94
38. H.G. Bogensberger, W.J. Oosterkamp, D. Wintzer, L. Caldarola, F. Mitzel
Analysis of SEFOR-Experiments
KfK-2095 (Jan. 1975)
EUR-5200e
39. L. Caldarola
Statusbericht, Methoden zur quantitativen Analyse von Kernenergie-Risiken
KfK-2100 (1975)
40. L. Caldarola
A Theoretical Model with Variable Masses for the Molten Fuel-Sodium
Thermal Interaction in a Nuclear Fast Reactor
3rd SMIRT Conf., London, Sept. 1975
Nucl. Engineering and Design, 34 (1975), S. 181-201
41. L. Caldarola
A Method for the Calculation of the Cumulative Failure Probability
Distribution of Complex Repairable Systems
Nucl. Engineering and Design, 36 (1975), S. 109-22
42. L. Caldarola, H. Beutel, P. Baraggioli, R. Ladisch
Brennstoff-Natrium-Reaktion
in Projekt Schneller Brüter, 3. Vierteljahresbericht 1976
KfK-1276/3 (Dez. 76), S. 123/55-61

43. H. Beutel, E. Bojarsky, L. Caldarola, H. Jacobs, H. Reiser, W. Zyszkowski
Current Status of Experimental and Theoretical Work on Sodium/
Fuel Interaction (SFI) at Karlsruhe
3rd Specialists' Meeting on Sodium/Fuel Interaction in Fast Reactors,
Tokio, März 1976
PNC-N251-76-12 (Vol. 1), S. 179-86 und 443-65
PNC-N251-76-12 (Vol. 2), S. 819-38
44. L. Caldarola
A Model for Fuel Fragmentation during Molten Fuel/Coolant Thermal
Interactions
Int. Conf. on Fast Reactor Safety and Related Physics, Chicago, Okt. 1976
45. L. Caldarola, P. Ferranti, F. Mitzel
Fast Reactor Transfer Functions with Special Reference to the Non-
linearities and to the Spatial Dependence of the Heat Transfer
Process
KfK-2027 (Okt. 1974)
EUR-4978e
46. L. Caldarola, A. Wickenhäuser
The Karlsruhe Computer Program for the Evaluation of the Availability
and Reliability of Complex Repairable Systems
Nuclear Engineering and Design, 43 (1977), S. 463-70
47. L. Caldarola
Unavailability and Failure Intensity of Components
Nuclear Engineering and Design, 44 (1977), S. 147-62
48. L. Caldarola
Recent Advancements in Fault Tree Methodology at Karlsruhe
Int. Conf. on Nucl. Systems Reliability Engineering and Risk Assessment,
Gatlinburg, June 1977, (invited paper)
49. S.J. Board, L. Caldarola
Fuel Coolant Interaction in Fast Reactors
ASME Symposium on the Thermal and Hydraulics Aspects of Nuclear
Reactor Safety, Winter Annual Meeting, New York, Nov. 1977
50. L. Caldarola
Fault Tree Analysis of Multistate Systems with Multistate Components
ANS Topical Meeting on Probabilistic Analysis of Nuclear Reactor
Safety, Los Angeles, Calif. Mai 1978 (invited paper)
51. L. Caldarola, H. Jacobs, R. Ladisch
Grundlagen der Brennstoff-Natrium-Wechselwirkung
KfK-Nachrichten 10 (1978), No. 3/4
52. L. Caldarola, H. Wenzelburger, A. Wickenhäuser, P. Schwab
Störfallablaufanalyse für die große Wiederaufarbeitungsanlage
(Explosionen)
In: Projekt Nukleare Sicherheit, Halbj.-Bericht 1978/1
KfK-2700 (Nov. 1978), S. 4500/1-4500/2

53. L. Caldarola
Fault Tree Analysis with Multistate Components
KfK-2761, Febr. 1979
54. L. Caldarola
Film Boiling Experiments at Karlsruhe
4th CSNI Specialist Meeting on FCI in Nuclear Reactor Safety,
Bournemouth, April, 1979
55. L. Caldarola
Generalized Fault Tree Analysis Combined with State Analysis
KfK-2530 (Februar 1980)
EUR-5754e (Febr. 1980)
56. L. Caldarola
Grundlagen der Booleschen Algebra mit beschränkten Variablen
KfK-2915 (Februar 1980)
EUR-6405d (Febr. 1980)
57. L. Caldarola
Coherent Systems with Multistate Components
Nucl. Eng. and Design, 58 (1980), S. 127-39
58. L. Caldarola
Fault Tree Analysis with Multistate Components
G. Apostolakis, S. Garribba (Hrsg.)
Synthesis and Analysis Methods for Safety and Reliability Studies,
Proc. of the NATO Advanced Study Institute on Synthesis and Analysis
Methods for Safety and Reliability Studies, Urbino, Italy,
3.-14. Juli 1978
New York: Plenum Pr. 1980, S. 199 - 248
59. L. Caldarola, A. Wickenhäuser
The Boolean Algebra with Restricted Variables as a Tool for Fault
Tree Modularization
KfK-3190 (August 1981)
EUR-7056e (Aug. 1981)
60. L. Caldarola, H. Schnauder, A. Wickenhäuser, E. Pamfilie
Fault Tree Analysis of a Reactor Protective System
Internat. Topical Meeting on Probabilistic Risk Assessment, Port Chester, N.Y.,
20.-24. September 1981
61. M. Ando, L. Caldarola
Triggered Fragmentation Experiments at Karlsruhe
U. Müller, G. Günter (Hrsg.)
Post Accident Debris Cooling. Proc. of the Post Accident Heat Removal
Information Exchange Meeting, Karlsruhe, 28. - 30. Juli 1982
Karlsruhe: Braun, 1982 S. 13-21
62. H. Schnauder, L. Caldarola, A. Wickenhäuser
Wie zuverlässig ist das Reaktorschutzsystem bei der Reaktor-
schnellabschaltung?
KfK-Nachrichten, 14 (1982), S. 253-60

63. L. Caldarola
Die Dampfexplosion - Ein Naturereignis und ein Sicherheitsproblem
der Industrie
Vortrag.: Deutsch-Italienische Gesellschaft, Karlsruhe, 12. Okt. 1982
64. L. Caldarola, Maschek, Fröhlich, Jacobs, Schikorr, Heusener, Royl, Struwe
Sicherheits- und Risikoanalysen für den SNR 300
KfK-Nachrichten 3/1983